MASTERARBEIT | MASTER'S THESIS

Titel | Title

The characterization of the mutant ΦCh1-ΔORF94 and complementation and investigation of ΦCh1-ΔORF75

verfasst von | submitted by

Helene Eliaçık BSc BSc

angestrebter akademischer Grad | in partial fulfilment of the requirements for the degree of

Master of Science (MSc)

Wien | Vienna, 2024

Studienkennzahl lt. Studienblatt | Degree programme code as it appears on the student record sheet:	UA 066 830
Studienrichtung lt. Studienblatt | Degree programme as it appears on the student record sheet:	Masterstudium Molecular Microbiology, Microbial Ecology and Immunobiology
Betreut von | Supervisor:	ao. Univ.-Prof. Dipl.-Biol. Dr. Angela Witte

Abstract

Natrialba magadii, a haloalkaliphilic archaea, is the only known host to the temperate head-tail virus ΦCh1, living under extreme environmental conditions of high salt concentrations and high pH values. The host-virus interaction, the molecular mechanisms of the virus and the functions of specific open reading frames are understudied and need investigation.

The virus ΦCh1 harbours a known methyltransferase gene, the open reading frame 94, which will be a focus in this study. An investigation of the deletion of the ORF94 was performed, the deletion verified by southern blot analysis and the effects on the growth and lysis behaviour, on the viral titer and on essential viral proteins, namely the methyltransferase, the major capsid protein E and the tail fibre protein gp34, were analysed. These provided evidence of the significant role of the ORF94 in many regulatory pathways, as in the lysis regulation, protein synthesis and viral particle production. Further the deletion strain was complemented with two plasmids pRo-5/Mev and pNB102 with different copy numbers, and the effects again analysed. This led to the partially restoration of the original functions and the different effects of the plasmids were determined. The methylation was further studied with restriction analysis, concluding that less than half of the virus populations genomes were methylated.

The second focus of this study was the verification of deletion and characterization of the ORF75 deletion mutant, concerning the effects on growth behaviour, on lysis and viral titer and on the above mentioned important viral proteins. The analysis showed that the ORF75 plays a role in the growth and lysis behaviour, but there was little evidence of effects on the proteins.

Zusammenfassung

Natrialba magadii, ein haloalkaliphiles Archaeon, ist der einzig bekannte Wirt des temperaten Kopf-Schwanz Virus ΦCh1 und lebt unter extremen Umweltbedingungen, wie hohe Salzkonzentrationen und einem hohen pH-Wert. Über die Wirt-Virus Interaktion, die molekularen Mechanismen des Virus und die Funktion spezifischer offener Leserahmen ist wenig bekannt und wurden wenig untersucht.

Der Virus ΦCh1hat ein bekanntes Methyltransferase-Gen, den offenen Leserahmen 94, welcher ein Fokus dieser Studie ist. Eine Untersuchung der Deletion des ORF94 wurde durchgeführt, die Deletion mittels Southern Blot verifiziert und die Effekte auf das Wachstum und das Lysis-Verhalten, auf den viralen Titer und auf essenzielle virale Proteine, der Methyltransferase, dem Hauptkapsidprotein E und dem Schwanzfaserprotein gp34 wurden analysiert. Diese Analysen gaben Hinweise auf die wichtige Rolle des ORF94 in vielen Regulationswegen, wie der Lysis-Regulation, der Protein-Synthese und der viralen Partikel Produktion. Weiters wurde der Stamm mit der Deletion komplementiert mittels zweiter Plasmide pRo-5/Mev und pNB102, mit verschiedenen Kopienzahlen, und der Effekt analysiert. Die ursprünglichen Funktionen konnten partiell wieder hergestellt werden und die verschiedenen Effekte der Plasmide wurden untersucht. Die Methylierung wurde weiters untersucht mit einer Restriktions-Analyse, welche ergab, dass weniger als die Hälfte der Genome der Viruspopulation methyliert waren.

Der zweite Fokus dieser Studie war die Verifikation der Deletion und Charakterisierung der ORF75 Deletationsmutante, bezüglich der Effekte auf das Wachstum, die Lysis, den viralen Titer und den oben erwähnten viralen Proteinen. Die Analyse zeigte, dass der ORF75 eine Rolle im Wachstumsverhalten und der Lysis hat, aber die Proteine nicht beeinflusst sind.

TABLE OF CONTENTS

1 Introduction

1.1 Archaea

Organisms belonging to Archaea (ancient Greek: αρχaios-original) are procaryotic and can be found in aquatic and in terrestrial habitats, as well as inside animals (DeLong, 1998; Karner *et al.*, 2001; Lloyd *et al.,* 2013; Lurie-Winberger & Gophna, 2015). The latest view of the domains of life is a partition of the living organisms into Eukarya, Bacteria and Archaea (Cavicchioli, 2007). Since 1990 the third domain of Archaea was added to this perspective, after the tree of life was reorganized in respect to 16S rRNA analysis (Woese & Fox, 1977; Woese *et al.,* 1990). Further research into the differentiation of these three domains concluded distinctions between Archaea and Bacteria, gave rise to the theory that Eukaryotes emerged from the Archaea clade and highlighted the great diversity of Archaea (Eme *et al.*, 2017; Guy & Ettema, 2011; Hug *et al.,* 2016; Woese *et al.,* 1990; Williams *et al.,* 2020; Yarza *et al.*, 2014; Figure 1). This field of research has still a lot of unanswered questions, which need further investigation. With the Archaea playing an important and fascinating role in the study of life, they offer a manifold of starting points for exploration.

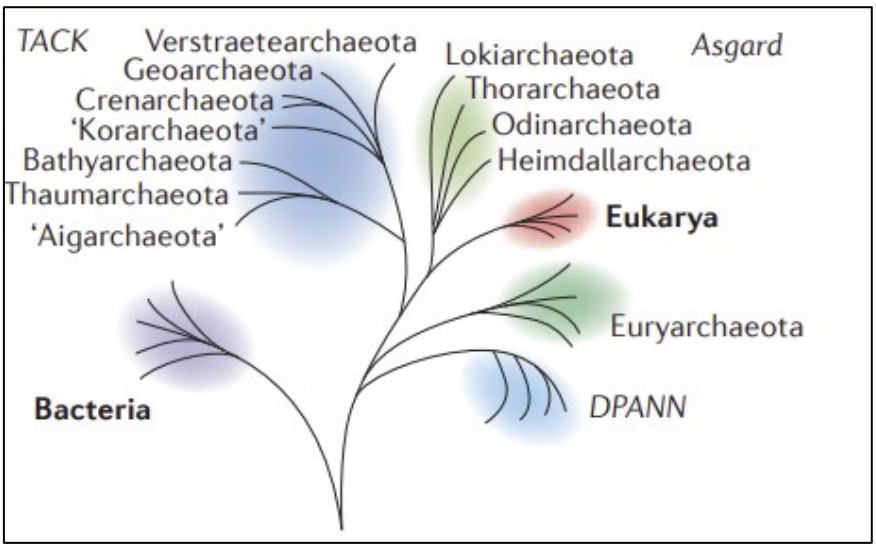

Figure 1. The tree of life. Schematic representation of the current idea of the relationship between Eukarya (red), Bacteria (purple) and Archaea (blue/green). (Eme *et al.,* 2017)

1.1.1 Distinction of Archaea

In previous times it was thought that Archaea and Bacteria are alike, since they both are procaryotes and show further similarities. Genomic analyses of Bacteria and Archaea showed similarities in their genomic organisation, metabolism, cellular morphology and intracellular composition (Allers & Mevarech, 2005; Bernander, 2000; Brown & Doolittle, 1997; Keeling *et al.*, 1994; Olsen & Woese, 1997; Woese, 1994). The chromosomes of both clades are small, circular and not inside of a nuclear envelope. The genomes of Archaea and Bacteria are organized, so that functionally related genes are arranged in operons (Forterre, 2013; Olsen & Woese, 1997; Zillig, 1991). Another characteristic of Archaea, which some Bacteria also have, is the pseudo-crystalline protein surface layer (S-layer), consisting of glycoproteins, around the cell surface (Jarrell *et al.*, 2010; Sleytr & Beveridge, 1999; Rodrigues-Oliveira *et al.*, 2017).

Nevertheless, similarities between Eukaryotes and Archaea have been discovered and are still explored. The transcriptional and translational mechanisms show great correspondence in both domains. The replication of DNA with the involved enzymes, like polymerases, shows higher consensus between Archaea and Eukaryotes compared to Bacteria (Edgell & Doolittle, 1997; Makarova *et al.*, 2014).

As mentioned, Archaea are now considered their own clade after 16S RNA analysis, this is supported by them having distinct features from the other domains. The membrane of Archaea consists of lipids with isoprenoid acyl chains with ether links to the glycerol backbone, instead of ester links between unbranched fatty acids and the backbone, which can be found in membranes of Bacteria and Eukaryotes (Albers & Meyer, 2011; Kates *et al*., 1993; Jarrell *et al.*, 2010; Jarrell *et al.*, 2011). These lipids are able to resist the harsh conditions Archaea live in (De Rosa & Gambacorta, 1988). The cell walls of Archaea do not contain murein, only some methanogens (*Euryarchaeota*) have pseudopeptidoglycan (Klingl *et al.*, 2019; Pohlschroder *et al.*, 2018).

1.1.2 Phylogeny

There are three superphyla of Archaea, named Asgard-, DPANN- and TACK-Archaea, after the phyla they contain (Baker et al, 2020; Figure 2). The Asgard Archaea contain the *Lokiarchaeota, Thorarchaeota, Odinarchaeota* and *Heimdallarchaeota* (Eme *et al.*, 2017). The *Aenigmarchaeota Diapherotrites, Nanoarchaeota, Nanohaloarchaeota* and *Parvarchaeota* belong to the DPANN Archaea (Sakai *et al.*, 2022). In the TACK superphyla are the phyla *Aigarchaeota*, *Crenarchaeota, Thaumarchaeota* and *Korarchaeota* (Guy & Ettema, 2011). The *Euryarchaeota* belong to no superphyla and are mainly methanogens, halophiles and hyperthermophiles (Woese *et al.*, 1990). With arising technologies, it will be possible to gain further understanding of the origin and evolution of Archaea and thereby life itself.

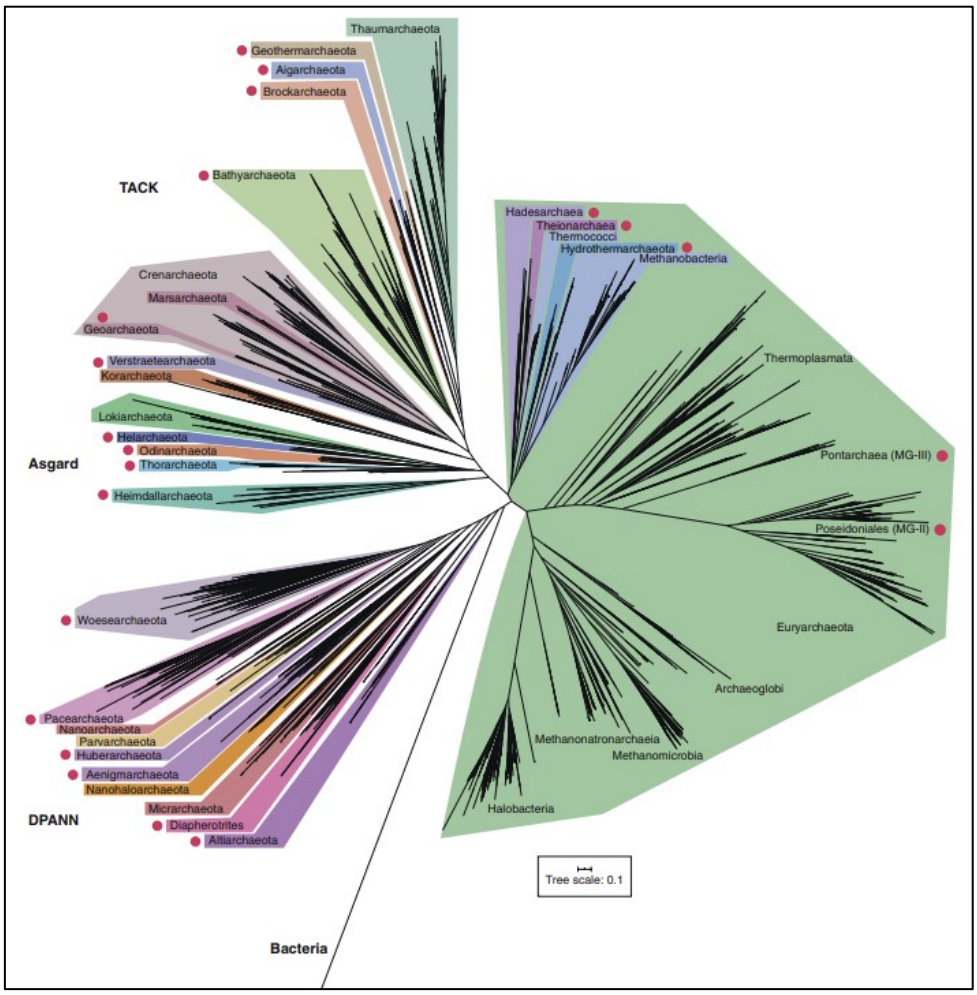

Figure 2. The updated archaeal tree of life. Phylogenetic analysis from 3.549 archaeal genomes and 40 bacterial genomes as outgroup, using 36 conserved marker proteins. Red dots indicate branches with no cultured representatives. (Baker *et al.*, 2020)

1.1.3 Habitats and extreme environments

A peculiarity of Archaea is their ability to live in extreme habitats and under distinct conditions, nevertheless they can be found mostly in moderate habitats (Rothschild *et al.*, 2001). This is the reason why many archaeal species are often referred to extremophiles (Pikuta *et al.*, 2007; Rothschild 2001). These are categorised into three groups: methanogens, thermoacidophiles and halophiles. The methanogens are anaerobic living organisms performing methanogenesis at aquatic habitats or in the gastrointestinal tracts of animals. As the name indicates, thermoacidophiles thrive at high temperatures above 80°C, like hydrothermal vents or volcanic environments. Halophilic Archaea live in hypersaline habitats, like the Dead Sea or saline lakes (Grant *et al.*, 1998).

1.1.4 Industrial potential, biotechnology and health

Working with Archaea can be exceedingly difficult, since their extreme living conditions lead to problems in cultivation, as well as handling difficulties because of their adaptations. Still there is a rising interest in studying and using Archaea in industrial applications, like bioremediation, wastewater treatments and organic pollutant degradation (Margesin & Schinner, 2001). The enzymes and proteins of Archaea are also of great interest since they show adaptations to extreme conditions and thereby stability in different environments or abilities to degrade substances, like cellulase (da Costa *et al.*, 1998; Gambacorta *et al.*, 1995; Norris *et al.*, 2000; Sauer and Galinski, 1998; Schumacher *et al.*, 2001). Archaea are a promising actor in biotechnologies and health sciences and show a range of applications. There are no known pathogenic Archaea, but there have been associations with diseases of the colon and the gum (Cavicchioli *et al.*, 2003).

1.1.5 Haloalkaliphilic Archaea

The superphylum *Euryarchaeota* includes the haloarchaea, which grow in high salt environments (Woese *et al.*, 1990). Haloalkaliphilic Archaea are adapted to high saline and alkaline conditions (Oren, 2002). These conditions can be ranging from 2.5-5.2 M NaCl and a pH between 8.5 to 11, but these extreme halophiles require salt and alkaline conditions to survive (Horikoshi, 1999; Kushner, 1978). In contrast to moderate

halophiles, which live at only a salt concentration of about 0.5 to 2.5 M NaCl (Andrei *et al.*, 2012). Most Archaea belonging to these extremophiles are in the class *Halobacteria* inside *Euryarchaeota* (Pikuta, 2011).

1.1.5.1 Adaptations

Archaea have evolved adaptations to withstand the high salt concentrations by accumulating inorganic ions, like KCl, inside the cytoplasm. They are able to achieve levels of ions for osmotic balance inside and outside the cell (Lanyi *et al.*, 1979; Madern *et al.*, 2000; Sehgal & Gibbons, 1960). The pH inside the cell is nearly neutral, for proteins to maintain their function, whilst living in environments with a high pH (Cook *et al.*, 1996; Guffanti & Hicks, 1991; Sturr *et al.*, 1994). The mechanisms behind these adaptations are transporter systems, like Na^+/H^+-antiporters, regulating the salt concentration inside the cell and a negatively charged cell envelope for aerobic respiration (Haines & Dencher, 2002; Hunte *et al.*, 2005; Kitada *et al.*, 1994; Ito *et al.*, 1997; Mesbah *et al.*, 2009; Oren, 1999; Tenchov *et al.*, 2006).

Mesophilic organisms have proteins which could not withstand the high salt concentrations and would precipitate under the high amount of KCl. The proteins of haloarchaea show adaptations in their amino acid compositions, so that their isoelectric point is low, having many hydrophobic and acidic and lesser basic amino acids (Lanyi, 1974; Mevarech *et al.*, 2000; Oren, 2002).

Most representatives of haloalkaliphilic archaea live as aerobe heterotrophs, but some can also grow anaerobically. The energy sources usually are proteins and amino acids, which also serve as carbon source (Andrei *et al.,* 2012).

Another adaptation which can be found in organisms living in extreme environments is containing multiple copies of their chromosome, called polyploidy (Comai, 2005). This leads to selection advantages, like the prospect of gene diversification, which could lead to new functions. In organisms with polyploidy, it is not highly likely that harmful recessive mutations will become homozygous (Breuert *et al.*, 2006). In addition, the increased number of chromosome copies can also be used as a phosphate storage.

1.1.5.2 *Natrialba magadii*

The Lake Magadi in Kenya is the first place of isolation (1980) and solely home of *Natrialba magadii*, a haloalkaliphilic Archaea (Tindall *et al.*, 1984). This alkaline soda lake has a salt concentration of 300g/L and a pH value of 11 (Ma *et al*., 2010; Oren 2002). These conditions are optimal for the growth of *N. magadii*, which requires salt concentrations of 3.5M to 4M NaCl and a pH of 8.5 to 11. In addition, temperatures between 37°C and 42°C, high levels of carbonate minerals and low concentrations of Mg^{2+}, which are beneficial for the growth (Kamekura *et al.*, 1997).

N. magadii is an obligate aerobe chemoorganotroph, getting energy from peptides and amino acids. The cells are rod shaped, 5 to 7 µm long and colonies appear red under stress conditions, because of a carotenoid pigment (α-bacterioruberin) in their membrane. The pigment also helps the cells to protect themselves from sunlight and UV radiation, to which they are usually exposed to in their habitats, since the pigment is an antioxidant protecting the DNA (Shahmohammadi *et al.*, 1998). For motility *N. magadii* uses a polar flagellum (Tindall *et al.,* 1984; Oren, 2006). The cells are polyploid, containing up to 50 copies of the chromosome per cell and leading to a generation time of around 9 hours (Breuert *et al.*, 2006).

There are two laboratory *N. magadii* strains, the lysogenic strain L11, the wildtype infected with the virus ΦCh1 and the non-lysogenic strain L13, which is cured and can be infected by ΦCh1. Once *N. magadii* is infected with the virus, it cannot be superinfected. (Figure 3)

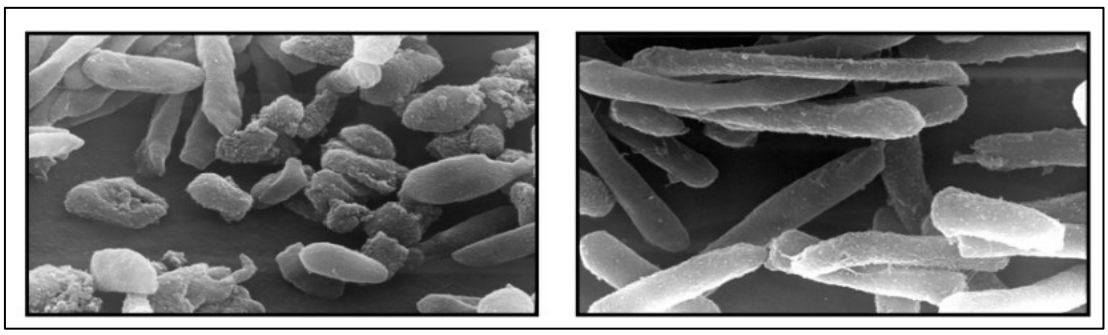

Figure 3. Electron micrograph of *N. magadii* strains. On the left side is the picture of *N. magadii* L11 the wild type. On the right side is the cured strain *N. magadii* L13 depicted (Iro, 2006).

To genetically work with *N. magadii*, there are two shuttle vectors available, pRo-5 and pNB102, which also are also suitable for working with *E. coli*. The first one is based on the vector pKS_{II}^{+}, contains the operon ORF53/ORF54 of ΦCh1 (*repH*) as the origin of replication, as well as an ampicillin and novobiocin resistances (Mayrhofer-Iro *et al.*, 2013; Figure 4). Novobiocin inhibits the B subunit of the DNA gyrase through blocking the ATP binding site (Holmes *et al.*, 1991). The vector pNB102 originates from the plasmid pNB101, isolated from *Natronobacterium* sp. strain AS7091, and contains the ColE1 origin of replication and the ampicillin and mevinolin resistances (Zhou *et al.*, 2004; Figure 4).

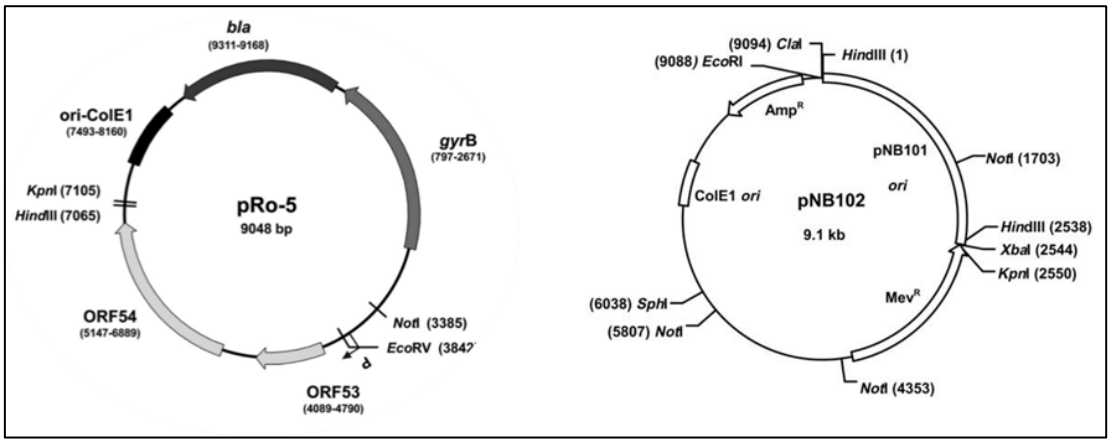

Figure 4. Maps of the shuttle vectors pRo-5 and pNB102. As arrows are the different fragments shown and restriction sites are indicated (Mayerhofer-Iro *et al.,* 2013; Zhou *et al.,* 2004)

Working with Archaea requires adapting the handling to the specific conditions the organism needs. The high salt concentrations which *N. magadii* requires, lead to adaptations being necessary in standard protocols and laboratory techniques. For example, when working with the proteins, adjustments need to be made when purifying and separating them (Holmes *et al.*, 1997). Another aspect deviating from standard work with microorganisms is the long generation time of 9 hours and 4 hours in logarithmic phase of *N. magadii*. For the process of making competent cells Proteinase K and bacitracin (antibiotic inhibiting cell wall synthesis) are necessary to create spheroplasts, since electroporation and using chemicals are ineffective because of the high salt concentration and high pH level (Mayrhofer-Iro *et al.*, 2013).

1.2 Archaeal virus

There are many families of viruses infecting Haloarchaea, like *Myoviridae, Fuselloviridae, Podoviridae, Pleilipoviridae, Pleioviridae, Sphaerolipoviridae* and *Siphjoviridae*. Each family has unique morphological features and a specific lifecycle. Viruses infecting Archaea are understudied and show cultivation difficulties, nevertheless, there have been a lot of findings in the last years (Luk *et al.*, 2014). The proteins of the viruses are similar to the proteins of haloarchaea, showing to be high in acidic amino acids, since the haloarchaea viruses are also confronted with extreme salt concentrations (Luk *et al.*, 2014). The viruses can be classified depending on their mode of infection. Virulent viruses cannot form stable lysogens with the host, rather a lytic cycle is active, with the result being the release of virions from the host. The temperate viruses can form lysogens with the host and activate the lytic lifecycle when necessary. Persistent infection leads to unstable carrier states, with the virus progeny being released without lysis of the host (Prangishvili, 2013).

The viruses show to drive the selection of the haloarchaea, which although their growth is slow, show great genetic variation (Bamford, 2003). Traditionally, the relationship between virus and host can be seen as predator-prey, but for the haloarchaeal viruses a more mutualistic relationship has been suggested, having a positive influence on the Archaea population and the genetic variation (Luk *et al.*, 2014; Oren *et al.*, 1997; Wais *et al.*, 1975).

1.2.1 Head-tailed viruses

The *Caudovirales*, also known as head-tailed viruses, are a group of viruses, with a distinct viral morphology, to which most bacteriophages belong to (Ackermann & Prangishvili, 2012). Even though they are the least abundant virus morphotype, they are the most studied. For analysis of them the plaque formation is used, which is an identification technique for lytic viruses. The *Myoviridae*, *Siphoviridae* and *Podoviridae* belong to the head-tailed viruses and form the three families, with different tails (Luk *et al.*, 2014). The *Caudovirales* have no envelope, but an icosahedral head, which harbours

the viral DNA and a flexible tail, which is necessary for adsorption to the host (Ackermann, 1998).

1.2.2 The virus ΦCh1

The virus ΦCh1 belongs to the family *Myoviridae* and is a temperate virus of *N. magadii*, integrating as a provirus in the chromosomal DNA. It is a model for the study of haloalkaliphilic viruses and was only found to have *N. magadii* as its host (Witte *et al.*, 1997). The extreme conditions under which *N. magadii* lives are also necessary for the stability and effectiveness of ΦCh1, otherwise the virus particles are segregated, or capsid proteins are changing their conformation (Witte *et al.*, 1997).

The tail of ΦCh1 consists of an internal shaft which is covered by a contractable tail. The total size of the head-tail virus is approximately 200 nm, with 70 nm head and 130 nm tail size (Witte *et al.*, 1997; Figure 5). The virus particle was found to be composed of four major and five minor proteins, with sizes ranging from 15 to 80 kDa and low isoelectric points (Lanyi, 1974).

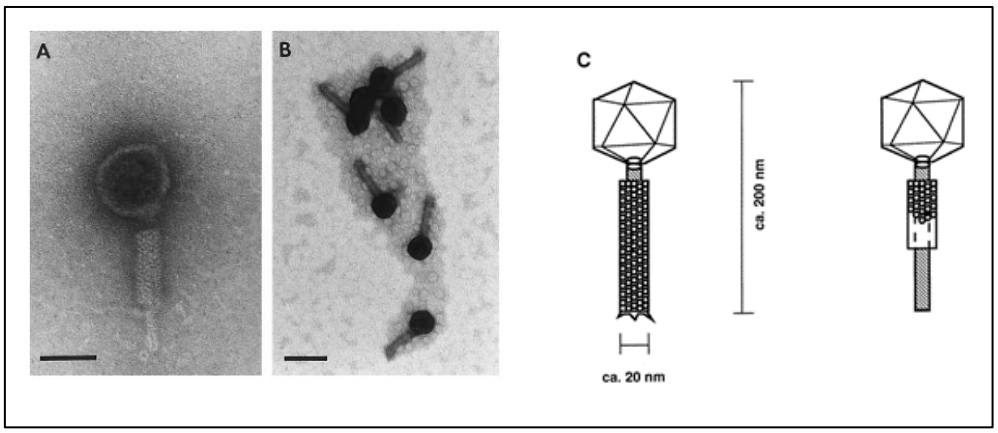

Figure 5. Electron micrographs of isolated ΦCh1 virus particles.
A. negatively strained virus particles with phospotungstate.
B. negatively strained virus particles with uranyl acetate
C. schematic representation of the ΦCh1 virus particles (Witte *et al.,* 1997)

The virus ΦCh1 integrates into the host genome as a prophage, where it can stable coexist. The lytic cycle is induced spontaneously while the cells are going into late stationary phase and is similarly regulated like the bacteriophage λ (Stolt & Zillig, 1994). The ORF48 was found to be analogous to the repressor in the lysis repressor- operator system in λ managing lysis, together with ORF94 (Iro *et al.*, 2007). The population of

viruses is at its highest during low salinity when the *N. magadii* population is low (Witte *et al.*, 1997).

The DNA of the virus is linear and double-stranded (58.5 kbp) and is packed with RNA which is host encoded and with unknown function (Klein *et al.*, 2000). The genome is divided into a part containing genes encoding for structural proteins and morphogenesis, a section for replication, stabilization of plasmids and gene expression regulation and lastly the segment including genes with unknown function, except from genes for DNA restriction and methylation (Figure 6). This organisation is comparable to the one of bacterial head-tail viruses, this could indicate horizontal gene transfer between viruses of Archaea and viruses of Bacteria or the existence of a common ancestor before the split into Bacteria and Archaea domains. In total there are 98 assigned open reading frames (ORFs) in the genome and the DNA contains 61.9% GC. The genes are thought to be organized in operons since some of the ORFs are overlapping (Klein *et al.,* 2002). A special feature of the viral DNA is that half the populations genomes are dam-like methylated at 5'-GATC-3', assumingly with a protective or regulatory function, whereas the host has no methylated DNA (Baranyi *et al.*, 2000; Bickle & Krüger, 1993; Haider, 2009; Kruger & Bickle, 1983). The ORF94, ORF80 and ORF82, each encode a methyltransferase M.*Nma*ϕCh1I, M.*Nma*ϕCh1II and M.*Nma*ϕCh1III, where the first one is an adenine and the other two are cytosine methyltransferases (Klein *et al.*, 2002).

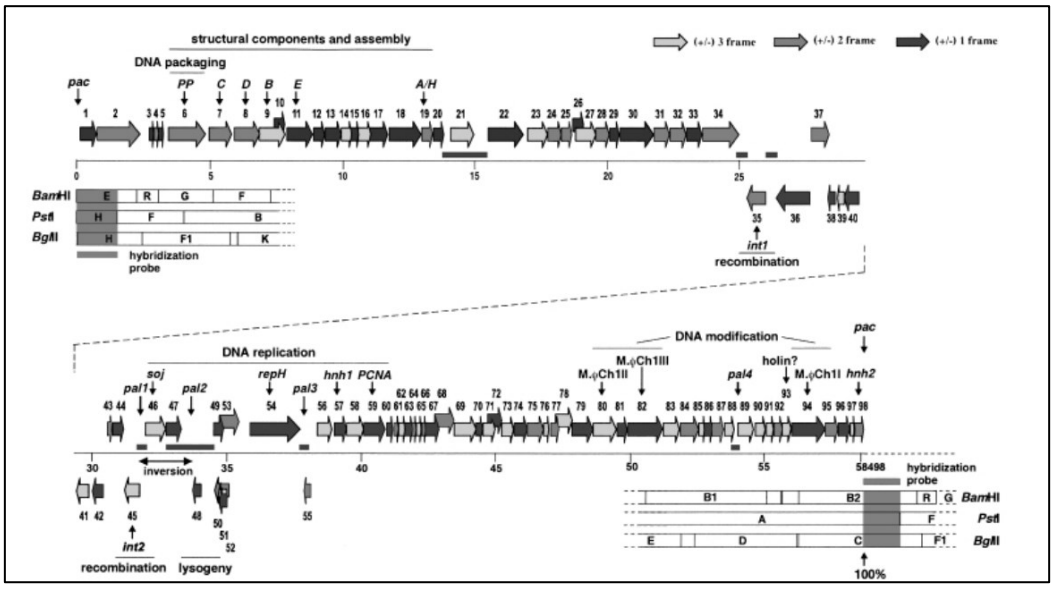

Figure 6. Linear scheme of the genome of ΦCh1, beginning at the *pac* site. Arrows indicate ORFs, with labelled known functions of predicted gene products. Reading frames are indicated with shades of grey: light is the third; mid is the second and dark is the first. (Klein *et al.,* 2002)

1.3 ORF94

Methylation of DNA is an epigenetic modification performed by methyltransferases and found in all kingdoms of life (Casadesús & Low, 2006; Jones & Takai, 2001; Modrich & Lahue, 1996). The enzymes recognize target sequences, depending on which residue is to be methylated, and add methyl groups from S-adenosyl-L-methionine, a donor molecule. There are DNA adenine methyltransferases (DAM), with the recognition site 5'-GATC-3', and cytosine methyltransferases (Dcm), with the sequencies 5'-CCTGG-3' and 5'-CCAGG-3' being recognised, where the C5 position is methylated (Marinus & Morris, 1975; May & Hattman, 1975).

As mentioned above, there are methyltransferases found in the virus ΦCh1, two cytosine (encoded by ORF80 and ORF82) and one adenine (encoded by ORF94) methyltransferase, which perform DNA modification (Klein *et al.*, 2002). The enzyme has a nuclease domain and a methyltransferase domain and belongs to the ß-subgroup of N^6-methyltransferases (Malone *et al.*, 1995; Wilson, 1991). The protein is 419 amino acids long, has a molecular weight of 46.6 kDa and a low isoelectric point at 4.17 (Baranyi *et al.*, 2000).

Previous studies showed that the protein is synthesized in the late phase during the lytic cycle, shortly before the release of virus particles from the host cell. It was examined how long the methylation of the DNA took, by comparing the methylated DNA levels of a lysogenic *N. magadii* L11 strains particles and a freshly infected *N. magadii* L13 strains particles. The progeny viruses of the freshly infected cells showed 5% of DNA methylation, whereas the lysogenic strain had 50% methylated genomes (Baranyi *et al.* 2000). The methylation pattern was further studied by restriction analysis and the ΦCh1 virus DNA showed to have partially adeno-methylated genomes (Witte *et al.*, 1997). It was shown, that the viral adenine methyltransferase M.*Nma*ϕCh1I can also work in low salt concentrations in *E. coli*, since it was able to restore dam^- mutants, even showing higher specificity in *E. coli* (Baranyi *et al.*, 2000; Nelson & McClelland, 1987; Palmer & Marinus, 1994; Witte *et al.*, 1997).

Earlier experiments regarding the better understanding the role of the ORF94 in the life of ΦCh1, suggested that the lysis regulation and the protein production are affected by the deletion of the ORF94 (Sommerkamp, 2022).

1.4 ORF75

The ORF75 is thought to play a role in the regulation of lysis but needs to be studied further to understand its function (Sommerkamp, 2022). The ORF75 is 620bp long and the protein gp75 has a size of 22.4 kDa (Klein *et al.,* 2002). The protein gp75 contains an ASCH (activating signal cointegrator-1 homology) domain, which has been shown to play a role in RNA metabolism, by having a potential RNA-binding cleft with a conserved sequence motif. This domain is often associated with bi-functional ribonucleoproteins and regulatory pathways including pre-mRNA processing and splicing (Iyer *et al.*, 2006; Kim *et al.*, 1999). ASCH domains are characterized by their central six-stranded beta-barrel structure surrounded by an alpha-helix, more than based on sequence similarities, since most of them show low sequence consensus (Bertonati *et al.*, 2009; Iyer *et al.*, 2006; Kim, 1998; Kim *et al.*, 2017; Sali, 1998; Teichmann *et al.*, 1999). Therefore, the hypothesis arose that the ORF75 is involved in the lytic cycle of ΦCh1 as a regulator. To investigate this possibility, experiments concerning the overexpression of the ORF75 were conducted and led to the conclusion that the ORF75 had an influence on the lytic pathway of ΦCh1. An earlier lysis and alterations of the expression of structural genes of ΦCh1 followed the overexpression of ORF75 (Sommerkamp, 2022).

2 Materials

2.1 Archaeal strains

Strain	Genotype	Reference
N. magadii L11	Wild type with integrated provirus ϕ Ch1	Witte *et al.*, 1997
N. magadii L13	ϕCh1 cured derivate of L11	Witte *et al.*,1997
N. magadii L11-ΔORF94 novR-R	ORF94 deficient derivate of L11	Witte, 2023
N. magadii L11-ΔORF75 novR	ORF75 deficient derivate of L11	Witte, 2023
N. magadii L13 pRo-5/Mev	ϕCh1 cured derivate of L11 with the plasmid pRo-5/Mev	Witte, 2019
N. magadii L13 pRo-5/Mev-ORF94	ϕCh1 cured derivate of L11 with the plasmid pRo-5/Mev-ORF94	This thesis
N. magadii L13 pNB102	ϕCh1 cured derivate of L11 with the plasmid pNB102	Witte, 2019
N. magadii L13 pNB102-ORF94	ϕCh1 cured derivate of L11 with the plasmid pNB102-ORF94	This thesis

Strain	Genotype	Reference
N. magadii L11-ΔORF94 novR-R pRo-5/Mev	ORF94 deficient derivate of L11 with the plasmid pRo-5/Mev	Witte, 2019
N. magadii L11-ΔORF94 novR-R pRo-5/Mev-ORF94	ORF94 deficient derivate of L11 with the plasmid pRo-5/Mev-ORF94	This thesis
N. magadii L11-ΔORF94 novR-R pNB102	ORF94 deficient derivate of L11 with the plasmid pNB102	Witte, 2019
N. magadii L11-ΔORF94 novR-R pNB102-ORF94	ORF94 deficient derivate of L11 with the plasmid pNB102-ORF94	This thesis

2.2 Bacterial strains

Strain	Genotype	Reference
E. coli XL1-Blue pRo-5/Mev-ORF94	*rec*A1, *end*A1, *gyr*A96, thi, *hsd*R17(r_K^-, m_K^+), *sup*E44, *rel*A1, *lac*, [F′, proAB$^+$, lacI^q, *lac*ZΔM15, Tn10(tet^R)]; with plasmid pRo-5/Mev-ORF94	Wali, 2019
E. coli XL1-Blue pNB102-ORF94	*rec*A1, *end*A1, *gyr*A96, thi, *hsd*R17(r_K^-, m_K^+), *sup*E44, *rel*A1, *lac*, [F′, proAB$^+$, lacI^q, *lac*ZΔM15, Tn10(tet^R)]; with plasmid pNB102-ORF94	Haider, 2014

2.3 Growth media

Lysogeny broth (LB) medium *(E. coli)*

10 g Peptone
5 g Yeast extract
5 g NaCl
pH 7.0
for plates added 15 g agar/L
ddH_2O added to a final volume of 1 L, autoclaved.

***N. magadii* rich medium (NVM^+)**

8.80 g Casaminoacids (CAA) or Casamino Hydrosylate (CH)
11.70 g Yeast extract
0.80 g Tri-Sodiumcitrate
2.35 g KCl
235 g NaCl
Add 5 pellets NaOH
For plates added 8 g/L agar or 4 g/L for soft agar.
Add ddH_2O to final volume 0.935 L, pH 9.5.
After sterilization added:
62 mL Na_2CO_3 (0.57 M; in sterile ddH_2O dissolved)
1 mL $MgSO_4$ (1 M; autoclaved)
1 mL $FeSO_4$ * 7 H_2O (0.02 M; in sterile ddH_2O dissolved)
1 mL Trace elements SL-6

1000x Trace elements SL-6

0.2 g $CoCl_2$ * 6 H_2O
10 mg $CuCl_2$ * 6 H_2O
0.3 g H_3BO_3
30 mg $MnCl_3$ * 4 H_2O
30 mg Na_2MoO_4 * H2O
20 mg $NiCl_2$ * 6 H_2O
0.1 g $ZnSO_4$ * 7 H_2O
Add ddH_2O to final volume of 100 mL and sterile filtered.

2.4 Antibiotics & additives

Compound	Stock concentration	Final concentration	Preparation
Novobiocin	3 mg/mL	3µg/mL	Dissolved in ddH_2O, sterile filtered, stored at -20°C
Mevinolin	5 mg/mL	4µg/mL	Lovastatin powder dissolved 96% EtOH, stored at -20°C
Ampicillin	20 mg/ml	100 µg/ml	Dissolved in ddH_2O, sterile filtered, stored at 4°C
Tetracycline	10 mg/ml	10 µg/ml	dissolved in half EtOH and half ddH_2O, stored at -20 °C
Bacitracin	7 mg/ml	70 µg/ml	dissolved in dH_2O, sterile filtered, stored at 4°C

2.5 Plasmids

Name	Features	Source
pRo-5/Mev	*bla*, ColE1 ori, *hmg* (Mev^R), ϕCh1 derived origin of replication	Sabic, 2019
pNB102	*bla*, ColE1 ori, *hmg* (Mev^R), ϕCh1 derived origin of replication	Zhou *et al.*, 2004
pRo-5/Mev-ORF94	*bla*, ColE1 ori, *hmg* (Mev^R), ϕCh1 derived origin of replication	Wali, 2019
pNB102-ORF94	*bla*, ColE1 ori, *hmg* (Mev^R), ϕCh1 derived origin of replication	Haider, 2014

2.6 Primers

Name	Sequence (5' to 3')
MT-Xba-3	GATCTCTAGATCACTCATTATCACCGGCGT
MT-Kpn-5	GAATGGTACCGCGAGTCGGACAACGTTC
5mt-1ba	GACGACGGTACCTCATGCAACTTGAAGAACTACCAA

Name	Sequence (5’ to 3’)
94-1-probe	GTTATCACACTACTGGCGCTGAT
94-2-probe	GTGACGCCTCGTAACCGAT
95-Bam	TTATGGATCCATGAGTGATGATATCGAGTACG
95-Hind	CAGGAAGCTTCAGTCGTCGACGTCG
NovR-1s	GATCCCCGGGTGTCGACTGGAACGAGG
NovR-2p	GTTACTGCAGGCCGTAATATCCAGCTGA
Δ75-5en1	GAGGCGCTCGAGTACTTC
Δ75-3en1	GTGCCCCTCTCGCTCG
Δ75-5en-3	GGGATCGACCTCCTCG
Δ75-3en-5	GAGGACAGCGTTTGCGTC

2.7 Enzymes & Nucleotides

Restriction Enzymes	**Reference**	**Product number**	**Source: *E. coli* strain carrying gene from …**
*Bam*HI-HF®	New England Biolabs	R3136	*Bacillus amyloliquefaciens*
*Bam*HI	New England Biolabs	ER0051	*Bacillus amyloliquefaciens*
*Nru*I-HF®	New England Biolabs	R3192	*Nocardia rubra*
*Pst*I-HF®	New England Biolabs	R3140	*Providencia stuartii*
*Eco*RV	ThermoFischer Scientific	R0195	plasmid J62 pLG74 (L.l. Glatman)
*Sau*3A	New England Biolabs	R0169	*Staphylococcus aureus* 3A
*Dpn*I	ThermoFischer Scientific	R0176	*Diplococcus pneumoniae*
*Mbo*I	ThermoFischer Scientific	R0147	*Moraxella bovis*

Polymerases	Reference	Product number
2x GoTaq green Master Mix	Promega	M7122
Other Enzymes	**Reference**	**Product number**
Proteinase K	Qiagen	19133
Nucleotides	**Reference**	**Product number**
Biotin-11-dUTP	Jena Bioscience	NU-803-BIOX-S

For all enzyme reactions the buffers according to the manufacturer were used.

2.8 DNA and Protein Ladders

DNA Ladder	Size [bp]	Reference	Product number
Generuler 1 kb Plus DNA Ladder	75, 200, 300, 400, 500, 700, 1000, 1500, 2000, 3000, 4000, 5000, 7000, 10000, 20000	ThermoFischer Scientific	SM1331

Protein Ladder	Size [kDa]	Reference	Product number
PageRuler™ Plus Prestained Protein Ladder, 10 to 250 kDa	10, 15, 25, 35, 55, 70, 100, 130, 250	ThermoFischer Scientific	26619

2.9 Kits

Name	Manufacturer	Product number
Wizard® SV Gel and PCR Clean-Up System	Promega	A9281
Wizard® Plus SV Minipreps DNA Purification System	Promega	A1460
Chemiluminescent Nucleic Acid Detection Module	ThermoFischer Scientific	89880

2.10 Antibodies

Primary Antibodies	Target	Dilution in 1x TBS, 0.3 % BSA, 0.02 % NaN_3	Reference
α-gp34$_{52}$ (rabbit #20)	ϕCh1 gp34	1:2500	Till, 2011
α- protein E	ϕCh1 gp11	1:2500	Klein *et al.,* 2000
α - methyltransferase	ϕCh1 gp94	1:1000	Baranyi *et al.*, 2000
Secondary Antibodies	**Target**	**Dilution in 1x TBS**	**Reference**
ECL™ Anti-Rabbit IgG, Horseradish peroxidase linked whole antibody from donkey	Rabbit IgG	1:5000	GE Healthcare (Product Number: NA934)

2.11 Membranes

Nitrocellulose Blotting Membrane Amersham Protean 0.2 µm GE Healthcare Life Science (Catalogue Number 10600001)

GE Healthcare, Amersham Hybond™-N, membrane otimized for nucleic acid transfer, 30 cm x 3 m

2.12 Buffers and Solutions

2.12.1 DNA methods

5x DNA Loading dye

0.1 %	SDS
0.05 %	Bromphenol blue
50 mM	Tris-HCl pH 8.2
0.05 %	Xylene cyanol

After autoclaving add 25% sterile sucrose

50x TAE

2 M	Tris-HCl pH 8.2
1 M	Acetic acid
0.1 M	EDTA

50x SuperBuffer

0.5 M	NaOH
1.82 M	boric acid

0.8 % Agarose Gel

Agarose melted in 1x TAE or 1x SuperBuffer.

Ethidiumbromide bath

10 µg/ml	ethidiumbromide

50x Denhardt's solution

1 g	Ficoll 400
1 g	Polyvinylpyrrolidone
1 g	BSA

filled up with ddH_2O to 100 mL

20X SSC solution

3 M	NaCl
0.3 M	Sodium citrate

pH 7.2, autoclaved

Hybridization buffer:

55 mL	ddH_2O
25 mL	20 x SSC
10 mL	50 x Denhardt´s Solution
5 mL	10 % BSA
5 mL	1 M Na_2HPO_4
500 µL	20 % SDS
200 µL	0,5 M EDTA

Denaturing solution

0.4 M	NaOH
0.6 M	NaCl

Add ddH_2O to final volume, autoclave.

Other Solutions

0.25 M HCl

1.5 M NaCl/ 0.5 M Tris-HCl pH 7.5

0.4 M NaOH

0.2 M Tris-HCl

100 µg/ml Salmon Sperm ssDNA

2x SSC/ 0.1 % SDS

0.1x SSC/ 0.1 % SDS

2.12.2 Protein methods

2x Laemmli buffer:

125 mM	Tris-HCl pH 6.8
4 % (v/v)	SDS
20 % (v/v)	Glycerol
10 % (v/v)	β-Mercapto-Ethanol
0.04 % (w/v)	Bromphenolblue

5 mM Sodiumphosphat buffer

1 M	NaH_2PO_4
1 M	Na_2HPO_4

10x SDS-PAGE running buffer

0.25 M	Tris
1.92 M	Glycine
1 % (w/v)	SDS

4x Stacking gel buffer

0.5 M	Tris-HCl pH 6.8
0.4 % (v/v)	SDS

4x Separating gel buffer

1.5 M	Tris-HCl pH 8.8
0.4 % (v/v)	SDS

30 % AA-Solution (29:1)

29 %	Acrylamide
1 %	N, N ‘-Methylenbisacrylamid

Coomassie staining solution

25 % (v/v)	Methanol
10 % (v/v)	Acetic acid
0.25% (w/v)	Coomassie Brilliant Blue R-250

Coomassie destaining solution

10 % (v/v)	Acetic acid

1x Towbin transfer buffer:

25 mM	Tris
192 mM	Glycine
20 % (v/v)	Methanol

10x TBS

1.37 M	NaCl
27 mM	KCl
0.25 M	Tris-HCl pH 8

Ponceau-S solution

0,5 % (w/v)	Ponceau-S
3 % (v/v)	TCA

Blocking solution

100 ml	1x TBS
5 %	Milk powder

500 mL ECL buffer

13.3 mL	1.5 M Tris-HCl pH 8.5
500 µL	Luminol
250 µL	Coumaric acid

ddH_2O filled up to 500 mL

Membrane Stripping Solution

ROTH ROTI® Free Stripping-Buffer

Coumaric acid solution

0.148 g	Coumaric acid
10 mL	DMSO

Luminol Solution

0.886 g	Luminol
20 mL	DMSO

2.12.3 *N. magadii* and haloalkaliphilic virus methods

Buffered high salt spheroplasting solution

2 M	NaCl
27 mM	KCl
50 mM	Tris-HCl pH 9.5

After autoclaving add 15% sterile sucrose

Unbuffered high salt spheroplasting solution

2 M	NaCl
27 mM	KCl

After autoclaving add 15% sterile sucrose

60 % PEG-600

60 % (v/v)	PEG-600
40 % (v/v)	Unbuffered high salt spheroplasting solution

High salt alkaline solution

4 M	NaCl
50 mM	Tris-HCl pH 9.5

Caesium chloride solution 1.5 (200 mL)

135 g	CsCl
23.4 g	NaCl
50 mM	Tris-HCl pH 9.5

Caesium chloride solution 1.3 (200 mL)

90 g	CsCl
23.4 g	NaCl
50 mM	Tris-HCl pH 9.5

Caesium chloride solution 1.1 (200 mL)

20 g	CsCl
23.4 g	NaCl
50 mM	Tris-HCl pH 9.5

3 Methods

3.1 DNA methods

3.1.1 Polymerase chain reaction (PCR)

For the analytical polymerase chain reactions, the 2x *GoTaq*® Mastermix from Promega was used. As templates diluted isolated DNA or probes of cultures, were used. For *N. magadii* the probes of cultures were prepared by spinning them down for 3 minutes at 13000 rpm and the pellet was resolved in 100 µL ddH_2O. For *E. coli* the cultures were taken directly as template. Primers were delivered in a lyophilized state, upon receiving were resolved in water to a concentration of 1 µg/µL and kept at -20°C for storage. The primers for the PCRs were diluted to a concentration of 0.1 µg/µL. The reaction included:

Component	Final volume
GoTaq® Mastermix (including the *GoTaq*® polymerase, reaction buffer and dNTPs)	12.5µL
Primer 1	1.5 µL
Primer 2	1.5 µL
Template DNA	1 µL
ddH_2O	8.5 µL
Total volume	25 µL

The optimal temperature for the polymerase to work is 72°C, where it can add 1000bp per minute. The settings of the PCR reaction were chosen according to the manufacturer's recommendation:

1. Preheating: 95°C for 5 minutes
2. Denaturation: 95°C for 10 seconds
3. Annealing of the primers: primer-specific temperature for 10 seconds
4. Extension: 72°C for as much time as was needed depending on the fragment length
5. Final extension: 72°C for 5 minutes
6. Ending: 4°C to 16°C until the PCR product was used

The annealing temperature was calculated by subtracting 4°C from the melting temperature of the primer with the lower melting point, which was estimated with the software GeneRunner from Hastings Software Inc. The steps 2 to 4 were repeated for 35 cycles. The PCR product was analysed via agarose gel electrophoresis.

In case an amplified fragment was to be isolated and purified, the Wizard® SV Gel and PCR Clean-Up System protocol from Promega was performed. Changes in these protocols were that the column was dried for 5 minutes at room temperature after the washing step and the elution was done in 25 µL. Afterwards the concentration was measured with the NanoDrop® spectrophotometer for nucleic acids.

3.1.2 Agarose gel electrophoresis

An agarose gel was prepared by melting the calculated amount of agarose in 1x TAE buffer or 1x SuperBuffer. This was poured into an electrophoresis trough with a comb inside. The solid gel was then put into the chamber and the buffer was added until the chamber was filled up. DNA was mixed with 5x or 6x Loading dye or in the case of PCR products, the *GoTaq*® Master Mix contained the loading dye. To separate DNA fragments up to 1500bp a 0.8% agarose gel with 1x Super Buffer was used. In case of fragments bigger than 1500bp 1x TAE Buffer was used. For the 1x TAE agarose gels a voltage between 70 to 150 V were applied. For 1x Super Buffer agarose gels a voltage of 200 V was used. To estimate the fragment size of samples a ladder, the GeneRuler 1kb

plus, was also applied to the gels. The agarose gel was stained in 10 µg/mL ethidium bromide for 10 to 15 minutes and afterwards rinsed in H_2O. Visualization was done with the ChemiDoc XRS+ Imager or in case of isolating fragments using an UV-trans illuminator (366nm).

3.1.3 Restriction

The restriction of DNA was needed for the southern blot analysis and for the restriction enzyme assay. Restriction reactions were performed with isolated DNA of ΦCh1 wildtype or deletion mutants. Therefore, the DNA was mixed with a restriction enzyme, the according 10x buffer and ddH_2O. The mixture was then incubated at 37°C for the time specified by the manufacturer, having a duration of 2 hours to overnight. For the double digest procedures, the ThermoFischer Scientific "DoubleDigest Calculator" was used to get the correct proportions of the enzymes and suitable buffer. Afterwards the restrictions were analysed on an 0.8% or 1.2% agarose TAE gel, by a separation at a low voltage of 60 to 90 V. The unrestricted ΦCh1 wildtype or deletion mutant DNA served as control for the restriction.

3.1.4 Southern blot

The restricted chromosomal DNA of ΦCh1 wild type and mutants was mixed with 5x loading dye and applied onto a 0.8% agarose TAE gel. The gel was run at 60-90 V and afterwards stained with ethidium bromide for 20 minutes. A picture of the gel was made with the ChemiDoc XRS+ imager. The gel was afterwards incubated in 0.25N HCl, then in 0.4N NaOH/ 0.6M NaCl denatured and then neutralized in 1.5M NaCl/0.5M Tris-HCl pH 7.5, each for 30 minutes. A Biodyne B membrane was cut out in the same size as the gel and the sides where the membrane could be cut were marked. A capillary blot was performed overnight to transfer the DNA from the gel onto the membrane, by laying the gel on top of a Whatman paper in a chamber, which is filled with 10x SSC and placing the membrane onto the gel and toping this off with paper towels and weights. The next day the membrane was transferred in 0.4N NaOH for 1 minute and then in 0.2M Tris-HCl pH 7.5 for 1 minute. To fixate the DNA on the membrane UV-crosslinking was performed and then the membrane was stored or directly used for hybridization.

The probes of the 5'- and 3'-end were isolated via 100 µL PCR reaction batch:

Component	Final volume
GoTaq® Mastermix (including the *GoTaq*® polymerase, reaction buffer and dNTPs)	50 µL
Primer 1	10 µL
Primer 2	10 µL
Template DNA	1 µL
ddH_2O	26.5 µL
Biotinylated dUTPs (1:4 in TE buffer)	2.5 µL
Total volume	100 µL

The primers had a concentration of 0.1 µg/µL and the biotinylated dUTPs from Jena Bioscience were diluted 1:4 in TE-buffer (original concentration of Biotin-11-dUTP: 1mM). This was then checked and isolated from a 0.8% agarose SuperBuffer gel.

The membrane with the fixed DNA was prehybridized for three hours at 65°C with 12 ml Hybridization buffer und 120 µl salmon sperm DNA (10 mg/ml). The probes where denatured for 10 minutes at 95°C and then added to the hybridization, which was kept at 65°C with rotation overnight. The 0.1 x SSC/ 0.1 % SDS solution was put at 65°C overnight. The next day the membrane was washed twice for 5 minutes at room temperature with 2 x SSC/ 0.1 % SDS and then washed twice for 15 minutes at 65°C with 0.1 x SSC/ 0.1 % SDS.

The detection of the nucleic acids was performed with the Chemiluminescent Nucleic Acid Detection Module from ThermoFischer Scientific and the steps of the belonging protocol were followed with adjusted volumes to the size of the membrane. The exposure of the membrane was then performed with the ChemiDoc XRS+ imager and 20 pictures were taken in 180 seconds with the Chemiluminescence High Sensitivity settings, where the intensity increased over time.

3.2 Protein methods

3.2.1 Crude extract protein probes

Protein samples were taken from *N. magadii* cultures to estimate certain protein concentrations over a period of 7 or 10 days. Therefore, the optical density (600) of a culture was measured and 1.5 mL of the culture was spun down for 3 minutes at 13 krpm. One millilitre supernatant from the first spin was used for viral titer analysis and kept with 20 µL chloroform at room temperature, the remaining supernatant was discarded. The chloroform was added to inhibit the growth in the samples. Afterwards, y µL 5 mM sodium-phosphate-buffer were added to the pellet and the pellet was scrap from the Eppendorf tube's surface.

$$\boldsymbol{y = 75 \times OD_{600}}$$

Then y µL 2x Laemmli-Buffer were added and the probe was incubated at 37°C overnight to break down the chromosomal DNA. Depending on the optical density, the step of spinning down 1.5 mL of culture was repeated until the overall volume of the protein probes reached 100 or 150 µL in total. The next day the probes were frozen at -20°C until usage or directly used. Before, applying the protein probes on a SDS gel, they were denatured for 10-15 minutes at 95°C.

3.2.2 SDS-PAGE

The SDS-Polyacrylamide gel electrophoresis was used to separate protein probes of *N. magadii* depending on their molecular weight. The BioRad Mini Protean apparatus

with 0.75mm spacers was used for the preparation of the discontinuous SDS gels. When preparing the gels on ice, APS and TEMED were added last, to start the polymerization reaction. First the 12% separating gel was poured into the gel apparatus, isopropanol was used to overlay the gel, and it took approximately 20 minutes for the separating gel to polymerize. Then the isopropanol was removed, and the 4% stacking gel was poured on top of the separating gel. The amounts of the components for one gel are depicted below:

Component	**Separating gel (12%)**	**Stacking gel (4%)**
Acrylamide solution	2 mL	267 µL
Separating gel buffer	1.25 mL	-
Stacking gel buffer	-	0.5 mL
ddH_2O	1.75 mL	1.233 mL
APS (10%)	60 µL	20 µL
TEMED	10 µL	5 µL

The comb was inserted into the gel and the gel took approximately 20 minutes to polymerize. Depending on the number of samples, combes with 10 or 15 lanes were used. SDS gels were prepared on the day they were used or one to two days before. If the gel was not used immediately, it was wrapped up in paper towels, which were soaked in water, and then put into a plastic bag, which was stored at 4°C.

The SDS gels were run in chambers with 1x SDS-PAGE running buffer, after the protein samples and the protein ladder were loaded. Because of the high salt concentrations found in the protein extracts the gels were run hat 40 V until the bromophenol blue reaches the end of the gels.

3.2.3 Coomassie staining

The SDS gels were stained with a Coomassie solution for 5 minutes with agnation. Afterwards the destaining solution was added to the gel overnight with agitation. The gel was destained until the background was no longer blue and sharp bands could be seen. Then the gel was transferred into water and pictures with the ChemiDoc XRS+ imager was made.

3.2.4 Western Blot

To analyse the gene expression patterns of selected ORFs, western blots were used. The gel was therefore placed on three pieces 3MM Whatman-Filter paper and an Amersham™ Protran® 0.2 µm nitrocellulose membrane (6.5 x 9 cm) membrane, which were both equilibrated in 1x Towbin transfer buffer. Finally, three Whatman-Filter paper pieces were dipped into transfer buffer and put on top of the gel. The blots performed at 83 V for 30 minutes for 4 gels. Afterwards the membrane was stained with Ponceau S solution for two minutes to make the bands visible. The standard proteins were marked, and the membrane washed with water until it was completely destained.

The primary antibody solution included the antibody serum, 1x TBS, 0.3% BSA, 0.02% NaN_3 and a spatula of acetone powder from *N. magadii* L13. This was stirred overnight at 4°C and was stored at 4°C. The antibody solution was diluted to the desired concentration.

The membrane was blocked overnight at 4°C with agnation in 5% milk powder in 1x TBS. The following day the blot was washed three times with 100 mL TBS. 10 mL of the primary antibody were poured onto the membrane and incubated for one hour at room temperature with agnation. The primary antibodies were recycled and could be used several times. The membrane was washed three times in 100 mL 1x TBS for each 10 minutes. The secondary antibody was freshly prepared for the reaction by making a 1:5000 dilution of α-Anti-Rabbit coupled with Horseradish peroxidase in 1x TBS, and 10 mL were added to the membrane. The secondary antibody reaction was incubated for one hour at room temperature with agnation. The membrane was again washed three times in

100 mL 1x TBS for 10 minutes. Then 3 mL of ECL were mixed with 3 µL H_2O_2 and this was poured on top of the membrane and left for one minute. The membrane was put on the ChemiDoc XRS+ imager and pictures were taken with the Chemiluminescence High Sensitivity settings, where in 180 seconds 20 pictures were taken, with increasing intensity. A picture of the ladder was made with the colorimetric settings.

Each lane of the blot was analysed with the Image Lab Software from Bio Rad concerning the adjusted total lane volume, which corresponds to the total amount of signals for all the pixels within a band, where the background is take into account. The sample value was then divided by the value of the positive control to get a relative value, which could then be compared.

3.2.5 Western blot membrane stripping

If the same membrane was to be used for another antibody, after the developing, the antibodies were stripped of the membrane. After developing with ECL and H_2O_2 and taking pictures of the western blot membrane, two washing steps with 1x TBS for 5 minutes were performed. Then 10 mL ROTI® Free Stripping Buffer (Roth) were added to the membrane and incubation was done for 30 minutes at 37°C with agnation. Afterwards the membrane was washed three times with 1x TBS for 10 minutes each. The re-blocking of the membrane was then performed overnight with blocking solution.

3.3 *N. magadii* Methods

3.3.1 Preparation of competent *N. magadii* cells

The preparation of competent *N. magadii* L13 cells was accomplished by inoculating three flasks with 50 mL NVM^+ CAA with 70 µg/ml bacitracin with different amounts of preculture *N. magadii* L13 (2, 4 and 6 mL). The cultures were kept at 37°C shaking until one of them reached an OD_{600} of 0.55 - 0.6. The cells then were harvested by centrifugation at 6 krpm for 15 minutes and resuspended in half the volume of the original culture in HS buffered spheroplasting solution. To this Proteinase K was added

to a final concentration of 20 µg/ml and the mixture was incubated at 42°C with agnation for approximately 48 hours until the cells lost their S-layer. This was observed by looking at the cells under the standard Nikon light microscope with 1000x magnification and seeing spheroplasts. The cells could be kept at room temperature for around one week.

3.3.2 Transformation of *N. magadii*

From the competent *N. magadii* L13 cells two times 1.5 mL were taken and centrifuged at 10 krpm for three minutes. The supernatant was discarded, and the cells resuspended in 150 µl HS buffered spheroplasting solution per transformation batch. Then an incubation of 10 minutes on room temperature was done, afterwards the plasmid was added (maximal 3 µg and 10 µL) and incubated for five minutes at room temperature. Then 150 µL 60% PEG-600 in HS unbuffered spheroplasting solution was added and incubated for 30 minutes on room temperature. One millilitre of NVM^+ CAA was carefully added and this was then centrifuged for three minutes at room temperature at 10 krpm. The pellet was resuspended in 1 mL NVM^+ CAA and this was transferred into a falcon tube, where another millilitre of NVM^+ CAA was added. The cells regenerated at 37°C with agnation for approximately two days, until the cells showed their rod shape. Then 100 µL of the cells were plated onto NVM^+ CAA plates with antibiotics, three times undiluted, three times 1:10 diluted and three times 1:100 diluted. The plates were sealed in plastic bags and incubated at 42°C until colonies formed. These single colonies were then inoculated in 500 µl NVM^+ CAA with antibiotics and incubated at 37°C with agitation. Following this an analytical PCR was performed to ensure the plasmid was in the cells.

3.3.3 *N. magadii* glycine cultures

To make stocks of cultures and freeze them at -80°C, 1 mL of the culture was put in a cryotube and mixed thoroughly with 800 µL glycine with 4M NaCl.

3.4 Haloalkaliphilic virus methods

3.4.1 Isolation of virus particles

To isolate virus particles 4.5 L NVM^+ CH were inoculated with 20-30 mL culture of *N. magadii* L11 wildtype or deletion mutant and kept at 37°C with agnation until the OD_{600} of the cultures was not going down anymore, showing that lysis was not occurring any longer. Afterwards the cells were collected by centrifugation for 20 minutes at 6 krpm at room temperature and the supernatant was collected. The supernatant was then mixed with 10% w/v PEG-6000 overnight at room temperature, thereby the virus precipitate. The cultures were again spun down and the pellet containing the virus, was resuspended in 7.5 mL 4M NaCl / 50 mM Tris-HCl (pH 9.5) overnight.

The virus particles were purified via a discontinuous CsCl gradient in Beckmann-centrifugation tubes, therefore 3.5 mL 1.5 solution, then 4 mL 1.3 solution, then 5 mL virus suspension and at last 1.1 solution to balance out the tubes, were put carefully into the tubes. These were centrifuged for around 20 hours at 30 krpm at room temperature with a SW40Ti swing-bucket rotor. After the centrifugation a light blue band, containing the virus particles, between the 1.5 solution and 1.3 solution was seen. This band was isolated and centrifuged with a continuous gradient with 1.3 solution. Therefore, the band and the 1.3 solution were mixed and centrifuged with the same settings as with the discontinuous gradient. After the centrifugation a light blue band was isolated and dialysed against 4M NaCl / 50mM Tris-HCl (pH 9.5) for 1 hour. The solution 4M NaCl / 50mM Tris-HCl (pH 9.5) was then exchanged for a fresh solution and dialysed overnight. The virus particles then were kept at room temperature and used for virus DNA isolation or infection of L13 via soft agar.

3.4.2 Virus DNA isolation (Phenol/Chloroform extraction)

100 µl of the virus particles after dialysis or after continuous gradient were mixed with 400 µl ddH_2O. The solution was extracted by adding 250 µl phenol and 250 µl chloroform by vortexing/shaking and centrifuging for 2 minutes at 13 krpm. The upper aqueous phase was transferred into new tube. This step was repeated 2-3 times, until no

white interface was seen. The solution then was extracted again with 500 µl chloroform twice to ensure no phenol residues were left. The aqueous phase was then precipitated with the same volume of isopropanol by centrifugation for 30 minutes at 13 krpm at 4°C. The supernatant was discarded, and the pellet washed once with 70% ethanol. The pellet was dried at 65°C for 10 minutes. Then the pellet was resolved in ddH_2O, and the DNA stored at -20°C.

3.4.3 Virus titer analysis: plaque assay

Either to determine the virus titer of a ΦCh1 variant or to generate new *N. magadii* L11 variant cultures, a plaque assay was performed. Therefore, *N. magadii* L11 variant cultures were grown in NVM^+ CAA at 37°C with agitation until they reached exponential growth and the ΦCh1 variant virus particles were harvested and used for the assay. For the determination of the virus titer of the time series the supernatant of a lysing culture was used. $CHCl_3$ was added to the supernatant, to stop growth.

To determine the viral titer, the concentration of infectious ΦCh1 variant particles in the suspension was calculated by soft agar technique. A dilution series was made from virus particles (dilutions: 10^{-2}, 10^{-4}, 10^{-6}, 10^{-8} in NVM^+ CAA). 100 µl of the dilutions were mixed with 300-500 µl (depending on growth state of cells) of growing *N. magadii* L13 cells and 5 ml soft agar, in preheated to 55°C glass tubes. The mixture was vortexed and poured on non-selective NVM^+ CH agar plates. The plates were dried overnight at room temperature. Then the plates were incubated at 37°C for 2 weeks in sealed plastic bags. The viral titer was determined by counting the plaques on the plates and calculating the plaque forming units per mL (PFU/mL).

$$\boldsymbol{PFU/mL = \frac{average\ number\ of\ plaques}{(dilution * 0,1)}}$$

The plaques from the plates were picked, inoculated in NVM^+ CAA and grown at 37°C with agitation for further analysis.

3.5 *E. coli* methods

3.5.1 Plasmid isolation

E. coli cells were used to isolate plasmid DNA, which was then used to transform into *N. magadii* L13. Therefor frozen cells, which contained the plasmid and were stored at -80°C, were inoculated in 15 mL LB with antibiotics. This was then kept overnight at 37°C with agnation and the plasmid was then isolated from this culture the next day with the Quick protocol Wizard® Plus SV Minipreps DNA Purification System by Promega with some deviations. Therefore, 1.5 mL of the culture was taken twice and spun down for 3 minutes at 13 krpm, then the cells were resuspended in 250 µL of Cell Resuspension Solution. The following steps were done according to the protocol, except that after the last washing step the column was dried for 5 minutes on room temperature and the cells were eluted in 30 µL of ddH_2O and this was then added to the column again and spun down again. Then the concentration of the nucleic acids was measured with the NanoDrop® spectrophotometer.

4 Results and Discussion

4.1 ORF94

4.1.1 Aim

Previous studies have performed a deletion of the ORF94 which was done by replacing it with the novobiocin resistance cassette in reverse by homologous recombination using the plasmid pKS_{II}^{+}. In this study the aim was to verify the deletion of the ORF94 and analyse the effects on the growth, viral titer and specific proteins. The deletion was verified via PCR of the methyltransferase gene and via a southern blot. Then the growth curve and infectious viral particles of the deletion strain were compared to the growth curve and infectious viral particles of the wild type. The proteins E, methyltransferase and gp34 were analysed via western blots and compared between the wild type strain and the deletion strain. Further, the complementation of the deletion strain was performed and the growth, viral titer and the same proteins as above were analysed. The loss of the methylating function of the methyltransferase was verified in the deletion strain and shown to be at least partially recovered in the complementation strain via a restriction analysis. The methylation pattern was further investigated with additional restriction tests.

4.1.2 Verification of the deletion and incorporation of the novobiocin resistance cassette

4.1.2.1 Qualitative assessment of methyltransferase gene

Single plaques of *N. magadii* L11-ΔORF94 novR-R were inoculated and a test PCR was performed to confirm the deletion of the ORF94. The primers 5mt-1ba and Mt-Xba-3 bind on the 3'- and 5'-end of the ORF94 and create a 1280bp long fragment in the wild type *N. magadii* L11 via PCR. The Figure 7 shows that that all 8 clones lack the fragment, which indicates that the deletion of ORF94 was successful. The first two clones were used for further experiments and inoculated in bigger flasks. To verify the homozygous deletion a southern blot was performed.

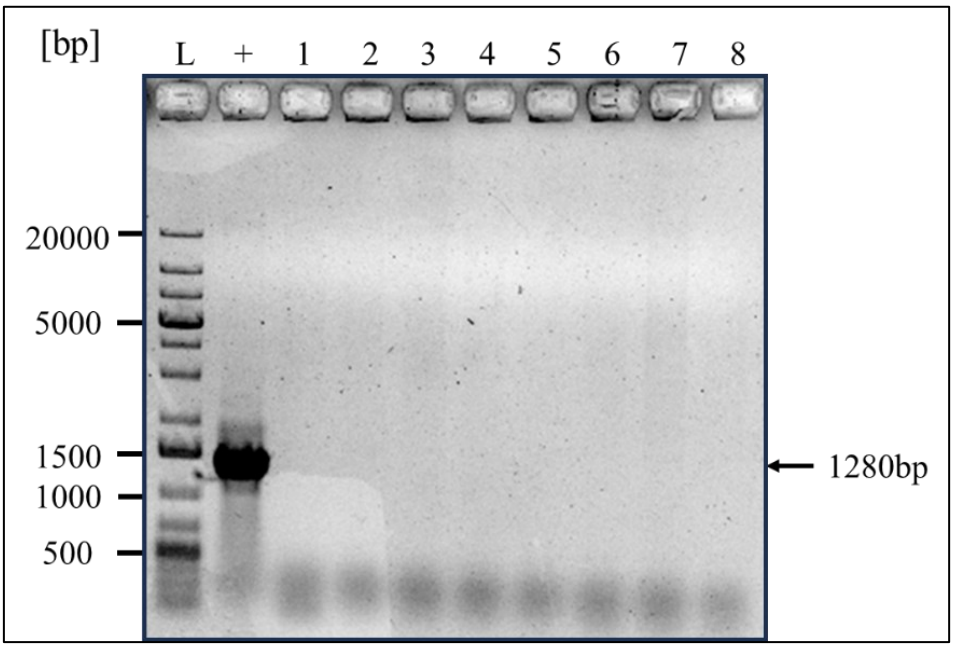

Figure 7. Agarose gel electrophoresis of ΦCh1-ΔORF94 novR-R from *N. magadii* for the ORF94. To test for the methyltransferase gene, a PCR with the primers 5mt-1ba and Mt-Xba-3 was performed on the ΦCh1-ΔORF94 novR-R DNA of eight clones (Lanes 1-8). The PCR products were separated on a 0.8% agarose gel. As a positive control ΦCh1 DNA from *N. magadii* L11 was used (Lane +). The ThermoFischer Scientific 1-kb plus DNA ladder (Lane L) was used as size control. The size of the fragment amplified by the PCR is indicated with an arrow on the right side (1280bp).

4.1.2.2 Confirmation of the homozygous deletion of the ORF94 via southern blot

The genome of ΦCh1 has several restriction sites for different restriction enzymes. This fact is used when performing a southern blot analysis. Here the enzymes *Nru*I and *Bam*HI were used to create specific restriction fragments. For the ΦCh1-ΔORF94 novR-R genome a different restriction site pattern is expected with the enzymes *Nru*I and *Bam*HI than in the wild type genome. For both strains the resulting fragment sizes were calculated with the SnapGene software, the fragments of interest were the ones differing in the deletion strain. To visualize these fragments, biotinylated probes were used, which cover overlapping regions at the 5‘- and 3‘-end. The southern blot designs for both restriction enzymes and for the 5’- and 3’-end respectively, can be seen in Figure 8 and Figure 9.

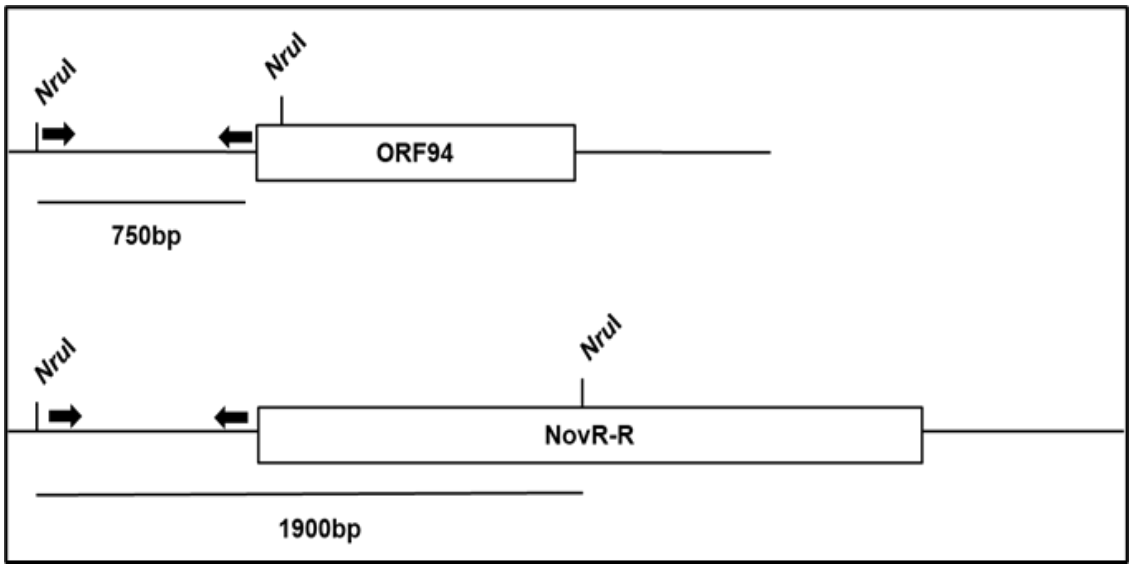

Figure 8. Schematic depiction of the fragment lengths after restriction and hybridization patterns of the southern blot of ΦCh1 and ΦCh1-ΔORF94 novR-R at the 5’-end. Parts of the genome of ΦCh1 and ΦCh1-ΔORF94 novR-R are depicted. After restriction of the ΦCh1 DNA of *N. magadii* L11 and of *N. magadii* L11-ΔORF94 novR-R with *Nru*I, fragments of the sizes 750bp for the ΦCh1 DNA and 1900bp for ΦCh1-ΔORF94 novR-R DNA can be found. The biotinylated probe, made with a PCR from the ΦCh1 DNA of *N. magadii* L11 with the primers 94-1-probe and 94-2-probe, binds between the shown arrows (→ ←) upstream of the target region. This fragment has a length of 600bp.

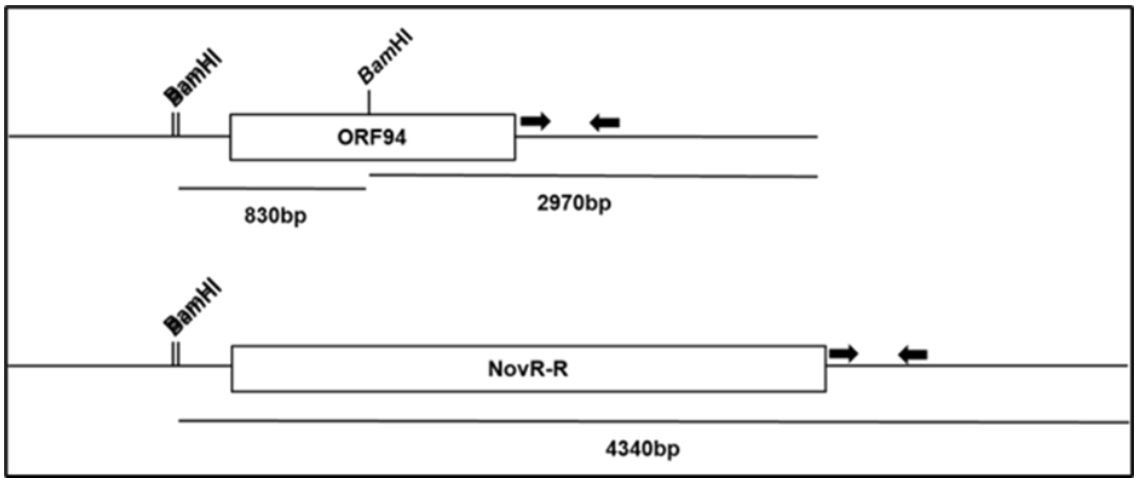

Figure 9. Schematic depiction of the fragment lengths after restriction and hybridization patterns of the southern blot of ΦCh1 and ΦCh1-ΔORF94 novR-R at the 3'-end. Parts of the genome of ΦCh1 and ΦCh1-ΔORF94 novR-R are depicted. After restriction of the ΦCh1 DNA of *N. magadii* L11 and of *N. magadii* L11-ΔORF94 novR-R with *Bam*HI, fragments of the sizes 830bp and 2970bp for the ΦCh1 DNA and 4340bp for ΦCh1-ΔORF94 novR-R DNA can be found. The biotinylated probe, made with a PCR from the ΦCh1 DNA of *N. magadii* L11 with the primers 95-Bam and 95-Hind, binds between the shown arrows (→ ←) downstream of the target region. This fragment has a length of 530 bp. For the ΦCh1 DNA of *N. magadii* L11 the probe binds the 2970bp fragment.

For the southern blot purified genomic DNA of ΦCh1 and ΦCh1-ΔORF94 novR-R were needed, so cultures of the wild type *N. magadii* L11 and *N. magadii* L11-ΔORF94 novR-R clone 1 were inoculated. These were used to isolate the chromosomal DNA and purify it with a CsCl gradient. Then the DNAs from *N. magadii* L11-ΔORF94 novR-R and *N. magadii* L11 were restricted with the enzymes *Nru*I and *Bam*HI. The digested DNA was loaded onto a 0.8% agarose gel (Figure 10 A/C) and from there transferred to a nylon membrane via capillary blot overnight.

A PCR was used to prepere the biotinylated probes for the 5'- and 3'-end analysis. Therefore, the wild type DNA was used as the template and biotinylated dUTPs were added to the reaction. The primers 94-1-probe and 94-2-probe were used to create the 5'-end probe with a length of 600bp. For the 3'-end probe the primers 95-Bam and 95-Hind were used, which resulted in a 537bp long fragment.

The probes were then hybridized to the DNA on the membrane. For the 5'-end the DNA restricted with *Nru*I was used and for the 3'-end the restriction with *Bam*HI was used. This resulted for the analysis of the 5'-end in a visualized fragment of 750bp for the ΦCh1 DNA and 1900bp for ΦCh1-ΔORF94 novR-R DNA (Figure 10 B). For the 3'-end

the fragment size for the ΦCh1 DNA was 2970bp and for the ΦCh1-ΔORF94 novR-R DNA was 4340bp (Figure 10 D).

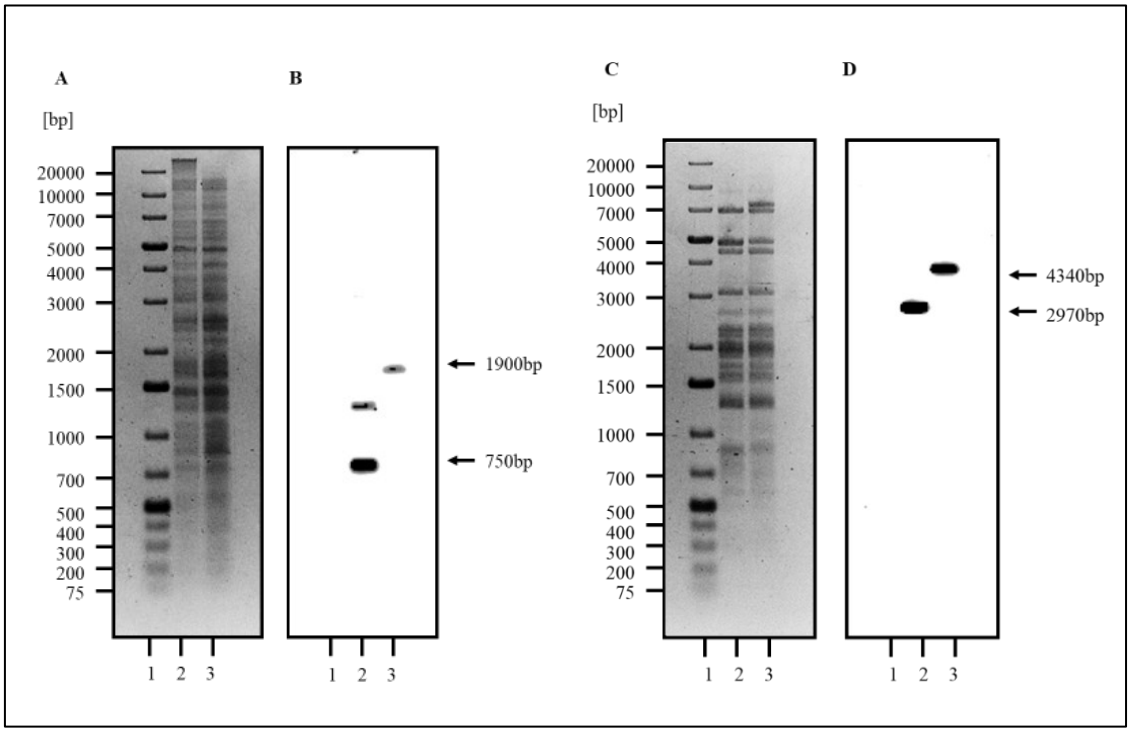

Figure 10. Southern blot analysis of ΦCh1 and ΦCh1-ΔORF94 novR-R at the 5'-end and 3'-end.
A. Restriction pattern on a 0.8% agarose gel of ΦCh1 (Lane 2) and ΦCh1-ΔORF94 novR-R (Lane 3) with the restriction enzyme *Nru*I. The ThermoFischer Scientific 1-kb plus DNA ladder (Lane 1) was used as size control.
B. Southern blot hybridization pattern of the 5'-end of ΦCh1 (Lane 2) and ΦCh1-ΔORF94 novR-R (Lane 3) with the biotinylated probe, made with a PCR from the ΦCh1 DNA of *N. magadii* L11 with the primers 94-1-probe and 94-2-probe. The size of the expected signals for ΦCh1 (750bp) and ΦCh1-ΔORF94 novR-R (1900bp) are indicated with an arrow on the right side. The ThermoFischer Scientific 1-kb plus DNA ladder (Lane 1) was used.
C. Restriction pattern on a 0.8% agarose gel of ΦCh1 (Lane 2) and ΦCh1-ΔORF94 novR-R (Lane 3) with the restriction enzyme *Bam*HI. The ThermoFischer Scientific 1-kb plus DNA ladder (Lane 1) was used as size control.
D. Southern blot hybridization pattern of the 3'-end of ΦCh1 (Lane 2) and ΦCh1-ΔORF94 novR-R (Lane 3) with the biotinylated probe, made with a PCR from the ΦCh1 DNA of *N. magadii* L11 with the primers 95-Bam and 95-Hind. The size of the expected signals for ΦCh1 (2970bp) and ΦCh1-ΔORF94 novR-R (4340bp) are indicated with an arrow on the right side. The ThermoFischer Scientific 1-kb plus DNA ladder (Lane 1) was used.

In the wild type restriction with *Nru*I an additional fragment can be seen, this could be due to a partial digestion of the DNA. The southern blot showed that the novobiocin resistance cassette was correctly incorporated and the ORF94 replaced. After

this conformation the deletion mutant was analysed concerning the effects of the deletion on the growth, viral titer and specific protein production.

4.1.3 Time course analysis of the deletion strain compared to the wild type

After showing that the deletion was done successfully, the influence of the deletion on *N. magadii* L11 was analysed. Cultures from *N. magadii* L11 and from *N. magadii* L11-ΔORF94 novR-R were grown for ten days in NVM^+ CAA media, were the media for the mutant included novobiocin. Over the course of these ten days the optical density (OD_{600}) was measured, and samples were taken every day of the proteins and the titer. These samples were then analysed concerning the growth behaviour, the lysis, the infectious virus particles and the gene expression of selected ORFs.

4.1.3.1 Growth kinetics and lysis behaviour of the deletion mutant

The optical density was measured of the cultures from the wild type and the deletion mutant for ten days (Figure 11).

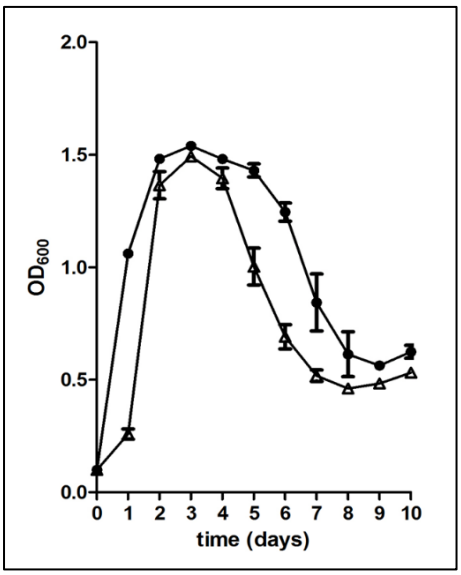

Figure 11. Growth kinetics analysis of *N. magadii* L11 and of *N. magadii* L11-ΔORF94 novR-R. *N. magadii* L11 was grown in NVM^+ CAA media for ten days and *N. magadii* L11-ΔORF94 novR-R was grown in NVM^+ CAA with novobiocin media for ten days. The optical densities of *N. magadii* L11 (●) and *N. magadii* L11-ΔORF94 novR-R (△) were measured at 600nm for every day. Error bars (±1SD) are indicated.

For the *N. magadii* L11 the growth from the inoculation to the first day showed a strong incline. The peak of cell density was on day three, which was followed by the beginning of lysis on the fourth day. The first stronger decline can be observed from days three to four. The strongest decrease in the optical density was from day six to seven. The *N. magadii* L11-ΔORF94 novR-R mutant started with a low optical density on the day after inoculation. The peak of the growth was on day three and was followed by the first stronger decline till day four, which indicated the lysis start. The strongest decrease of cell density was from day four until day five.

Comparing the growth kinetics of the wild type and the deletion strain, it can overall be observed that the mutant grew at a lower density. The mutant showed a lower cell density on the first day after inoculation. The peaks of both strains where at the same time point and followed by a stronger decrease in optical density. In general, the lysis of the mutant strain was more pronounced than for the wild type strain.

4.1.3.2 Plating efficiency and viral titer analysis

A plaque assay was used to quantify the actively infectious viral particles. Therefore, the titer samples of the time series were used to infect *N. magadii* L13 by soft agar plaque assay and from these resulting plates the plaque forming units (PFU) were calculated. The plating efficiency of the viral titer from *N. magadii* L11 and of *N. magadii* L11-ΔORF94 novR-R are depicted in Figure 12.

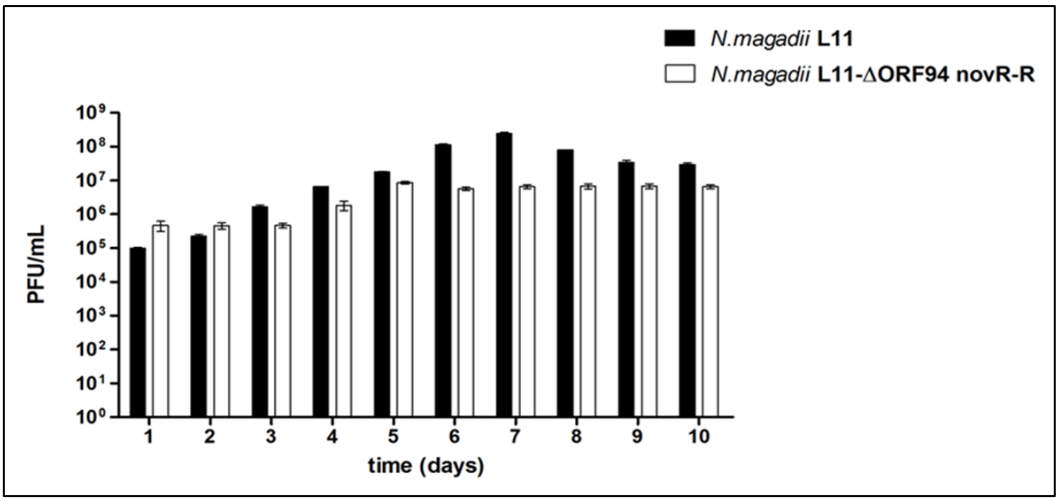

Figure 12. Plating efficiency and viral titer of *N. magadii* L11 and of *N. magadii* L11-ΔORF94 novR-R. *N. magadii* L11 was grown in NVM$^+$ CAA media for ten days and *N. magadii* L11-ΔORF94 novR-R was grown in NVM$^+$ CAA with novobiocin media for ten days. Every day the supernatant of *N. magadii* L11 (black bars) and *N. magadii* L11-ΔORF94 novR-R (white bars) was collected and used to infect the cured strain *N. magadii* L13, to estimate the viral titer. Error bars (±1SD) are indicated.

The viral titer of *N. magadii* L11 ranged from 10^5 to 10^8 PFU/ mL, with the lowest viral load on the first day and the highest on the seventh day. From day one until day seven the viral load increased every day. After the peak the viral titer slowly declined until the tenth day down one power of ten. The PFU/mL of the titer from *N. magadii* L11-ΔORF94 novR-R stayed the same at around 10^5 until the fourth day, from this day on the viral titer increased a power of ten and reached its peak on day five. The viral load did not change significantly from the days six to ten.

The PFU/mL of the deletion mutant did not increase as strong as the wild type and showed lower values from day three on. The plating efficiency of the deletion strain was lower than of the wild type strain, which means that the deletion has a negative impact on the quantity of the actively infectious viral particles.

4.1.3.3 Western Blot analysis of *N. magadii* L11-ΔORF94 novR-R

The whole protein-extract samples, which were taken every day from the time course of *N. magadii* L11 and of *N. magadii* L11-ΔORF94 novR-R, were used to analyse the gene expression of the methyltransferase, the major capsid protein E and the tail fiber protein gp34. The samples and controls were loaded onto SDS gels and western blots were performed. These could then be analysed and compared concerning the protein concentrations at each time point.

Methyltransferase

The adenine methyltransferase was shown to be detectable from day three on in the wild type strain, which is one day before the lysis occurs, since the viral proteins are synthesised shortly before the release. From there on the concentration increased until day six and then decreased the following four days. The western blot analysis of the deletion strain provided further assurance that the methyltransferase gene was deleted, since no gene product was detected (Figure 13).

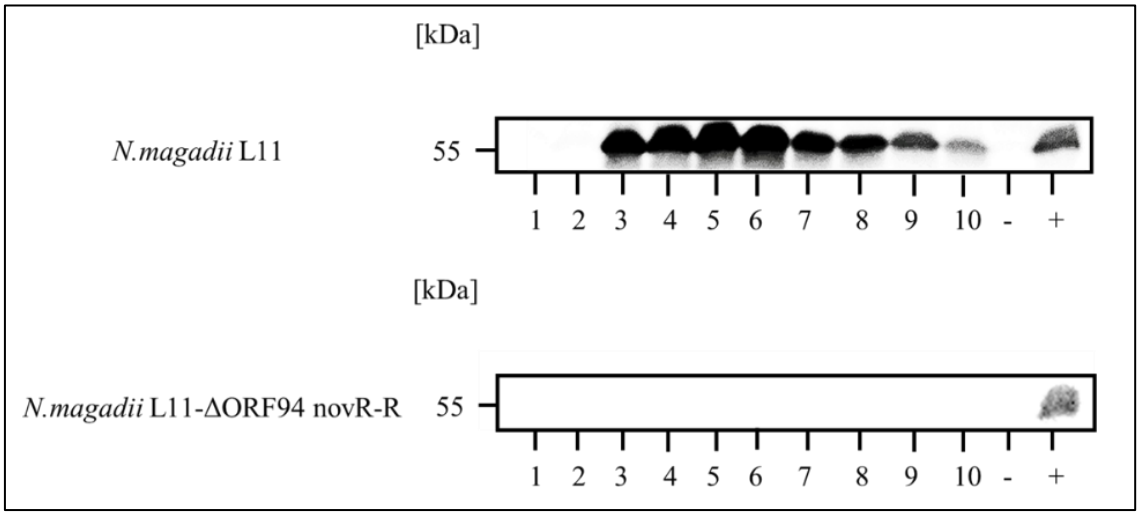

Figure 13. Western blot of *N. magadii* L11 and of *N. magadii* L11-ΔORF94 novR-R time series samples with antibodies against the methyltransferase. *N. magadii* L11 was grown in NVM^+ CAA media for ten days and *N. magadii* L11-ΔORF94 novR-R was grown in NVM^+ CAA with novobiocin media for ten days. Every day whole protein-extract samples of *N. magadii* L11 (top panel; Lanes 1-10) and *N. magadii* L11-ΔORF94 novR-R (bottom panel; Lanes 1-10) were collected and used for western blot analysis. As positive and negative control the whole protein-extract of *N. magadii* L11 (+) and *N. magadii* L13 (-), respectively, were used. For the detection of the methyltransferase the α - methyltransferase antibody was used, and the protein has a size of 46 kDa, calculated from the sequence. Due to the low pI, the protein migrates app at a size of 60kDa.

protein E

The major capsid protein E is produced on day three, one day before the lysis starts in *N. magadii* L11. The protein concentration increased until day six and then declined over the following days, so that it was barely or not detectable on the last days. The protein E production in *N. magadii* L11-ΔORF94 novR-R was visible from the third day on, which is also one day before lysis started. From that day on the concentration increased till day six, and then did not recede but stayed strongly detectable. Comparing the mutant to the wild type strain, the protein E stayed detectable longer and stronger than in the wild type. From the fourth day on the mutant had a significantly higher protein concentration. (Figure 14 and Figure 15)

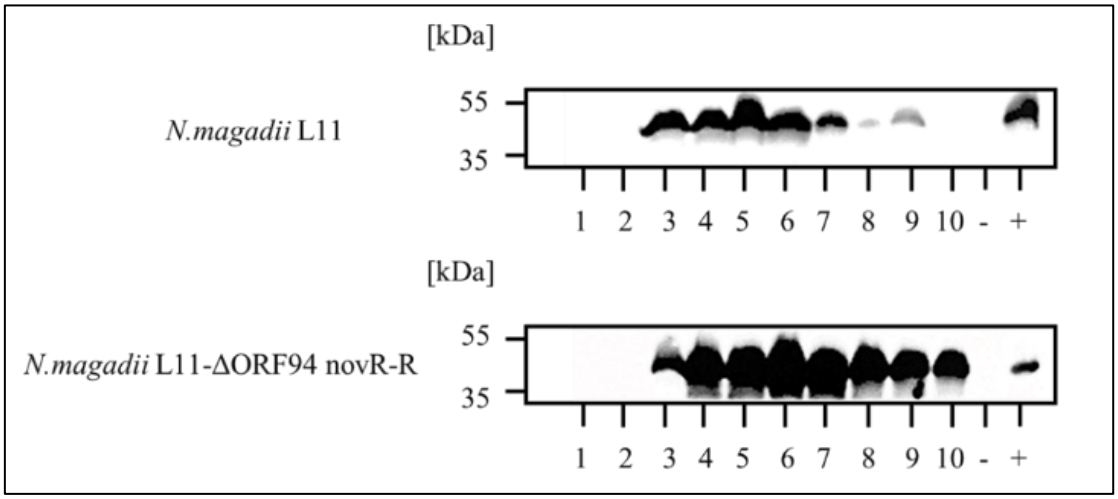

Figure 14. Western blot of *N. magadii* L11 and of *N. magadii* L11-ΔORF94 novR-R time series samples with antibodies against the major capsid protein E. *N. magadii* L11 was grown in NVM$^+$ CAA media for ten days and *N. magadii* L11-ΔORF94 novR-R was grown in NVM$^+$ CAA with novobiocin media for ten days. Every day whole protein-extract samples of *N. magadii* L11 (top panel; Lanes 1-10) and *N. magadii* L11-ΔORF94 novR-R (bottom panel; Lanes 1-10) were collected and used for western blot analysis. As positive and negative control the whole protein-extract of *N. magadii* L11 (+) and *N. magadii* L13 (-), respectively, were used. For the detection of the protein E the α-protein E antibody was used, and the protein has a size of 50 kDa.

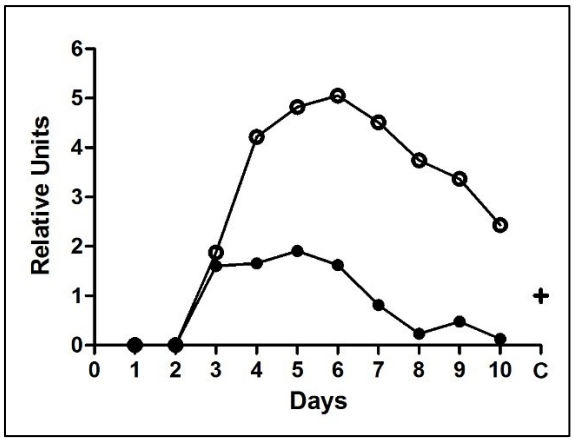

Figure 15. Relative protein levels of *N. magadii* L11 and of *N. magadii* L11-ΔORF94 novR-R with antibodies against the major capsid protein E. Every day whole protein-extract samples of *N. magadii* L11 (●) and *N. magadii* L11-ΔORF94 novR-R (o) were collected and used for western blot analysis. As positive control the whole protein-extract of *N. magadii* L11 (+, C) was used. The relative values were calculated in respect to the positive control. For the western blot detection of the protein E the α-protein E antibody was used. The analysis was performed with Image Lab Software from Bio Rad.

The difference in concentration of the protein E was further investigated, by comparing the samples from the fifth day next to each other (Figure 16). This provided further evidence that the concentration of the protein E in the deletion mutant showed an approximately 2.2-fold increase in amount compared to the wild type, while the Coomassie gel showed that the wild type and deletion samples had the same total amount in the lanes (Figure 17).

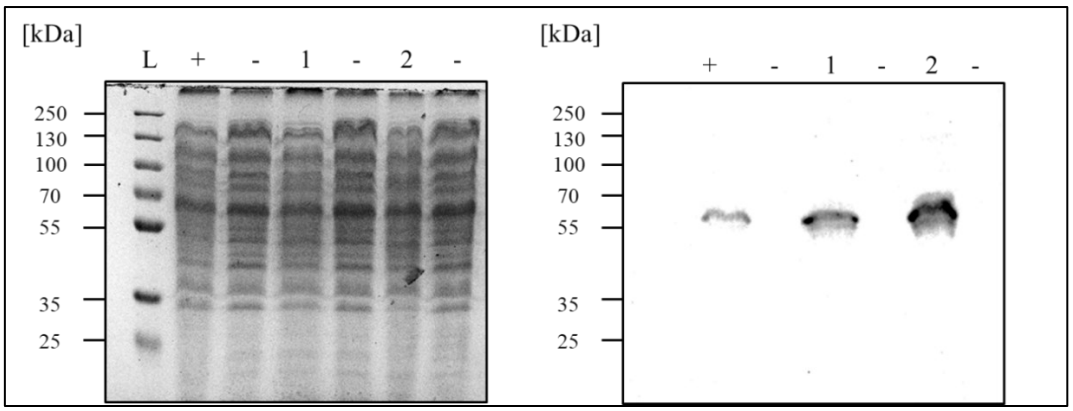

Figure 16. Coomassie gel (left) and western blot (right) of probes from *N. magadii* L11 and of *N. magadii* L11-ΔORF94 novR-R time series samples with antibodies against the protein E. *N. magadii* L11 was grown in NVM^+ CAA media for ten days and *N. magadii* L11-ΔORF94 novR-R was grown in NVM^+ CAA with novobiocin media for ten days. Every day whole protein-extract samples of *N. magadii* L11 and *N. magadii* L11-ΔORF94 novR-R were collected. In the lane labelled 1 is the probe of *N. magadii* L11 day 5 and in lane labelled 2 the probe of *N. magadii* L11-ΔORF94 novR-R day 5. As positive and negative control the whole protein-extract of *N. magadii* L11 (+) and *N. magadii* L13 (-), respectively, were used. For the western blot detection of protein E the α- protein E antibody was used and the protein has a size of 50 kDa.

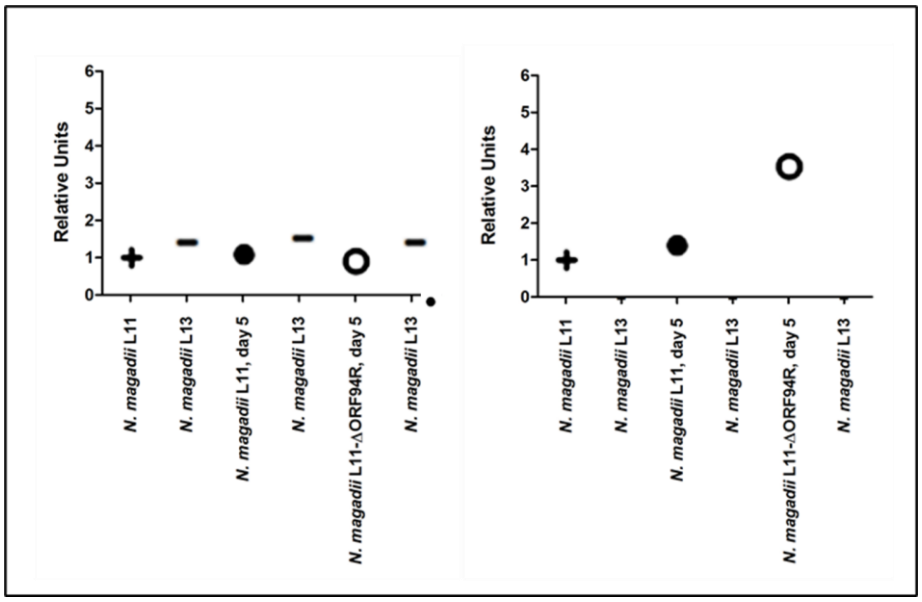

Figure 17. Relative protein levels in the Coomassie gel (left) and western blot (right) of *N. magadii* L11 and of *N. magadii* L11-ΔORF94 novR-R with antibodies against the major capsid protein E. Every day whole protein-extract samples of *N. magadii* L11 and *N. magadii* L11-ΔORF94 novR-R were collected and used for western blot analysis. For this analysis the probe of *N. magadii* L11 day 5 (●) and the probe of *N. magadii* L11-ΔORF94 novR-R day 5 (o) were used. As positive and negative control the whole protein-extract of *N. magadii* L11 (+) and *N. magadii* L13 (-), respectively, were used. The relative values were calculated in respect to the positive control. For the western blot detection of the protein E the α-protein E antibody was used. The strains are shown in the order as depicted on the picture in Figure 16. The analysis was performed with Image Lab Software from Bio Rad.

gp34

The viral tail fiber protein gp34 was produced since day three, the day before the lysis started, in *N. magadii* L11. Then the concentration of the protein increased until day six, and from there on decreased until it was only lightly detectable on day ten. The protein was produced also from day three on in *N. magadii* L11-ΔORF94 novR-R, but then did not decrease significantly but stayed strongly detectable till day ten. In comparison did the mutant strain show an approximately 1.5-fold higher concentration of gp34 over the time course than the wild type and was longer stronger detectable in the cell (Figure 18 and Figure 19).

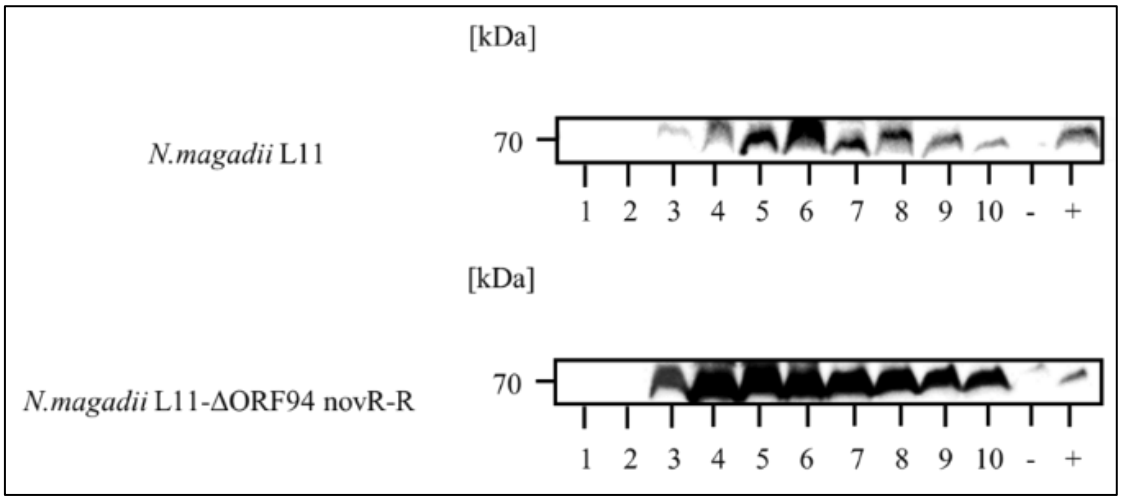

Figure 18. Western blot of *N. magadii* L11 and of *N. magadii* L11-ΔORF94 novR-R time series samples with antibodies against gp34. *N. magadii* L11 was grown in NVM^+ CAA media for ten days and *N. magadii* L11-ΔORF94 novR-R was grown in NVM^+ CAA with novobiocin media for ten days. Every day whole protein-extract samples of *N. magadii* L11 (top panel; Lanes 1-10) and *N. magadii* L11-ΔORF94 novR-R (bottom panel; Lanes 1-10) were collected and used for western blot analysis. As positive and negative control the whole protein-extract of *N. magadii* L11 (+) and *N. magadii* L13 (-), respectively, were used. For the detection of gp34 the α-$gp34_{52}$ (rabbit #20) antibody was used and the protein has a size of 66 kDa.

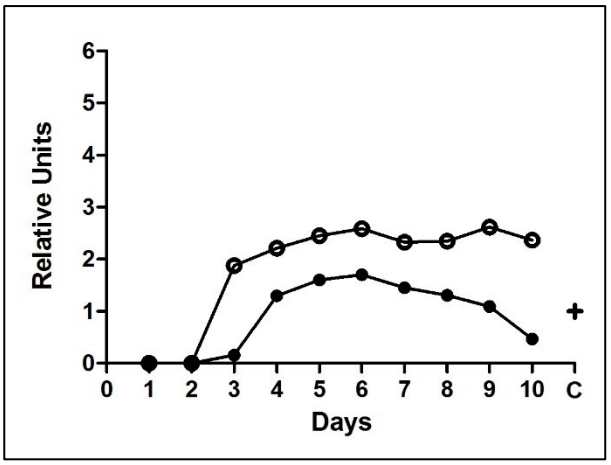

Figure 19. Relative protein levels of *N. magadii* L11 and of *N. magadii* L11-ΔORF94 novR-R with antibodies against gp34. Every day whole protein-extract samples of *N. magadii* L11 (●) and *N. magadii* L11-ΔORF94 novR-R (o) were collected and used for western blot analysis. As positive control the whole protein-extract of *N. magadii* L11 (+, C) was used. The relative values were calculated in respect to the positive control. For the western blot detection of gp34 the α-gp34$_{52}$ (rabbit #20) antibody was used. The analysis was performed with Image Lab Software from Bio Rad.

4.1.4 Complementation of the deletion mutant with the plasmids pRo-5/Mev and pNB102

The next step after the verification of the deletion and deletion analysis was the complementation of the deletion mutant with two different vectors to reintroduce the ORF94 into the cell. The plasmids pRo-5/Mev and pNB102 were chosen, since the first has a copy number of 1 to 5 and the second has a copy number of about 20. Using these plasmids allows analysing the effects of the complementation better and gain further understanding of the function of the gp94. Control cultures infected with the mutant virus and containing the respective plasmid, were used to compare the influence of solely the plasmid on the cell.

The complementation was performed and quantitatively verified via PCR. Then the complementation and control cultures were analysed in the same way as the deletion and wild type strain, with an analysis of their growth, titer and proteins.

4.1.4.1 Preparation for complementation of *N. magadii* L11-ΔORF94 novR-R

For this study four strains were needed, the two control strains *N. magadii* L11-ΔORF94 novR-R with the plasmids pRo-5/Mev and pNB102 respectively and the two complementation strains *N. magadii* L11-ΔORF94 novR-R with the plasmids pRo-5/Mev-ORF94 and pNB102-ORF94 respectively. Therefore, cultures of *N. magadii* L13 containing the needed plasmids were inoculated from the laboratory collection and tested for the methyltransferase gene via analytical PCR with the primers MT-Kpn-5 and MT-Xba-3 (Figure 20). The ORF94 should be present in the complementation strains and the positive control *N. magadii* L11, but not in the control strains and the negative control *N. magadii* L13. The resulting fragment should be 1280bp long.

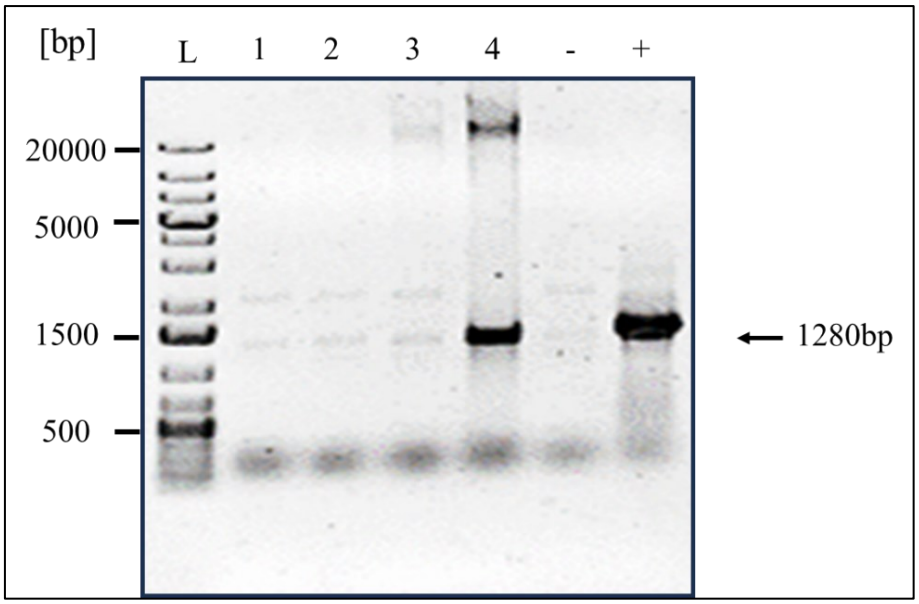

Figure 20. Agarose gel electrophoresis of *N. magadii* L11-ΔORF94 novR-R complementation and control strains for the ORF94. To test for the methyltransferase gene, a PCR with the primers MT-Kpn-5 and MT-Xba-3 was performed on the *N. magadii* L11-ΔORF94 novR-R complementation and control strains (Lane 1: *N. magadii* L11-ΔORF94 novR-R pNB102, Lane 2: *N. magadii* L11-ΔORF94 novR-R pNB102-ORF94, Lane 3: *N. magadii* L11-ΔORF94 novR-R pRo-5/Mev, Lane 4: *N. magadii* L11-ΔORF94 novR-R pRo-5/Mev-ORF94). The PCR products were separated on a 0.8% agarose gel. As a positive control *N. magadii* L11 was used (Lane +) and as negative control *N. magadii* L13 was used (Lane -). The ThermoFischer Scientific 1-kb plus DNA ladder (Lane L) was used as size control. The size of the fragment amplified by the PCR is indicated with an arrow on the right side (1280bp).

In the Figure 20 it is visible that the plasmid control strains correctly show no band indicating the absence of the ORF94, but also *N. magadii* L11-ΔORF94 novR-R pNB102-ORF94 showed no band. The complementation strain with the plasmid pNB102 was therfore freshly transformed. The strain *N. magadii* L11 ΔORF94 novR-R pRo-5/Mev-ORF94 showed a band at the correct length. To ensure these results a western blot analysis was performed for the complementation and control strain with the plasmid pRo-5/Mev.

Crude whole-protein extracts were taken from *N. magadii* L11-ΔORF94 novR-R pRo-5/Mev and *N. magadii* L11-ΔORF94 novR-R pRo-5/Mev-ORF94 and loaded onto an SDS gel, which was then used for western blotting against the methyltransferase antibody. The results showed that the methyltransferase was lighter visible in the complementation strain than the wild type and therefore it was decided to transform this plasmid freshly (Figure 21).

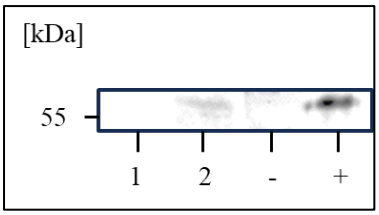

Figure 21. Western blot of *N. magadii* L11-ΔORF94 novR-R pRo-5/Mev and *N. magadii* L11-ΔORF94 novR-R pRo-5/Mev-ORF94 samples with antibodies against the methyltransferase. Whole protein-extract samples of *N. magadii* L11-ΔORF94 novR-R pRo-5/Mev (Lanes 1) and *N. magadii* L11-ΔORF94 novR-R pRo-5/Mev-ORF94 (Lane 2) were collected and used for western blot analysis. As positive and negative control the whole protein-extract of *N. magadii* L11 (+) and *N. magadii* L13 (-), respectively, were used. For the detection of the methyltransferase the α - Methyltransferase antibody was used, and the protein has a size of 46 kDa, calculated from the sequence. Due to the low pI, the protein migrates app at a size of 60kDa.

4.1.4.2 Complementation with the plasmids pRo-5/Mev-ORF94 and pNB102-ORF94

The plasmids pRo-5/Mev-ORF94 and pNB102-ORF94 were isolated from the *E. coli* and transformed it into *N. magadii* L13 competent cells. These cells were plated on selective plates with mevinolin and after growth six colonies were inoculated. These were tested for the ORF94 via a PCR with the primers 5mt-1ba and Mt-Xba-3 (Figure 22 and Figure 23).

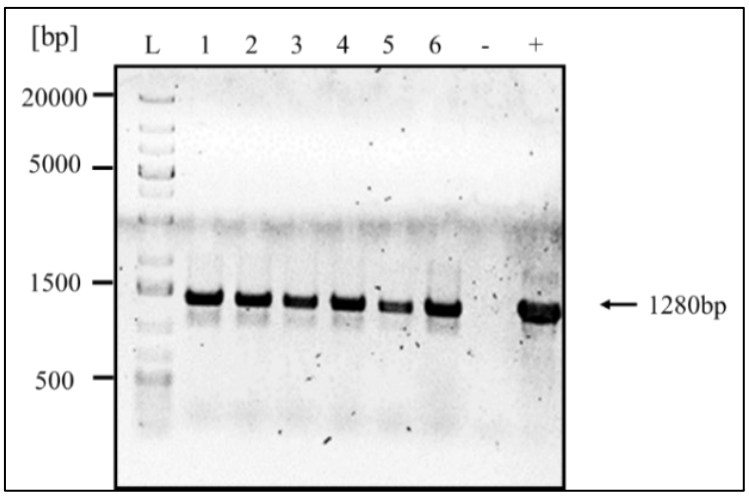

Figure 22. Agarose gel electrophoresis of *N. magadii* L13 pRo-5/Mev-ORF94 for the ORF94. To test for the methyltransferase gene, a PCR with the primers 5mt-1ba and Mt-Xba-3 was performed on six clones of *N. magadii* L13 pRo-5/Mev-ORF94 (Lanes 1-6). The PCR products were separated on a 0.8% agarose gel. As a positive control *N. magadii* L11 was used (Lane +) and as negative control *N. magadii* L13 was used (Lane -). The ThermoFischer Scientific 1-kb plus DNA ladder (Lane L) was used as size control. The size of the fragment amplified by the PCR is indicated with an arrow on the right side (1280bp).

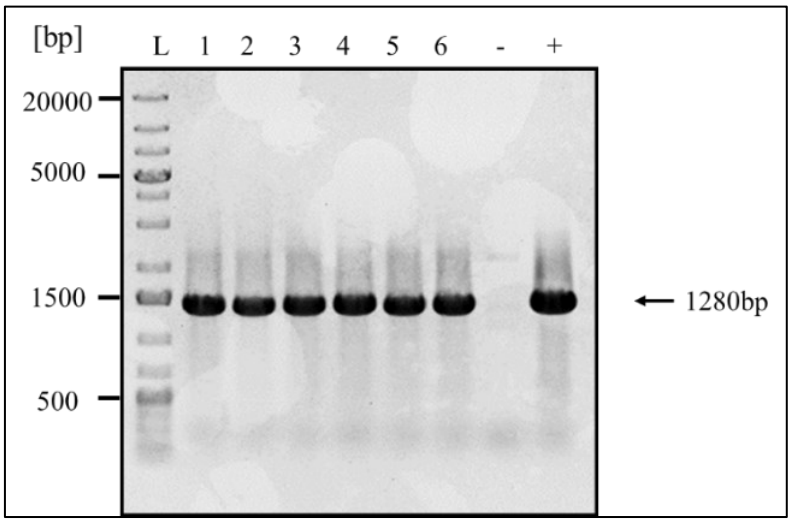

Figure 23. Agarose gel electrophoresis of *N. magadii* L13 pNB102-ORF94 for the ORF94. To test for the methyltransferase gene, a PCR with the primers 5mt-1ba and Mt-Xba-3 was performed on six clones of *N. magadii* L13 pNB102-ORF94 (Lanes 1-6). The PCR products were separated on a 0.8% agarose gel. As a positive control *N. magadii* L11 was used (Lane +) and as negative control *N. magadii* L13 was used (Lane -). The ThermoFischer Scientific 1-kb plus DNA ladder (Lane L) was used as size control. The size of the fragment amplified by the PCR is indicated with an arrow on the right side (1280bp).

All cultures showed the correct fragment length of 1280bp. Three of these cultures were taken for further experiments and for the control cultures containing the plasmids pRo-5/Mev and pNB102 the cultures from above were used. These *N. magadii* L13 cultures containing the plasmids were infected with ΦCh1-ΔORF94 novR-R. PCR analyses were done to test the cultures for the ORF94 and the novobiocin resistance cassette. The primers 5mt-1ba and Mt-Xba-3 were used for the ORF94 PCR, and bands of the length of 1280bp were expected for the complementation strains but not for the control strains (Figure 24 and Figure 25). The PCR for the novobiocin resistance cassette used the primers NovR-1s and NovR-2p, which resulted in a fragment length of 2680bp in all cultures (Figure 26 and Figure 27).

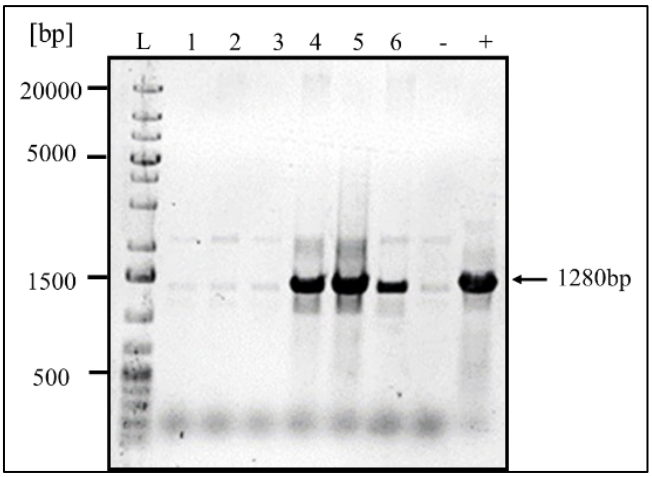

Figure 24. Agarose gel electrophoresis of *N. magadii* L11-ΔORF94 novR-R pRo-5/Mev and *N. magadii* L11-ΔORF94 novR-R pRo-5/Mev-ORF94 for the ORF94. To test for the methyltransferase gene, a PCR with the primers 5mt-1ba and Mt-Xba-3 was performed on three clones of *N. magadii* L11-ΔORF94 novR-R pRo-5/Mev (Lanes 1-3) and *N. magadii* L11-ΔORF94 novR-R pRo-5/Mev-ORF94 (Lanes 4-6). The PCR products were separated on a 0.8% agarose gel. As a positive control *N. magadii* L11 was used (Lane +) and as negative control *N. magadii* L13 was used (Lane -). The ThermoFischer Scientific 1-kb plus DNA ladder (Lane L) was used as size control. The size of the fragment amplified by the PCR is indicated with an arrow on the right side (1280bp).

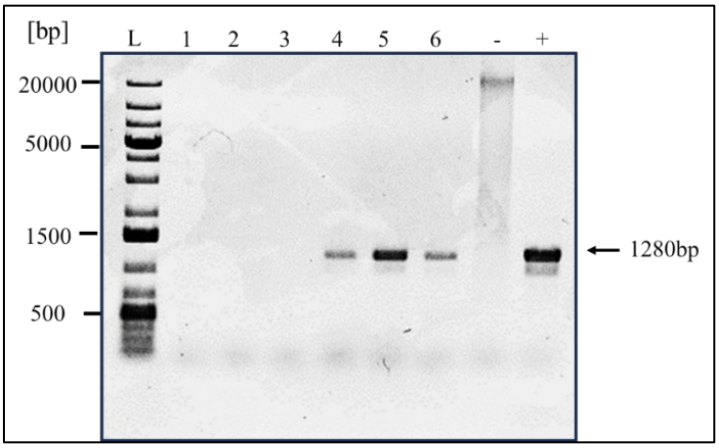

Figure 25. Agarose gel electrophoresis of *N. magadii* L11-ΔORF94 novR-R pNB102 and *N. magadii* L11-ΔORF94 novR-R pNB102-ORF94 for the ORF94. To test for the methyltransferase gene, a PCR with the primers 5mt-1ba and Mt-Xba-3 was performed on three clones of *N. magadii* L11-ΔORF94 novR-R pNB102 (Lanes 1-3) and *N. magadii* L11-ΔORF94 novR-R pNB102-ORF94 (Lanes 4-6). The PCR products were separated on a 0.8% agarose gel. As a positive control *N. magadii* L11 was used (Lane +) and as negative control *N. magadii* L13 was used (Lane -). The ThermoFischer Scientific 1-kb plus DNA ladder (Lane L) was used as size control. The size of the fragment amplified by the PCR is indicated with an arrow on the right side (1280bp).

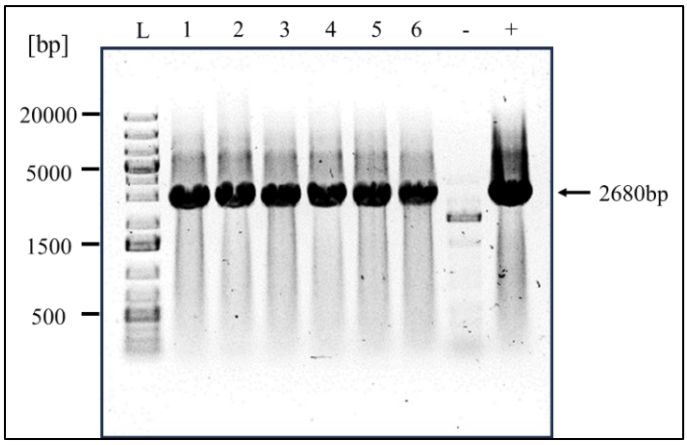

Figure 26. Agarose gel electrophoresis of *N. magadii* L11-ΔORF94 novR-R pRo-5/Mev and *N. magadii* L11-ΔORF94 novR-R pRo-5/Mev-ORF94 for the novobiocin resistance cassette. To test for the methyltransferase gene, a PCR with the primers NovR-1s and NovR-2p was performed on three clones of *N. magadii* L11-ΔORF94 novR-R pRo-5/Mev (Lanes 1-3) and *N. magadii* L11-ΔORF94 novR-R pRo-5/Mev-ORF94 (Lanes 4-6). The PCR products were separated on a 0.8% agarose gel. As a positive control *N. magadii* L11-ΔORF94 novR-R was used (Lane +) and as negative control *N. magadii* L11 was used (Lane -). The ThermoFischer Scientific 1-kb plus DNA ladder (Lane L) was used as size control. The size of the fragment amplified by the PCR is indicated with an arrow on the right side (2680bp).

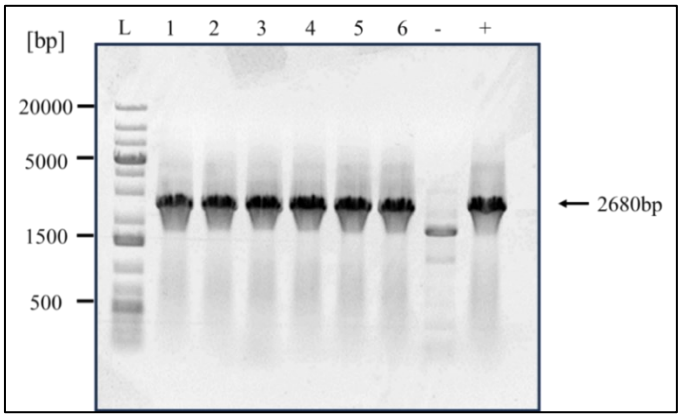

Figure 27. Agarose gel electrophoresis of *N. magadii* L11-ΔORF94 novR-R pNB102 and *N. magadii* L11-ΔORF94 novR-R pNB102-ORF94 for the novobiocin resistance cassette. To test for the methyltransferase gene, a PCR with the primers NovR-1s and NovR-2p was performed on three clones of *N. magadii* L11-ΔORF94 novR-R pNB102 (Lanes 1-3) and *N. magadii* L11-ΔORF94 novR-R pNB102-ORF94 (Lanes 4-6). The PCR products were separated on a 0.8% agarose gel. As a positive control *N. magadii* L11-ΔORF94 novR-R was used (Lane +) and as negative control *N. magadii* L11 was used (Lane -). The ThermoFischer Scientific 1-kb plus DNA ladder (Lane L) was used as size control. The size of the fragment amplified by the PCR is indicated with an arrow on the right side (2680bp).

The PCR results showed that all clones of all cultures were correctly containing the desired constructs. Two clones of each strain were used for further analysis and were therefore inoculated in NVM^+ CAA with novobiocin and a time series was performed.

Optical density measurements, protein probes and titer samples were taken for 10 days and analysed afterwards.

4.1.4.3 Time series analysis of the complementation and control strains

As for the deletion and wild type strain analyses, the cultures of the complementation and control strains were grown in NVM^+ CAA with novobiocin for 10 days and the influence of the plasmids was analysed and compared. Since the plasmids alone are expected to have an influence on the growth, titer and proteins, comparison to the empty plasmid cultures was done. Carrying a plasmid can affect the cells by adding metabolic stress since maintaining the plasmid is energetically costly. The strength of the effect is also dependent on the copy number of the plasmid. Therefore, in this study plasmids with different copy numbers were chosen and analysed in the following.

4.1.4.3.1 Growth of the complementation and control strains

During the 10-day period, samples for optical density measurements were taken and a growth curve was made for each strain (Figure 28 and Figure 29).

The growth kinetics of *N. magadii* L11-ΔORF94 novR-R pRo-5/Mev started with a weaker growth from inoculation day to the first day, like *N. magadii* L11-ΔORF94 novR-R. The lysis started on day four, with the peak of the optical density occurring on day three, this corresponds to the day lysis started in the deletion strain. The control strain showed a lower growth behaviour than the deletion strain. The first strong decline of the control strain was from days five to six, which is two days later than in the deletion strain. The strongest decline of this control strain occurred from days nine to ten, which is five days later than in the deletion strain. Furthermore, the strongest decline of the growth curve in the control strain was about two-times weaker than in the deletion strain. This means that *N. magadii* L11-ΔORF94 novR-R pRo-5/Mev grew similarly to *N. magadii* L11-ΔORF94 novR-R, but at a lower optical density with the density decreasing slower and with a less steep lysis (Figure 28 and Figure 11).

N. magadii L11-ΔORF94 novR-R pRo-5/Mev-ORF94 showed an increased growth from the day inoculation happened to the first day compared to the control strain *N. magadii* L11-ΔORF94 novR-R pRo-5/Mev. The lysis started on day five, which is also the day the first strong decline began going to day six, this corresponds to the same pattern

seen in the control strain. This relation can also be observed in the wild type and deletion strains. The strongest decline happened from days seven to eight. Overall did the growth curve of *N. magadii* L11-ΔORF94 novR-R pRo-5/Mev-ORF94 show increased optical density values compared to the control strain *N. magadii* L11-ΔORF94 novR-R pRo-5/Mev, which matches the relationship between *N. magadii* L11 and *N. magadii* L11-ΔORF94 novR-R (Figure 28 and Figure 11).

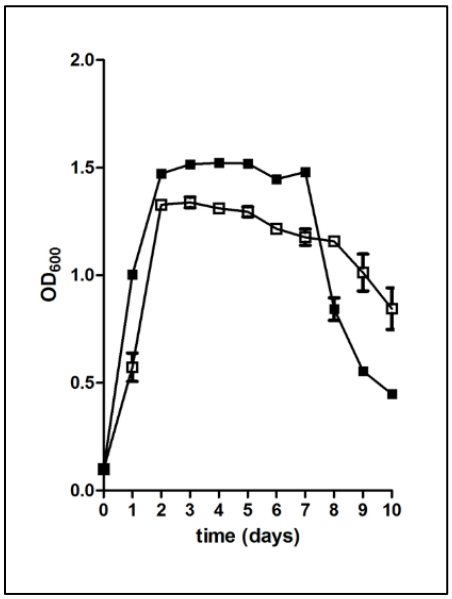

Figure 28. Growth kinetics analysis of *N. magadii* L11-ΔORF94 novR-R pRo-5/Mev-ORF94 and of *N. magadii* L11-ΔORF94 novR-R pRo-5/Mev. *N. magadii* L11-ΔORF94 novR-R pRo-5/Mev-ORF94 (■) and *N. magadii* L11-ΔORF94 novR-R pRo-5/Mev (□) were grown in NVM$^+$ CAA with novobiocin media for ten days and the optical densities were measured at 600nm every day. Error bars (±1SD) are indicated.

The control strain *N. magadii* L11-ΔORF94 novR-R pNB102 grew weak from inoculation to day one, like *N. magadii* L11-ΔORF94 novR-R. When comparing the lysis behaviour to the deletions strain it is noticeable that the lysis was pushed back two days, until day six. Another difference to the deletion strain is the plateau from day three until day six, which is followed by a first strong decline. The steepest decrease in cell density was from day seven to eight. The introduction of the plasmid lead to the control strain growing for a longer time at a high optical density and lysis therefore starting later (Figure 29 and Figure 11).

The complementation strain *N. magadii* L11-ΔORF94 novR-R pNB102-ORF94 began its growth from inoculation analogously to the wild type strain *N. magadii* L11 with as steep increase in cell density. This was followed by the plateau phase like in the control strain, which lasted from day two until day seven. Lysis started on day six, like the control strain, two days later than the wildtype strain. The growth curve first started to strongly decline from day seven to eight. The strongest decline was from day eight to nine, which is later than the control strain. Overall is the growth of *N. magadii* L11-ΔORF94 novR-R pNB102-ORF94 stronger and reaches a higher optical density than the control strain *N. magadii* L11-ΔORF94 novR-R pNB102, this relationship can also be seen in the wild type and deletion strain (Figure 29 and Figure 11).

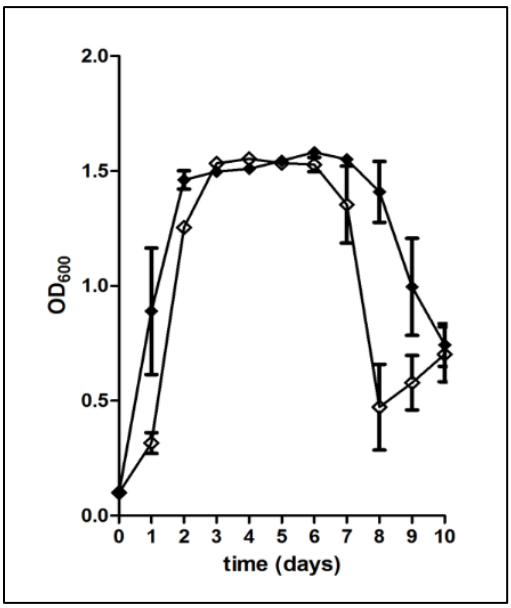

Figure 29. Growth kinetics analysis of *N. magadii* L11-ΔORF94 novR-R pNB102-ORF94 and of *N. magadii* L11-ΔORF94 novR-R pNB102. *N. magadii* L11-ΔORF94 novR-R pNB102-ORF94 (♦) and *N. magadii* L11-ΔORF94 novR-R pNB102 (◊) were grown in NVM$^+$ CAA with novobiocin media for ten days and the optical densities were measured at 600nm every day. Error bars (±1SD) are indicated.

4.1.4.3.2 Viral titer analysis of the complementation and control strain

The first three days both the complementation and the control strain with the plasmid pRo-5/Mev, show approximately the same low viral load. The viral titer of *N. magadii* L11-ΔORF94 novR-R pRo-5/Mev increased on day four, the day lysis started. From that point on a steady increase in plaque forming units per millilitre can be seen up to day ten, reaching values between 10^5 and 10^9. For *N. magadii* L11-ΔORF94 novR-R pRo-5/Mev-ORF94 a similar graph was made, with a stronger increase on day five, the day lysis started, but on day four a slight increase from the day before can be seen. After this the plaque forming units per millilitre increased every day until day ten, ranging from 10^5 to 10^9. The relationship between these strains is like the relation between the wild type *N. magadii* L11 and the deletion strain *N. magadii* L11-ΔORF94 novR-R, with the complementation strain showing overall higher values from the day lysis starts on, even though beginning with slightly lower values than the control strain (Figure 30 and Figure 12).

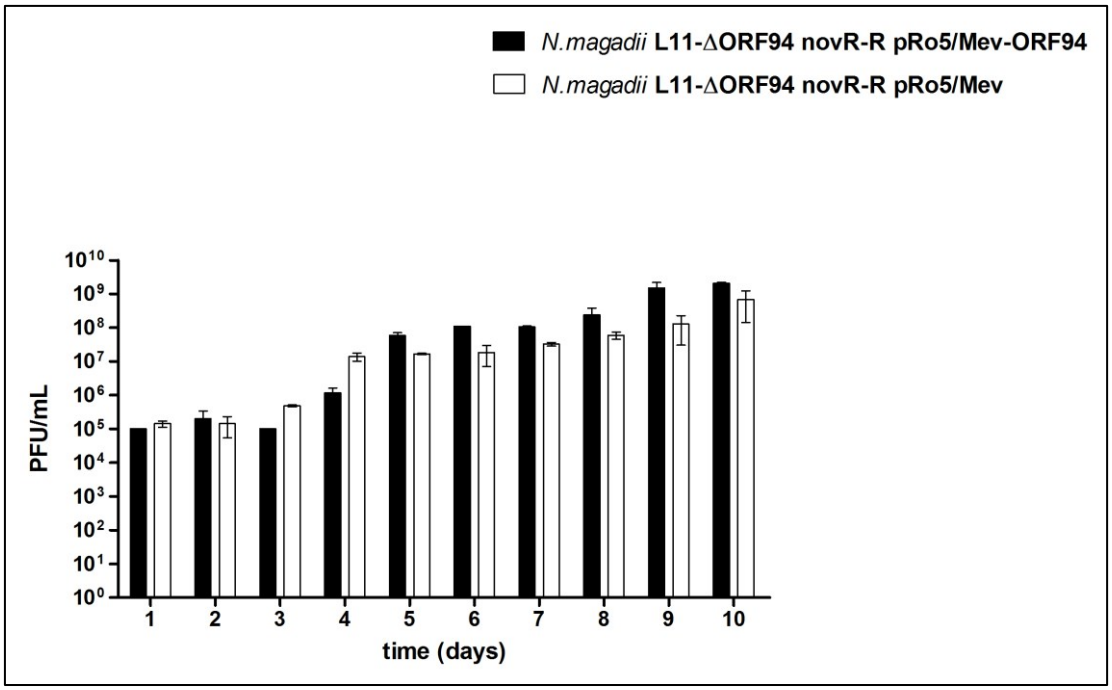

Figure 30. Plating efficiency and viral titer of *N. magadii* L11-ΔORF94 novR-R pRo-5/Mev-ORF94 and of *N. magadii* L11-ΔORF94 novR-R pRo-5/Mev. *N. magadii* L11 was grown in NVM^+ CAA media for ten days and *N. magadii* L11-ΔORF94 novR-R was grown in NVM^+ CAA with novobiocin media for ten days. Every day the supernatant of *N. magadii* L11-ΔORF94 novR-R pRo-5/Mev-ORF94 (black bars) and *N. magadii* L11-ΔORF94 novR-R pRo-5/Mev (white bars) was collected and used to infect the cured strain *N. magadii* L13, to estimate the viral titer. Error bars (±1SD) are indicated.

The analysis of the plating efficiency of *N. magadii* L11-ΔORF94 novR-R pNB102-ORF94 and of *N. magadii* L11-ΔORF94 novR-R pNB102 showed a shift of the viral titer graph to later days. The strains started the first there days at 10^3 and the days four to six resembled the pattern of the wild type *N. magadii* L11 and the deletion strain *N. magadii* L11-ΔORF94 novR-R on the first three days, with the control being slightly higher than the complementation strain. On day six lysis did start and the plaque forming units of the complementation strain started to increase from this day on until day ten reaching higher values, up to 10^9, than the control strain, which showed only slight increases from day to day reaching values of 10^7 (Figure 31 and Figure 12).

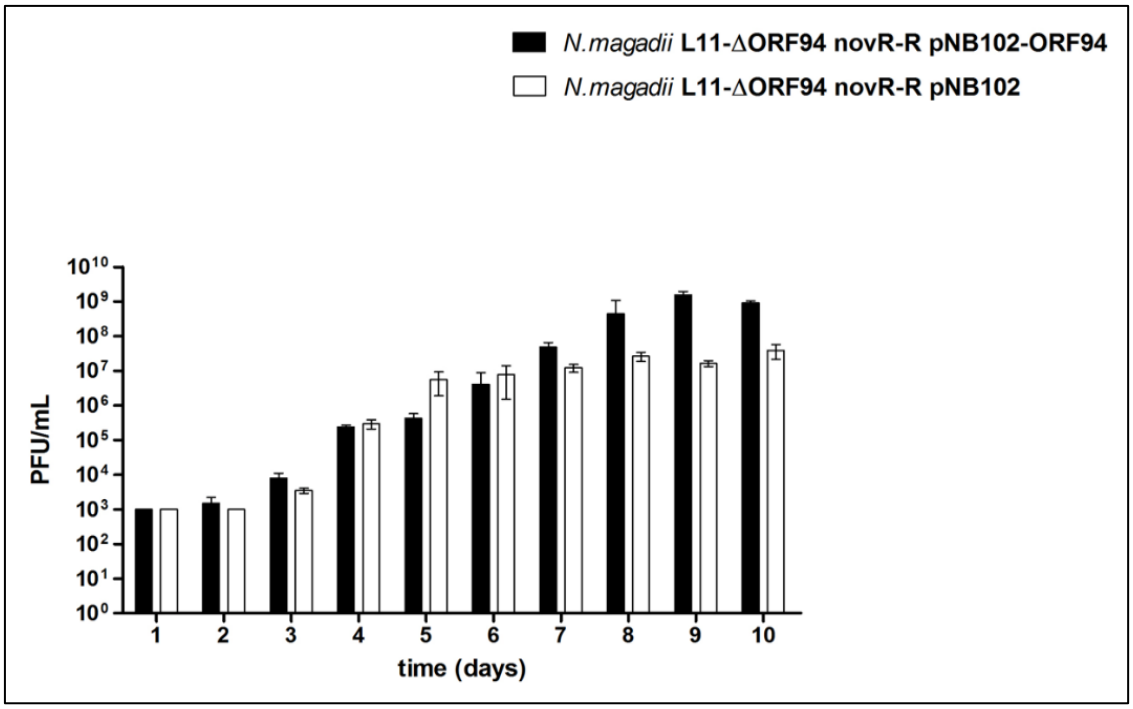

Figure 31. Plating efficiency and viral titer of *N. magadii* L11-ΔORF94 novR-R pNB102-ORF94 and of *N. magadii* L11-ΔORF94 novR-R pNB102. *N. magadii* L11-ΔORF94 novR-R pNB102-ORF94 and *N. magadii* L11-ΔORF94 novR-R pNB102 was grown in NVM^+ CAA with novobiocin media for ten days. Every day the supernatant of *N. magadii* L11-ΔORF94 novR-R pNB102-ORF94 (black bars) and *N. magadii* L11-ΔORF94 novR-R pNB102 (white bars) was collected and used to infect the cured strain *N. magadii* L13, to estimate the viral titer. Error bars (±1SD) are indicated.

4.1.4.3.3 Western blot analysis of the complementation and control strain

Methyltransferase

The western blot analysis of the time series for *N. magadii* L11-ΔORF94 novR-R pRo-5/Mev showed no signal at any day as to be expected. The strain *N. magadii* L11-ΔORF94 novR-R pRo-5/Mev-ORF94 showed a constant expression of the methyltransferase gene from the second day on, with a lighter band on day one. Comparing this to the wild type strains pattern it can be seen that the constant expression pattern is lighter (Figure 13, Figure 32, Figure 33).

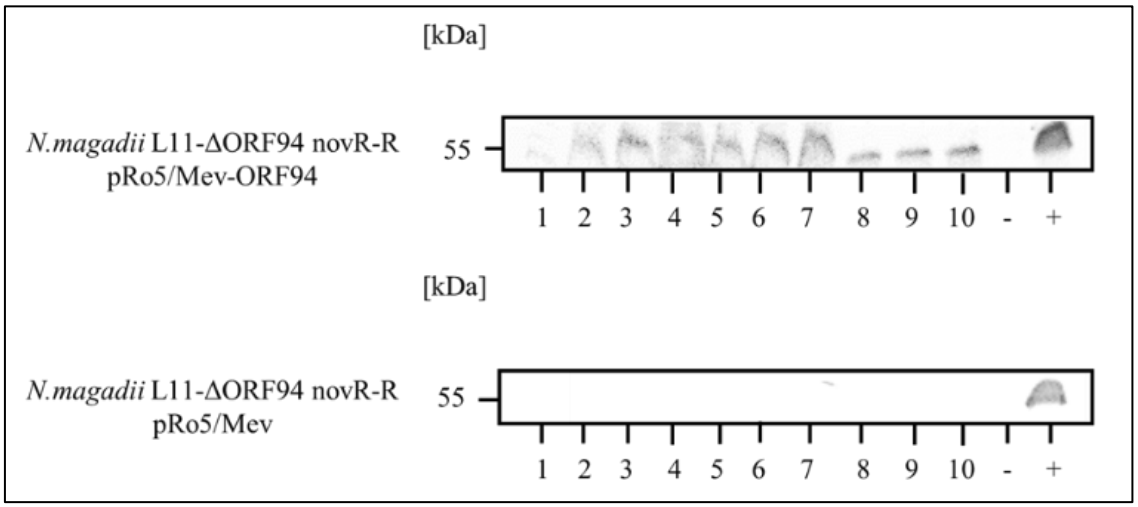

Figure 32. Western blot of *N. magadii* L11-ΔORF94 novR-R pRo-5/Mev-ORF94 and of *N. magadii* L11-ΔORF94 novR-R pRo-5/Mev time series samples with antibodies against the Methyltransferase. *N. magadii* L11-ΔORF94 novR-R pRo-5/Mev-ORF94 and of *N. magadii* L11-ΔORF94 novR-R pRo-5/Mev were grown in NVM$^+$ CAA with novobiocin media for ten days. Every day whole protein-extract samples of *N. magadii* L11-ΔORF94 novR-R pRo-5/Mev-ORF94 (top panel; Lanes 1-10) and *N. magadii* L11-ΔORF94 novR-R pRo-5/Mev (bottom panel; Lanes 1-10) were collected and used for western blot analysis. As positive and negative control the whole protein-extract of *N. magadii* L11 (+) and *N. magadii* L13 (-), respectively, were used. For the detection of the methyltransferase the α-methyltransferase antibody was used, and the protein has a size of 46 kDa, calculated from the sequence. Due to the low pI, the protein migrates app at a size of 60kDa.

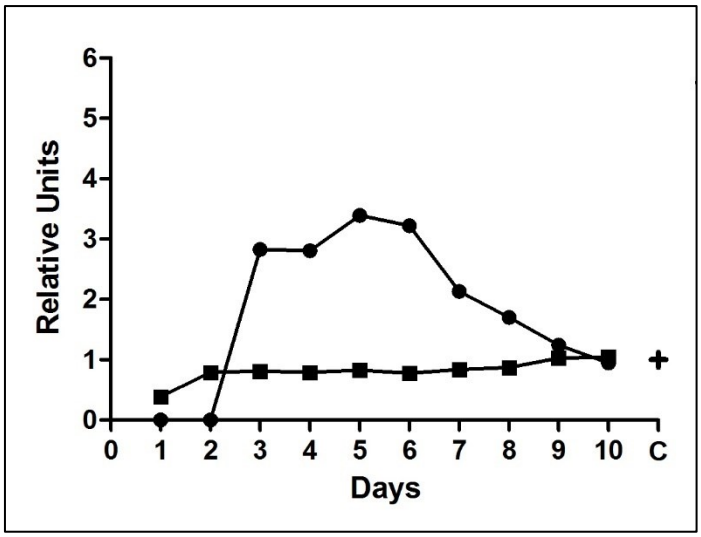

Figure 33. Relative protein levels of *N. magadii* L11 and of *N. magadii* L11-ΔORF94 novR-R pRo-5/Mev-ORF94 with antibodies against the methyltransferase. Every day whole protein-extract samples of *N. magadii* L11 (●) and *N. magadii* L11-ΔORF94 novR-R pRo-5/Mev-ORF94 (■) were collected and used for western blot analysis. As positive control the whole protein-extract of *N. magadii* L11 (+, C) was used. The relative values were calculated in respect to the positive control. For the western blot detection of α - methyltransferase antibody was used. The analysis was performed with Image Lab Software from Bio Rad.

The expression pattern of the methyltransferase gene in *N. magadii* L11-ΔORF94 novR-R pNB102 showed like the deletion strain no protein at any timepoint. *N. magadii* L11-ΔORF94 novR-R pNB102-ORF94 showed an increasing gene expression from day one forward. The protein concentrations stayed constant from day five to day ten. Considering the growth curve, it was visible that the growth and lysis behaviour was shifted two days further in the complementation strain compared to the wild type strain. Nevertheless, slightly higher concentrations overall were detectable in the complementation strain over a longer period, than in the wild type (Figure 13, Figure 34 and Figure 35).

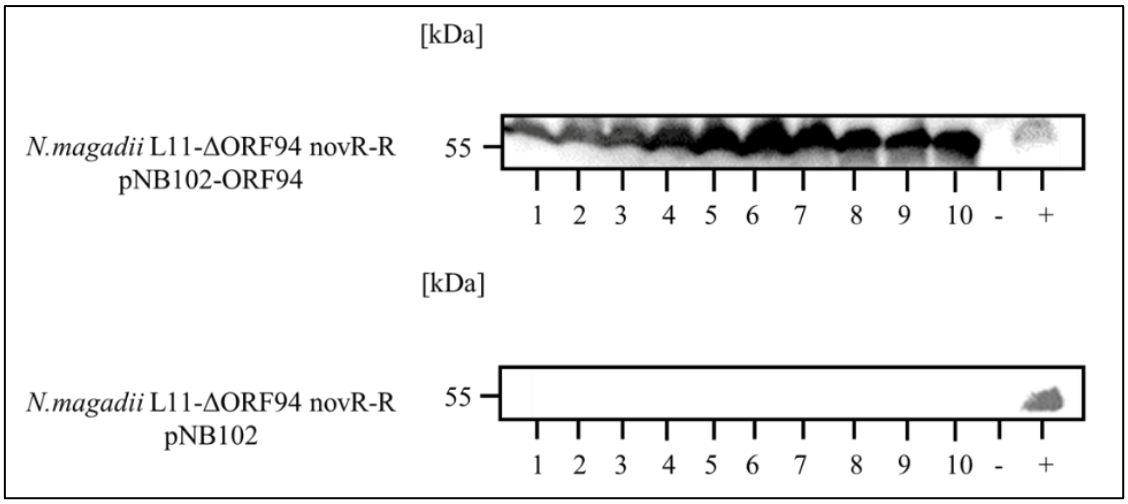

Figure 34. Western blot of *N. magadii* L11-ΔORF94 novR-R pNB102-ORF94 and of *N. magadii* L11-ΔORF94 novR-R pNB102 time series samples with antibodies against the methyltransferase. *N. magadii* L11-ΔORF94 novR-R pNB102-ORF94 and of *N. magadii* L11-ΔORF94 novR-R pNB102 were grown in NVM$^+$ CAA with novobiocin media for ten days. Every day whole protein-extract samples of *N. magadii* L11-ΔORF94 novR-R pNB102-ORF94 (top panel; Lanes 1-10) and *N. magadii* L11-ΔORF94 novR-R pNB102 (bottom panel; Lanes 1-10) were collected and used for western blot analysis. As positive and negative control the whole protein-extract of *N. magadii* L11 (+) and *N. magadii* L13 (-), respectively, were used. For the detection of the methyltransferase the α - methyltransferase antibody was used and the protein has a size of 46 kDa, calculated from the sequence. Due to the low pI, the protein migrates app at a size of 60kDa.

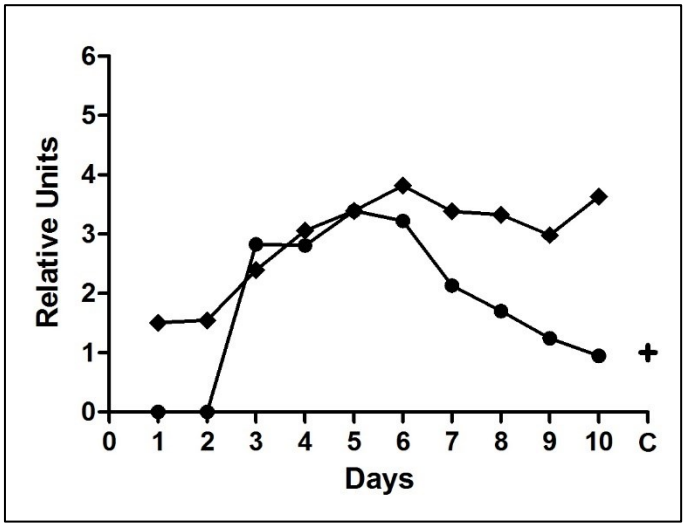

Figure 35. Relative protein levels of *N. magadii* L11 and of *N. magadii* L11-ΔORF94 novR-R pNB102 -ORF94 with antibodies against the methyltransferase. Every day whole protein-extract samples of *N. magadii* L11 (●) and *N. magadii* L11-ΔORF94 novR-R pNB102-ORF94 (♦) were collected and used for western blot analysis. As positive control the whole protein-extract of *N. magadii* L11 (+, C) was used. The relative values were calculated in respect to the positive control. For the western blot detection of α - methyltransferase antibody was used. The analysis was performed with Image Lab Software from Bio Rad.

protein E

The analysis of the protein E concentrations of both *N. magadii* L11-ΔORF94 novR-R pRo-5/Mev-ORF94 and of *N. magadii* L11-ΔORF94 novR-R pRo-5/Mev showed the signal beginning on day three and increasing afterwards but staying constant after day four until day ten. Overall, the concentrations of the control strain were lower than in the deletion mutant *N. magadii* L11-ΔORF94 novR-R and the concentration of the complementation strain were higher than wild type *N. magadii* L11, leading to both strains having similar concentrations values (Figure 14, Figure 15, Figure 36 and Figure 37).

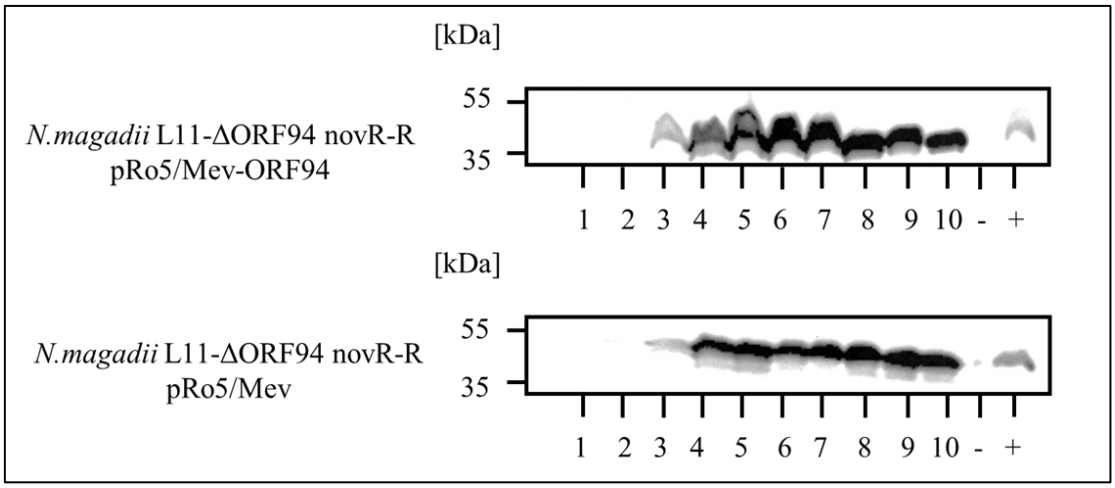

Figure 36. Western blot of *N. magadii* L11-ΔORF94 novR-R pRo-5/Mev-ORF94 and of *N. magadii* L11-ΔORF94 novR-R pRo-5/Mev time series samples with antibodies against the protein E. *N. magadii* L11-ΔORF94 novR-R pRo-5/Mev-ORF94 and of *N. magadii* L11-ΔORF94 novR-R pRo-5/Mev were grown in NVM^+ CAA with novobiocin media for ten days. Every day whole protein-extract samples of *N. magadii* L11-ΔORF94 novR-R pRo-5/Mev-ORF94 (top panel; Lanes 1-10) and *N. magadii* L11-ΔORF94 novR-R pRo-5/Mev (bottom panel; Lanes 1-10) were collected and used for western blot analysis. As positive and negative control the whole protein-extract of *N. magadii* L11 (+) and *N. magadii* L13 (-), respectively, were used. For the detection of the protein E the α-protein E antibody was used and the protein has a size of 50 kDa.

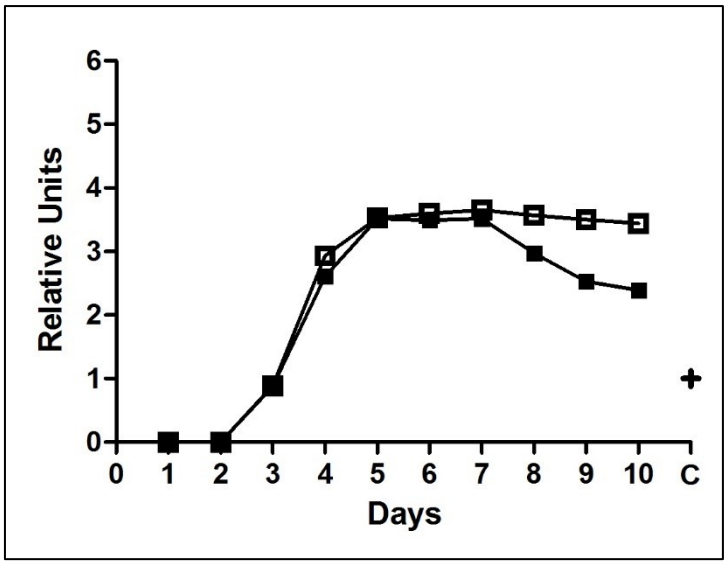

Figure 37. Relative protein levels of *N. magadii* L11-ΔORF94 novR-R pRo-5/Mev-ORF94 and of *N. magadii* L11-ΔORF94 novR-R pRo-5/Mev with antibodies against the major capsid protein E. Every day whole protein-extract samples of *N. magadii* L11-ΔORF94 novR-R pRo-5/Mev-ORF94 (■) and *N. magadii* L11-ΔORF94 novR-R pRo-5/Mev (□) were collected and used for western blot analysis. As positive control the whole protein-extract of *N. magadii* L11 (+, C) was used. The relative values were calculated in respect to the positive control. For the western blot detection of the protein E the α-protein E antibody was used. The analysis was performed with Image Lab Software from Bio Rad.

The western blot of *N. magadii* L11-ΔORF94 novR-R pNB102-ORF94 and of *N. magadii* L11-ΔORF94 novR-R pNB102 for the protein E had similar concentrations depicted, starting from day three on. The peak in concentration of protein E is shifted one day later for the complementation strain, which aligns with the results from the growth curve. In both strains barely any reduction of protein E was visible, and the concentrations stayed from day four until day ten rather constant. The analysis showed that the concentrations of the control strain were a bit lower than in the deletion strain and the complementation strain showed a higher concentration of protein E than the wild type (Figure 14, Figure 15, Figure 38 and Figure 39).

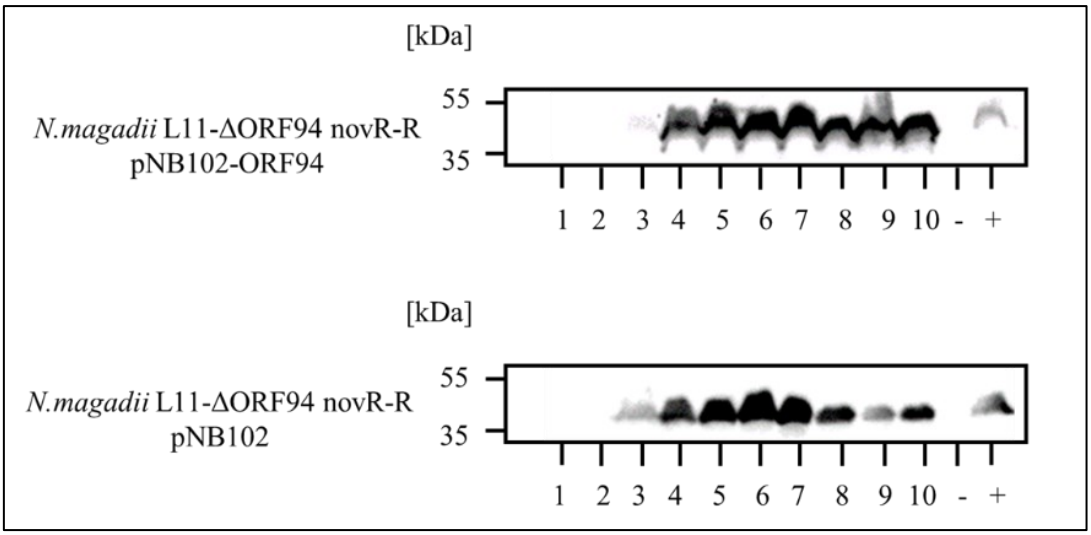

Figure 38. Western blot of *N. magadii* L11-ΔORF94 novR-R pNB102-ORF94 and of *N. magadii* L11-ΔORF94 novR-R pNB102 time series samples with antibodies against the major capsid protein E. *N. magadii* L11-ΔORF94 novR-R pNB102-ORF94 and of *N. magadii* L11-ΔORF94 novR-R pNB102 were grown in NVM$^+$ CAA with novobiocin media for ten days. Every day whole protein-extract samples of *N. magadii* L11-ΔORF94 novR-R pNB102-ORF94 (top panel; Lanes 1-10) and *N. magadii* L11-ΔORF94 novR-R pNB102 (bottom panel; Lanes 1-10) were collected and used for western blot analysis. As positive and negative control the whole protein-extract of *N. magadii* L11 (+) and *N. magadii* L13 (-), respectively, were used. For the detection of the protein E the α-protein E antibody was used, and the protein has a size of 50 kDa.

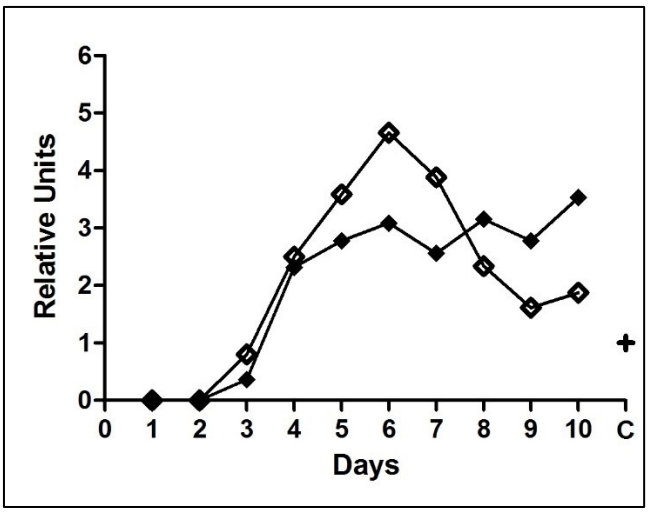

Figure 39. Relative protein levels of *N. magadii* L11-ΔORF94 novR-R pNB102-ORF94 and of *N. magadii* L11-ΔORF94 novR-R pNB102 with antibodies against the major capsid protein E. Every day whole protein-extract samples of *N. magadii* L11-ΔORF94 novR-R pNB102-ORF94 (♦) and *N. magadii* L11-ΔORF94 novR-R pNB102 (◊) were collected and used for western blot analysis. As positive control the whole protein-extract of *N. magadii* L11 (+, C) was used. The relative values were calculated in respect to the positive control. For the western blot detection of the protein E the α-protein E antibody was used. The analysis was performed with Image Lab Software from Bio Rad.

gp34

The strains *N. magadii* L11-ΔORF94 novR-R pRo-5/Mev-ORF94 and of *N. magadii* L11-ΔORF94 novR-R pRo-5/Mev both began synthesising the protein gp34 on day three. The protein concentration was in both strains similar, with an increase on day four and then a stagnation in concentration, which stayed strong until the last day. Compared to the deletion strain a decrease in concentration can be seen in the control strain. For the complementation strain a slight increase in concentration at certain time points compared to the wild type can be seen (Figure 18, Figure 19, Figure 40 and Figure 41).

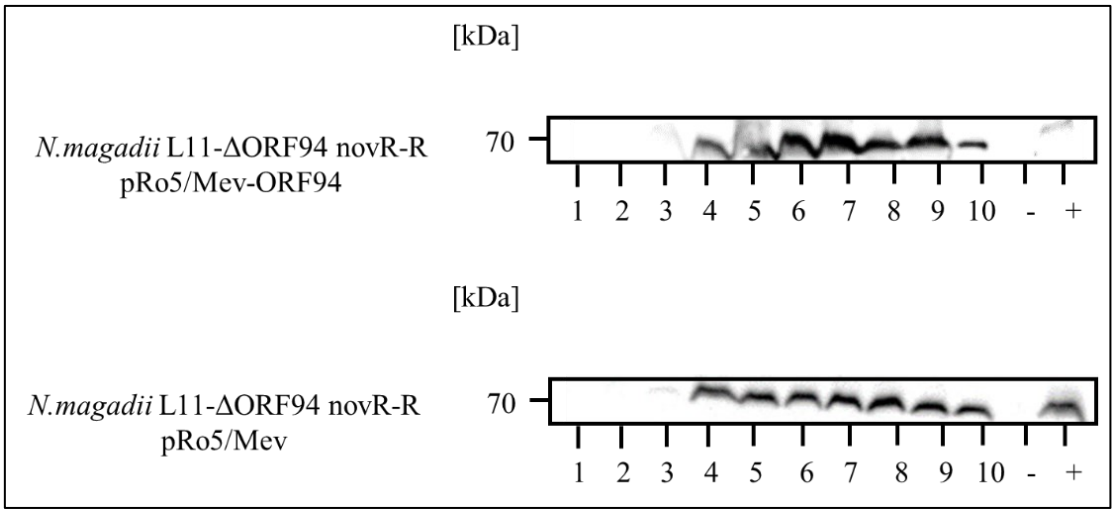

Figure 40. Western blot of *N. magadii* L11-ΔORF94 novR-R pRo-5/Mev-ORF94 and of *N. magadii* L11-ΔORF94 novR-R pRo-5/Mev time series samples with antibodies against gp34. *N. magadii* L11-ΔORF94 novR-R pRo-5/Mev-ORF94 and of *N. magadii* L11-ΔORF94 novR-R pRo-5/Mev were grown in NVM^+ CAA with novobiocin media for ten days. Every day whole protein-extract samples of *N. magadii* L11-ΔORF94 novR-R pRo-5/Mev-ORF94 (top panel; Lanes 1-10) and *N. magadii* L11-ΔORF94 novR-R pRo-5/Mev (bottom panel; Lanes 1-10) were collected and used for western blot analysis. As positive and negative control the whole protein-extract of *N. magadii* L11 (+) and *N. magadii* L13 (-), respectively, were used. For the detection of gp34 the α-gp34$_{52}$ (rabbit #20) antibody was used and the protein has a size of 66 kDa.

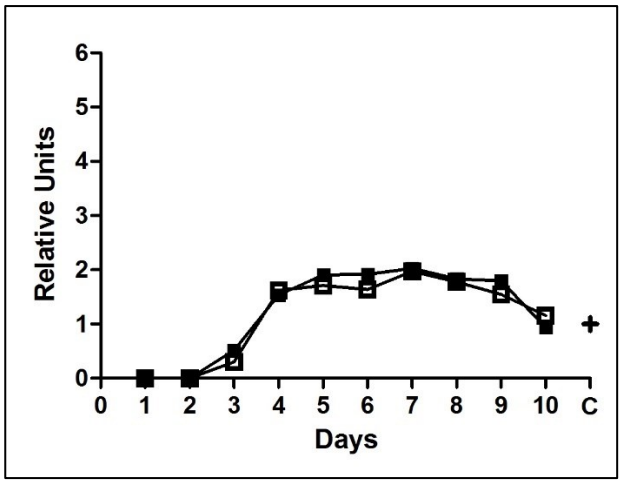

Figure 41. Relative protein levels of *N. magadii* L11-ΔORF94 novR-R pRo-5/Mev-ORF94 and of *N. magadii* L11-ΔORF94 novR-R pRo-5/Mev with antibodies against gp34. Every day whole protein-extract samples of *N. magadii* L11-ΔORF94 novR-R pRo-5/Mev-ORF94 (■) and *N. magadii* L11-ΔORF94 novR-R pRo-5/Mev (□) were collected and used for western blot analysis. As positive control the whole protein-extract of *N. magadii* L11 (+, C) was used. The relative values were calculated in respect to the positive control. For the western blot detection of gp34 the α-gp34$_{52}$ (rabbit #20) antibody was used. The analysis was performed with Image Lab Software from Bio Rad.

The protein gp34 started to appear lightly on day three in both *N. magadii* L11-ΔORF94 novR-R pNB102-ORF94 and *N. magadii* L11-ΔORF94 novR-R pNB102. From the fourth day on both strains showed a constant concentration of protein until day ten, whereas the control strain had higher values. The deletion strain had slightly higher concentrations overall than the control strain. The wild type strain declined towards the last days, which cannot be seen in the complementation strain (Figure 18, Figure 19, Figure 42 and Figure 43).

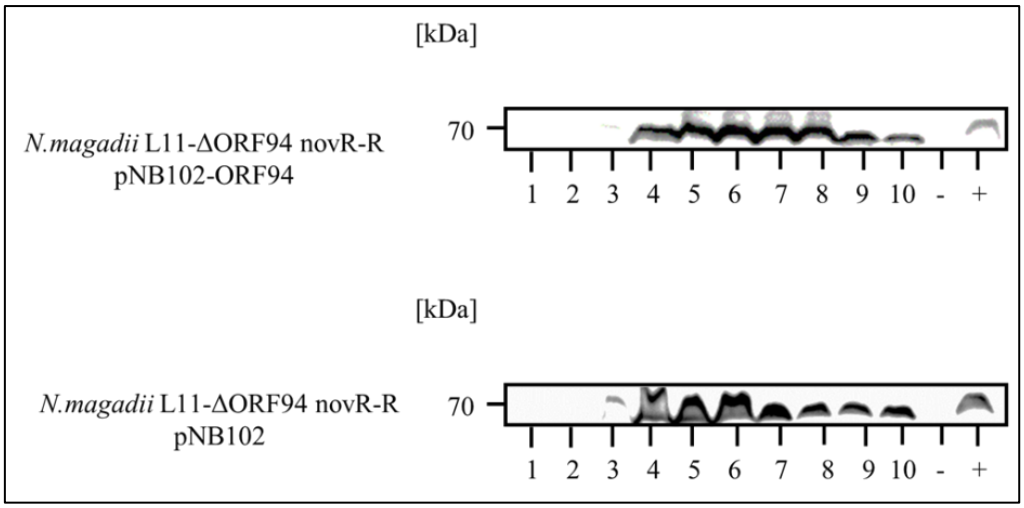

Figure 42. Western blot of *N. magadii* L11-ΔORF94 novR-R pNB102-ORF94 and of *N. magadii* L11-ΔORF94 novR-R pNB102 time series samples with antibodies against gp34. *N. magadii* L11-ΔORF94 novR-R pNB102-ORF94 and of *N. magadii* L11-ΔORF94 novR-R pNB102 were grown in NVM^+ CAA with novobiocin media for ten days. Every day whole protein-extract samples of *N. magadii* L11-ΔORF94 novR-R pNB102-ORF94 (top panel; Lanes 1-10) and *N. magadii* L11-ΔORF94 novR-R pNB102 (bottom panel; Lanes 1-10) were collected and used for western blot analysis. As positive and negative control the whole protein-extract of *N. magadii* L11 (+) and *N. magadii* L13 (-), respectively, were used. For the detection of gp34 the α-gp34$_{52}$ (rabbit #20) antibody was used and the protein has a size of 66 kDa.

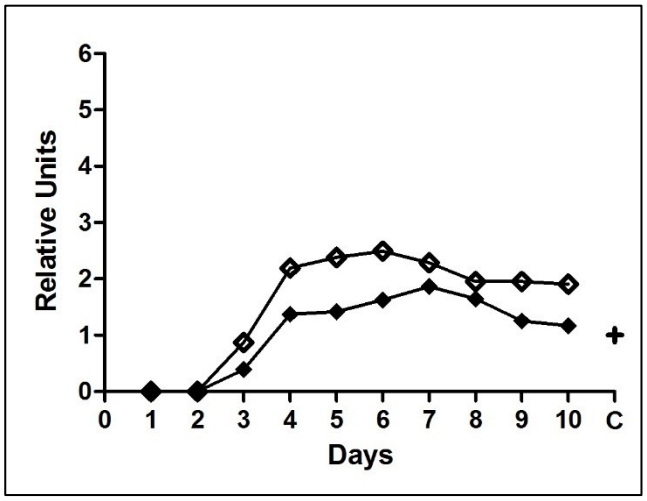

Figure 43. Relative protein levels of *N. magadii* L11-ΔORF94 novR-R pNB102-ORF94 and of *N. magadii* L11-ΔORF94 novR-R pNB102 with antibodies against gp34. Every day whole protein-extract samples of *N. magadii* L11-ΔORF94 novR-R pNB102-ORF94 (♦) and *N. magadii* L11-ΔORF94 novR-R pNB102 (◊) were collected and used for western blot analysis. As positive control the whole protein-extract of *N. magadii* L11 (+, C) was used. The relative values were calculated in respect to the positive control. For the western blot detection of gp34 the α-gp34$_{52}$ (rabbit #20) antibody was used. The analysis was performed with Image Lab Software from Bio Rad.

4.1.5 Restriction analysis to verify loss of the adenine methylation in the deletion strain and restoration in complementation strain

In this study a restriction analysis was used to investigate the adenine methylation, which should be non-existent in the deletion strain and recovered in the complementation strain. Therefor the isolated DNA of *N. magadii* L11, *N. magadii* L11-ΔORF94 novR-R and *N. magadii* L11-ΔORF94 novR-R pNB102-ORF94 were restricted with isoshizomeric enzymes with different responses to methylated DNA, recognizing the sequence 5‘-GATC-3‘. First the DNA was restricted with the enzyme *Dpn*I, an enzyme which cuts only the methylated sequence. Then the enzyme *Mbo*I was used, which is prevented from cutting by methylation. Both enzymes mentioned above were added to a third reaction, thereby ensuring a complete restriction of both methylated and unmethylated DNA. In previous studies it was found that a fraction of the populations virus DNA is site-specifically cleaved by *Mbo*I, while the other part stayed resistant (Witte *et al*., 1997). The last enzyme was *Sau*3A, whose activity is unaffected by the methylation, creating the same pattern as the reaction with both enzymes *Dpn*I and *Mbo*I. All restriction reactions were loaded onto an 1.2% agarose gel and their patterns analysed afterwards (Figure 44).

The fragment pattern of the ΦCh1 wild type DNA showed the unrestricted DNA above 20000bp. This was followed by the restriction with *Dpn*I, were a large fraction of DNA remained unrestricted and only a small fraction was cleaved. Reversely in the restriction reaction with *Mbo*I a small fraction of DNA was uncut, and most virus DNA was cut. The double-digest showed all the DNA to be cleaved, same as the reaction with *Sau*3A (Figure 44).

The ΦCh1-ΔORF94 novR-R virus DNA showed a similar pattern of fragments with two differences. First the mutant did not show restricted DNA in the reaction with the enzyme *Dpn*I and no uncut DNA in the *Mbo*I reaction. This showed that the deletion of the ORF94 lead to the loss of methylation in the virus DNA. The second deviation of the fragment pattern from the wild type, was the appearance of fragments at approximately 2000bp. This corresponds to the fragment pattern of the novobiocin

resistance cassette being cleaved with the selected enzymes. This indicated further that the deletion was correctly done (Figure 44).

The ΦCh1-ΔORF94 novR-R pNB102-ORF94 virus DNA restriction pattern was matching the fragment pattern of the wild type, with the fragments corresponding to the novobiocin resistance cassette. Nevertheless, the relation between unrestricted virus DNA in the reactions with *Dpn*I and *Mbo*I, indicated a smaller fraction of unrestricted DNA in the *Mbo*I reaction than in the *Dpn*I reaction, in the complementation strain compared to the wild type strain (Figure 44).

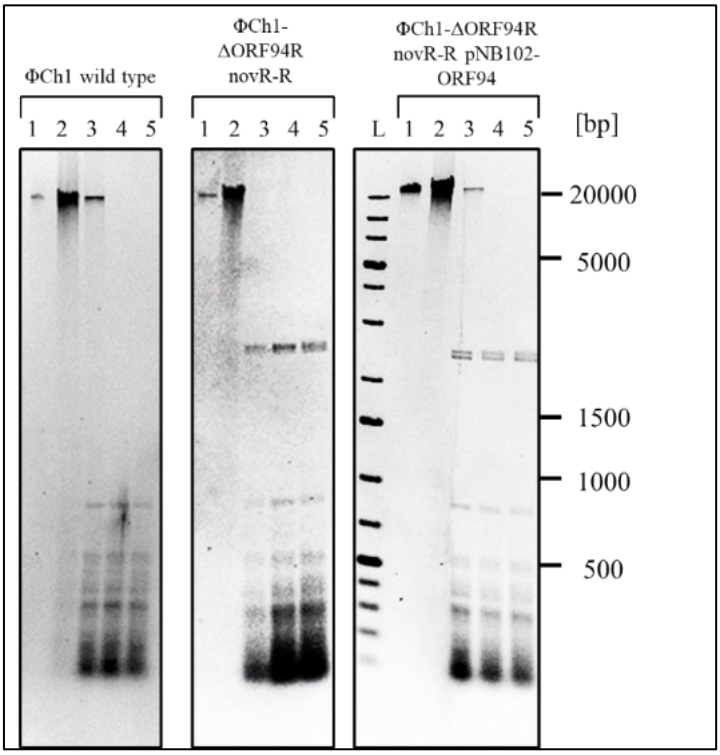

Figure 44. Restriction analysis of ΦCh1 DNA, ΦCh1-ΔORF94 novR-R DNA and ΦCh1-ΔORF94 novR-R pNB102-ORF94 DNA with the enzymes *Dpn*I, *Mbo*I, *Dpn*I/*Mbo*I and *Sau*3A. Purified ΦCh1 DNA (first picture from the left), ΦCh1-ΔORF94 novR-R DNA (picture in the middle) and ΦCh1-ΔORF94 novR-R pNB102-ORF94 DNA (last picture from the left) were digested with different restriction endonucleases (Lane 1: unrestricted, Lane 2: *Dpn*I, Lane 3: *Mbo*I, Lane 4: double digest with *Dpn*I and *Mbo*I, Lane 5: *Sau*3A), and separated on an 1.2% agarose gel. The ThermoFischer Scientific 1-kb plus DNA ladder (Lane L) was used as size control.

The relationship between methylated and unmethylated virus DNA, showed to be unequal in the wild type and the complementation strain. Previous findings suggested that the viral DNA of the ΦCh1 population was partially methylated and partially unmethylated, but the results in this study showed lesser methylated virus DNA than unmethylated, although the western blot analysis showed that the methyltransferase was

synthesised. Therefore, further investigations were done to investigate the relation with the adenine-methylation-sensitive endonucleases *Eco*RV and *Pst*I. These enzymes restricted the sequence 5'-GAT*ATC-3' and 5'-CTGC*AG-3' respectively, corresponding to cognate adenine methylation (McClelland *et al.*, 1994). The restrictions with the wild type, deletion and complementation strains DNA were again loaded to an 1.2% agarose gel. This showed that the wild type and complementation virus DNA had a small portion of unrestricted DNA, whereas the deletion showed non. The ΦCh1-ΔORF94 novR-R pNB102-ORF94 virus DNA indicated in both restriction reactions with both enzymes a lower fraction of methylated DNA. In the restrictions with the enzyme *Pst*I an additional fragment, of the length of approximately 5000bp, to the ΦCh1 wild type virus DNA restriction can be seen in the pattern of the ΦCh1-ΔORF94 novR-R and the ΦCh1-ΔORF94 novR-R pNB102-ORF94 DNA, corresponding to the novobiocin resistance cassette. The relation of methylated to unmethylated DNA showed to be nonequal again, with more unmethylated DNA (Figure 45).

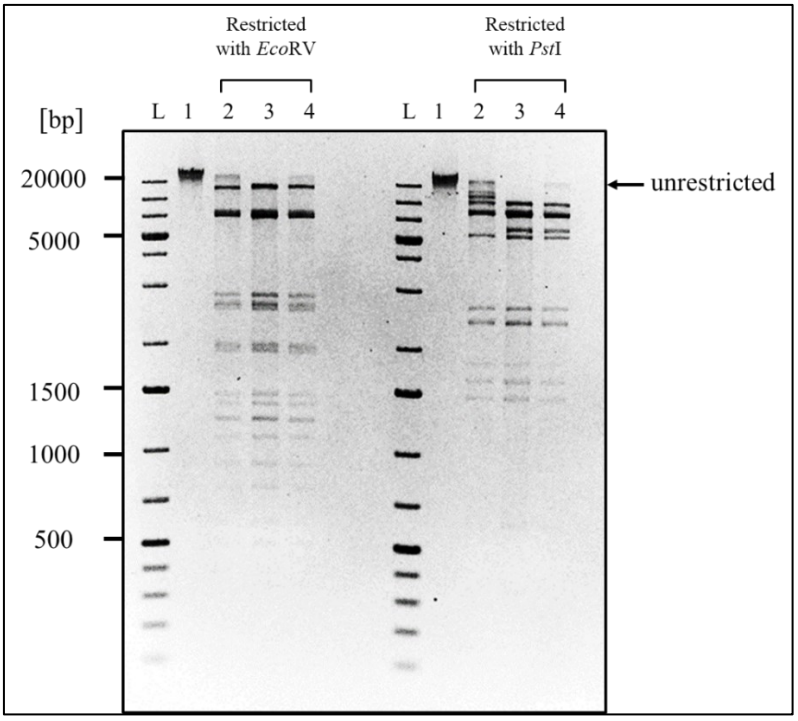

Figure 45. Restriction analysis of ΦCh1 DNA, ΦCh1-ΔORF94 novR-R DNA and ΦCh1-ΔORF94 novR-R pNB102-ORF94 DNA with the enzymes *Eco*RV and *Pst*I. Purified ΦCh1 DNA (Lane 1: unrestricted and Lane 2: restricted), ΦCh1-ΔORF94 novR-R DNA (Lane 3) and ΦCh1-ΔORF94 novR-R pNB102-ORF94 DNA (Lane 4) were digested with different the restriction endonucleases *Eco*RV and *Pst*I and separated on an 1.2% agarose gel. The ThermoFischer Scientific 1-kb plus DNA ladder (Lane L) was used as size control.

4.1.6 Discussion

The deletion of the ORF94 and thereby the loss of the adenine methyltransferase in ΦCh1, in its natural host *N. magadii*, was shown to have been successfully performed. The effects of the deletion, via homologous recombination of the novobiocin resistance cassette, were analysed by growth behaviour, western blots and viral titer plaque assay. These further provided evidence of the loss of the methyltransferase and gave inside into its function and role in the viral life cycle. The growth of the deletion strain *N. magadii* L11-ΔORF94 novR-R was impaired, which could be because of the stress the cells are under, since the methyltransferase is not there to methylate and thereby regulate gene expression or other critical cellular processes. The amount of actively infectious viral particles was shown to be reduced in the deletion strain *N. magadii* L11-ΔORF94 novR-R compared to the wild type *N. magadii* L11, possibly also effects of the stress or because the methyltransferase plays a role in the lysis regulation pathway. This is a possible starting point for further investigations. The protein synthesis analysis gave further prove of the deletion, since the methyltransferase was not detectable any more in the deletion strain *N. magadii* L11-ΔORF94 novR-R. The other proteins under investigation, were the protein E, the major capsid protein and the protein gp34, tail fibre protein of ΦCh1. Two proteins which are important in the lytic cycle, and which are produced shortly before lysis starts. It was determined that both showed a much higher and a longer stronger concentration in the deletion strain *N. magadii* L11-ΔORF94 novR-R than the wild type *N. magadii* L11. This could be due to the missing methylation which could regulate the protein synthesis of these two proteins, so an unregulated expression pattern is seen.

The next analysis was conducted by complementing the deletion strain *N. magadii* L11-ΔORF94 novR-R to see the effects of bringing the ORF94 back into the system. This was done in two ways, with two plasmids having different copy numbers, the plasmids pRo-5/Mev, with the lower copy number and pNB102, with the higher copy number. In addition, control strains harbouring only the empty plasmids were used to determine the effect of the plasmids on the cell. The control strains, *N. magadii* L11-ΔORF94 novR-R pRo-5/Mev and *N. magadii* L11-ΔORF94 novR-R pNB102, showed a delay in the growth behaviour and viral titer production, with the plasmid pNB102 showing to induce a stronger shift to a later lysis than the strain with pRo-5/Mev. The plasmids showed to have a stressing effect on the cells, since the maintenance of them can be energy

consuming. The proteins E and gp34, showed the timely shift effects in their protein concentrations and slightly diverged from the concentrations of the deletion strain *N. magadii* L11-ΔORF94 novR-R by being lower. With this information was it possible to conclude the effects coming from the complementation of the ORF94 and not from the plasmids themselves.

The protein analysis showed that the methyltransferase was restored in the complementation strains *N. magadii* L11-ΔORF94 novR-R pRo-5/Mev-ORF94 and *N. magadii* L11-ΔORF94 novR-R pNB102-ORF94, but the regulation seamed not present. As expected, the complementation strain *N. magadii* L11-ΔORF94 novR-R pRo-5/Mev-ORF94 showed a lower concentration of methyltransferase than *N. magadii* L11-ΔORF94 novR-R pNB102-ORF94, which showed a slightly higher concentration than the wildtype. Nevertheless, both strains had a signal for the methyltransferase showing from day one and the concentration seemed not to go down in the last days but rather stayed strong, in contrast to the wild type *N. magadii* L11. These two findings hint towards a missing regulation of the expression of the ORF94 from the plasmids, but the mechanism behind this need's further investigation. Since the rest of the viral genome is available, it could be that the regulation of the methyltransferase gene does work in cis but not in trans. The other proteins which were under examination, protein E and gp34, showed no significant differences in both complementation strains, *N. magadii* L11-ΔORF94 novR-R pRo-5/Mev-ORF94 and *N. magadii* L11-ΔORF94 novR-R pNB102 -ORF94 to the control strains, *N. magadii* L11-ΔORF94 novR-R pRo-5/Mev and *N. magadii* L11-ΔORF94 novR-R pNB102, and had strong concentrations detectable until the last days. It was not possible to restore the regulation of the proteins completely, opening the question of how the methyltransferase plays a part in their regulation.

To further analyse the methylation activity of the methyltransferase and gain insight into the methylation pattern in the genome, a restriction analysis was done with the virus particles of the wild type *N. magadii* L11, the deletion strain *N. magadii* L11-ΔORF94 novR-R and the complementation strain with the plasmid pNB102 *N. magadii* L11-ΔORF94 novR-R pNB102-ORF94. This was done based on earlier studies performed on the genomic DNA of ΦCh1 (Witte *et al.*, 1997). The restriction of the wild type strain *N. magadii* L11 showed that not half the genomes were methylated but a much lesser part, whereas previous studies showed about half the population's DNA being methylated (Witte *et al.*, 1997). This was an unexpected finding, opening new questions.

The adenine methylation showed importance in many cellular mechanisms and the western blot analysis in this study showed that the methyltransferase is being produced, but the restriction analysis showed a smaller part of the genomes being methylated than in previous analyses. This must be analysed further, and the implications of lesser ΦCh1 DNAs being methylated than over 20 years ago should be investigated. The restriction analyses provided again evidence that the methylation was not present in the deletion strain *N. magadii* L11-ΔORF94 novR-R but could be restored at least partially in the complementation strain *N. magadii* L11-ΔORF94 novR-R pNB102-ORF94. This was surprising, since the methyltransferase was stronger and longer produced in the complementation strain *N. magadii* L11-ΔORF94 novR-R pNB102-ORF94, but the restriction pattern showed that lesser DNA was methylated than in the wild type strain *N. magadii* L11. Since this analysis gave only the information of if and how much DNA was methylated, the next steps could be to investigate which sites are and are not methylated in the wild type strain *N. magadii* L11 and in the complementation strain *N. magadii* L11-ΔORF94 novR-R pNB102-ORF94. With a restriction enzyme based 6mA sequencing (6mA-RE-seq) it is possible to detect 6mA sites at single nucleotide resolution, if its only desired to obtain the genome-wide distribution of the 6mA a photo-crosslinking with exonuclease digestion could be done (6mA-CLIP-exo; Fu *et al.*, 2015).

4.2 ORF75

4.2.1 Aim

Before this study was concluded, a deletion of the ORF75 was done by replacing it with the novobiocin resistance cassette by homologous recombination. The aim of this analysis was to provide evidence for the deletion of the ORF75 and investigate if the growth, viral titer and gene expression of chosen proteins are affected by the deletion. Verification of the deletion was gathered via PCR of the ORF75 and by performing a southern blot analysis. Following an inspection of the growth curve and active infectious viral titer of the deletion strain in comparison to the wild type strain. A western blot analysis was used to analyse the protein E, methyltransferase and gp34 concentrations in the deletion strain and compare them to the wild type strain.

4.2.2 Verification of the deletion and integration of the novobiocin resistance cassette

4.2.2.1 Agarose gel analysis

Different cultures were tested via PCR for the integration of the novobiocin resistance cassette, by amplification of the fragment between the upstream and downstream sequence of ORF75 with the primers Δ75-5en1 and Δ75-3en1. The fragment size of the deletion strain has the length of 3739bp with the 2673bp long novobiocin resistance cassette inserted.

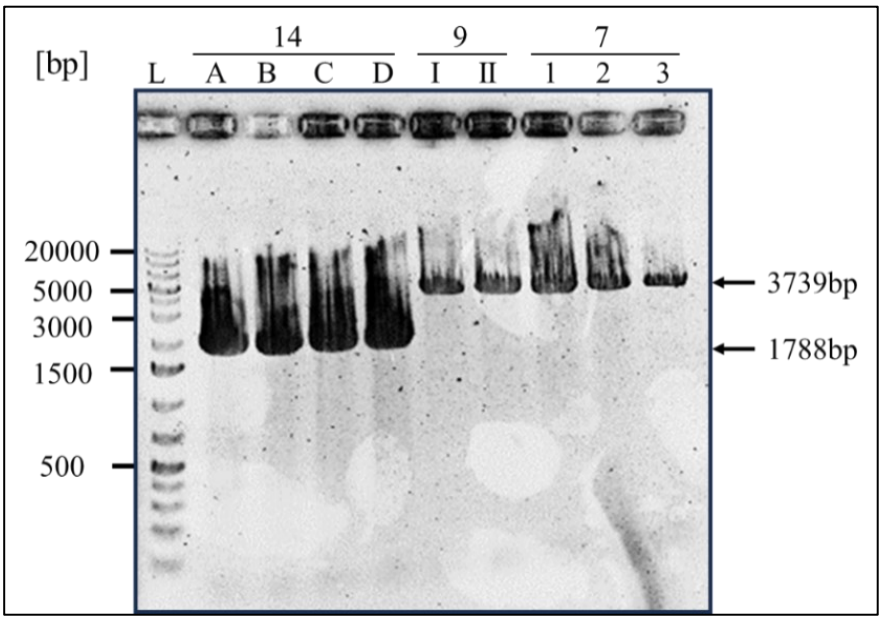

Figure 46. First agarose gel electrophoresis of ΦCh1-ΔORF75 novR from *N. magadii* for the ORF75 deletion mutant. To test for the novobiocin resistance cassette a PCR with the primers Δ75-5en1 and Δ75-3en1 was performed on the ΦCh1 DNA of nine clones (Lanes A-D, I, II, 1-3) from different plates (14, 9 and 7), supposably with the deleted ORF75 and containing the novobiocin resistance cassette. The PCR products were separated on a 0.8% agarose gel. The ThermoFischer Scientific 1-kb plus DNA ladder (Lane L) was used as size control. The size of the fragment amplified by the PCR with the novobiocin cassette inserted is 3739bp long and indicated with an arrow on the right side. The size of the fragment amplified by the PCR without the novobiocin cassette inserted is 1788bp long and indicated with an arrow on the right side.

The results from the agarose gel analysis shows that the cultures 14 (A, B, C and D) have the expected fragment size of the wild type and the cultures 9 (I and II) and 7 (1,2 and 3) have the expected fragment size of the deletion (Figure 46).

The cultures of 7:1 and 9:I were grown and their titer used to infect L13 via soft agar. Form the plaques on the plates four fresh cultures were inoculated in total, two from each 7:1 and 9:I. A test PCR was done on the grown cultures like before with the primers Δ75-5en1 and 1,5 primer Δ75-3en1 (Figure 47).

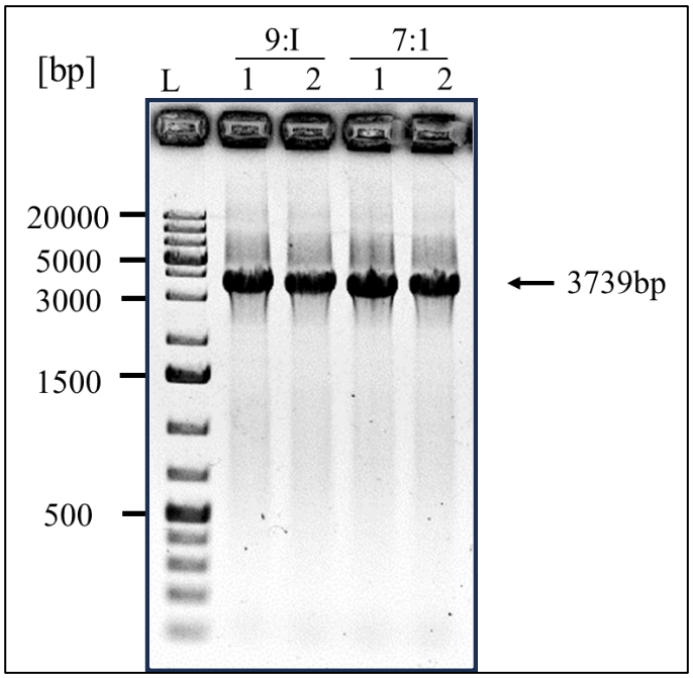

Figure 47. Agarose gel electrophoresis of ΦCh1-ΔORF75 novR from *N. magadii* for the ORF75 deletion mutant. To test for the novobiocin resistance cassette a PCR with the primers Δ75-5en1 and Δ75-3en1 was performed on the ΦCh1 DNA of four clones (Lanes 9:I:1,1 and 7:1:1,2). The PCR products were separated on a 0.8% agarose gel. The ThermoFischer Scientific 1-kb plus DNA ladder (Lane L) was used as size control. The size of the fragment amplified by the PCR with the novobiocin cassette inserted is 3739bp long and indicated with an arrow on the right side.

The test PCR results showed that all four clones have the correct fragment length of 3739bp (Figure 47). The cultures 7:1:1 and 9:I:1 were used for further analysis. Following these results a southern blot analysis was performed to verify the deletion by examining the 5'-and 3'-end of ΔORF75 novR.

4.2.2.2 Verification of the deletion via southern blot

The genome of ΦCh1 has several restriction sites for the enzymes *Bam*HI and *Pst*I. The resulting restriction site pattern is changed by the homologous recombination between the ORF75 and the novobiocin resistance cassette. The fragments of ΦCh1 and ΦCh1-ΔORF75 novR have different sizes after the restriction, which is used to analyse

the 5'- and 3'-end of ΦCh1 and ΦCh1-ΔORF75 novR (Figure 48 and Figure 49). Biotinylated probes hybridized at the 5'- and 3'-end of the DNA fragments target region and were used to make the difference in the fragment sizes of ΦCh1 and ΦCh1-ΔORF75 novR visible.

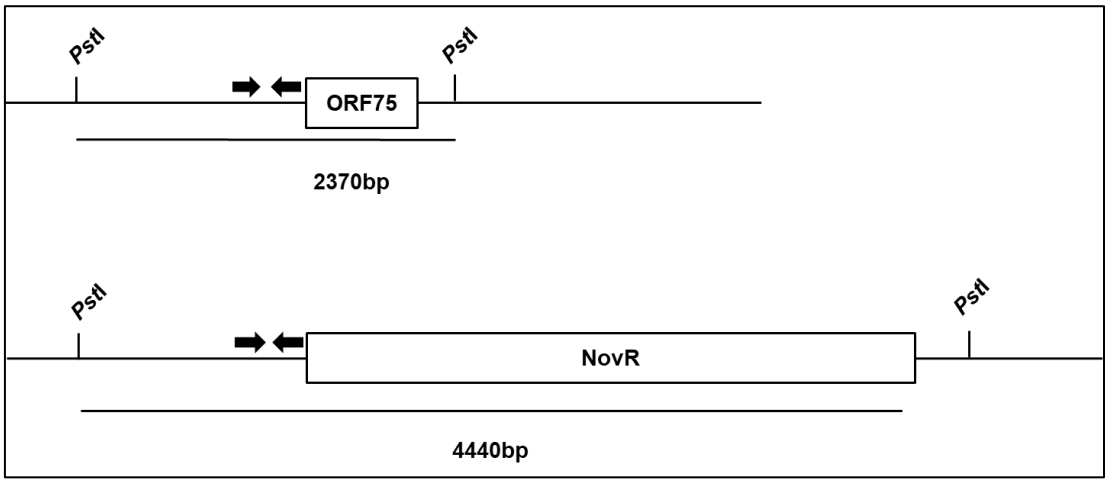

Figure 48. Schematic depiction of the fragment lengths after restriction and hybridization patterns of the southern blot of ΦCh1 and ΦCh1-ΔORF75 novR at the 5'-end. Parts of the genome of ΦCh1 and ΦCh1-ΔORF75 novR are depicted. After restriction of the ΦCh1 DNA of *N. magadii* L11 and of *N. magadii* L11-ΔORF75 novR with *Pst*I, fragments of the sizes 2370bp for the ΦCh1 DNA and 4440bp for ΦCh1-ΔORF75 novR DNA can be found. The biotinylated probe, made with a PCR from the ΦCh1 DNA of *N. magadii* L11 with the primers Δ75-5en1 and Δ75-5en-3, binds between the shown arrows (→ ←) upstream of the target region. This probe fragment has a length of 568 bp.

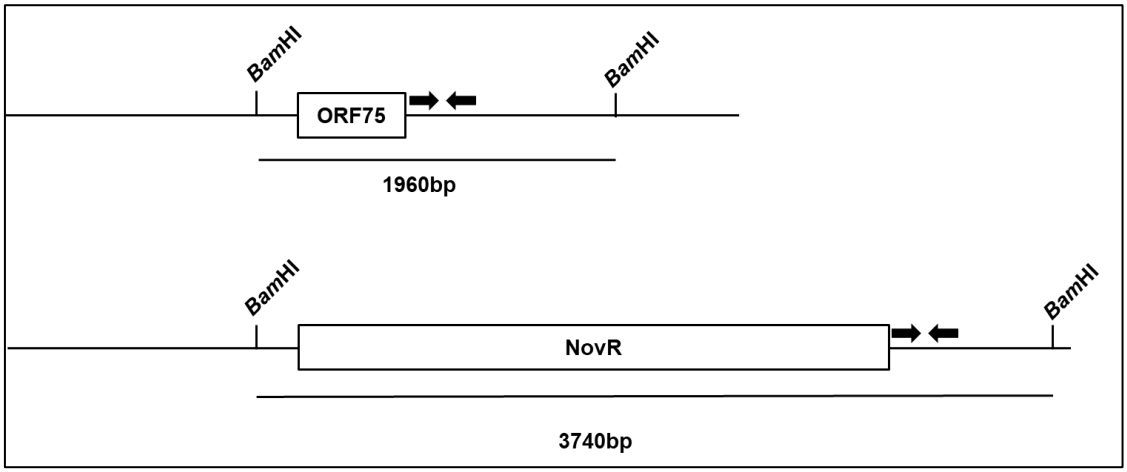

Figure 49. Schematic depiction of the fragment lengths after restriction and hybridization patterns of the southern blot of ΦCh1 and ΦCh1-ΔORF75 novR at the 3'-end. Parts of the genome of ΦCh1 and ΦCh1-ΔORF75 novR are depicted. After restriction of the ΦCh1 DNA of *N. magadii* L11 and of *N. magadii* L11-ΔORF75 novR with *Bam*HI, fragments of the sizes 1960bp for the ΦCh1 DNA and 3740bp for ΦCh1-ΔORF75 novR DNA can be found. The biotinylated probe, made with a PCR from the ΦCh1 DNA of *N. magadii* L11 with the primers Δ75-3en1 and Δ75-3en-5, binds between the shown arrows (→ ←) downstream of the target region. This probe fragment has a length of 290 bp.

A positive culture of *N. magadii* L11-ΔORF75 novR from the PCR results and a wild type *N. magadii* L11 culture were grown until complete lysis and the virus particles were isolated. The DNA of both viruses ΦCh1 and ΦCh1-ΔORF75 novR was isolated and purified. Following this, the restrictions of the DNA with *Bam*HI and *Pst*I were performed. The DNA which was restricted with *Pst*I was used for the 5'-end analysis and the DNA restricted with *Bam*HI was used for the 3'-end analysis. The digested DNA was loaded onto a 0.8% agarose gel (Figure 50 A and C), from which the DNA was transferred to a nylon membrane via a capillary blot. The biotinylated probes for the 5'- and 3'-end were amplified via PCR from the ΦCh1 DNA of *N. magadii* L11 with the primers Δ75-5en1 and Δ75-5en-3, and with the primers Δ75-3en1 and Δ75-3en-5, respectively. The resulting probes have a length of 568bp for the 5'-end and 290bp for the 3'-end. The probes were hybridized to the corresponding regions on the fragments of the ΦCh1 and ΦCh1-ΔORF75 novR DNA (Figure 50 B and D).

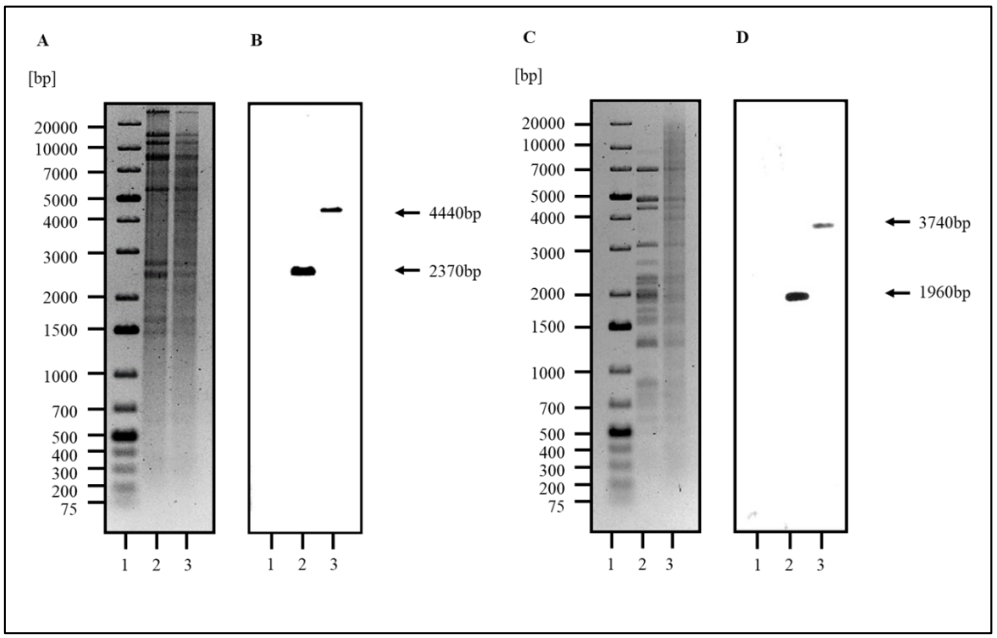

Figure 50. Southern blot analysis of ΦCh1 and ΦCh1-ΔORF75 novR at the 5'-end and 3'-end.
A. Restriction pattern on a 0.8% agarose gel of ΦCh1 (Lane 2) and ΦCh1-ΔORF75 novR (Lane 3) with the restriction enzyme *Pst*I. The ThermoFischer Scientific 1-kb plus DNA ladder (Lane 1) was used as size control.
B. Southern blot hybridization pattern of the 5'-end of ΦCh1 (Lane 2) and ΦCh1-ΔORF75 novR (Lane 3) with the biotinylated probe, made with a PCR from the ΦCh1 DNA of *N. magadii* L11 with the primers Δ75-5en1 and Δ75-5en-3. The size of the expected signals for ΦCh1 (2370bp) and ΦCh1-ΔORF75 novR (4440bp) are indicated with an arrow on the right side. The ThermoFischer Scientific 1-kb plus DNA ladder (Lane 1) was used.
C. Restriction pattern on a 0.8% agarose gel of ΦCh1 (Lane 2) and ΦCh1-ΔORF75 novR (Lane 3) with the restriction enzyme *Bam*HI. The ThermoFischer Scientific 1-kb plus DNA ladder (Lane 1) was used as size control.
D. Southern blot hybridization pattern of the 3'-end of ΦCh1 (Lane 2) and ΦCh1-ΔORF75 novR (Lane 3) with the biotinylated probe, made with a PCR from the ΦCh1 DNA of *N. magadii* L11 with the primers Δ75-3en1 and Δ75-3en-5. The size of the expected signals for ΦCh1 (1960bp) and ΦCh1-ΔORF75 novR (3740bp) are indicated with an arrow on the right side. The ThermoFischer Scientific 1-kb plus DNA ladder (Lane 1) was used.

For the 5'-end hybridization pattern a signal is, as expected, at 2370bp for ΦCh1 and at 4440bp for ΦCh1-ΔORF75 novR. Analogous, the 3'-end signals can be seen at 1960bp for ΦCh1 and at 3740bp for ΦCh1-ΔORF75 novR (Figure 50 B and D). These results verify the correct incorporation of the novobiocin resistance cassette, replacing the ORF75. After the confirmation of the deletion, the growth kinetics, viral titer and gene expression of selected ORFs can be analysed.

4.2.3 Time series analysis

The next step, after verifying the deletion of the ORF75, was the analysis of the time course of the deletion strain compared to the *N. magadii* L11 wild type. Over the time span of seven days cultures from *N. magadii* L11 and from *N. magadii* L11-ΔORF75 novR were grown in NVM^+ CAA media, with novobiocin for the mutant strain. Every day the optical density (OD_{600}) was measured and samples of the whole-protein extract and the titer were taken. These were afterwards analysed concerning their growth, the lysis, the active virus particles and the protein concentrations of selected proteins.

4.2.3.1 Growth kinetics of *N. magadii* L11-ΔORF75 novR

Every 24 hours, for seven days, the optical density (OD_{600}) of *N. magadii* L11-ΔORF75 novR cultures and, for comparison, a *N. magadii* L11 culture were measured, to analyse the growth kinetics (Figure 51).

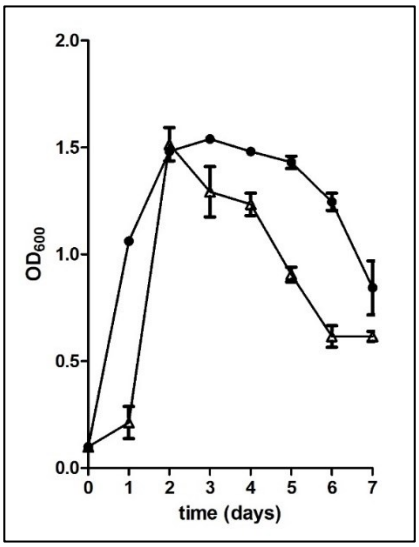

Figure 51. Growth kinetics analysis of *N. magadii* L11 and of *N. magadii* L11-ΔORF75 novR. *N. magadii* L11 was grown in NVM^+ CAA media for seven days and *N. magadii* L11-ΔORF75 novR was grown in NVM^+ CAA with novobiocin media for seven days. The optical densities of *N. magadii* L11 (●) and *N. magadii* L11-ΔORF75 novR (△) were measured at 600nm for every day. Error bars (±1SD) are indicated.

N. magadii L11 starts with a strong incline from inoculation to day one. The culture reaches its peak on day three, which is followed by the beginning of the lysis on day four, with the first strong decline. The strongest decrease in cell density was from day

six to seven. The growth curve of *N. magadii* L11-ΔORF75 novR begins with a weak increase in optical density but reaches fast its maximum on day two and declines on day three. This first decrease showed a steep curve, but the strongest decline was observed from day four to day five.

In comparison, the wild type strain shows a faster growth from the day of the inoculation to the first day, but from day one to day two the deletion mutant strain shows a stronger increase of optical density, resulting in the same optical density of both strains on day two. The different growth speed at the beginning could have been because of different states in the pre-culture, but these were grown to approximately the same optical density. The deletion strain shows an earlier lysis, than the wild type and an overall lower density, except on day two. The decline of the growth curve after lysis of the mutant strain is stronger than the one from the wild type strain. (Figure 51). These differences indicate that the influence of the deletion of ORF75 on the growth and lysis behaviour, shows to be negative on the growth, with a decreased cell density, but positive on the lysis behaviour, with strong declines. To further analyse the effects on the lysis and infectious viral particles the next step was a viral titer analysis.

4.2.3.2 Viral titer analysis of *N. magadii* L11-ΔORF75 novR

Each day of the seven-day time series viral titer probes were collected from *N. magadii* L11 and *N. magadii* L11-ΔORF75 novR and used to quantify the actively infectious viral particles. Therefore, a soft agar plaque assay was performed, where a *N. magadii* L13 strain was infected with the viral particles and the infected *N. magadii* formed plaques on the soft agar. The plaque forming units were estimated from these plates every day.

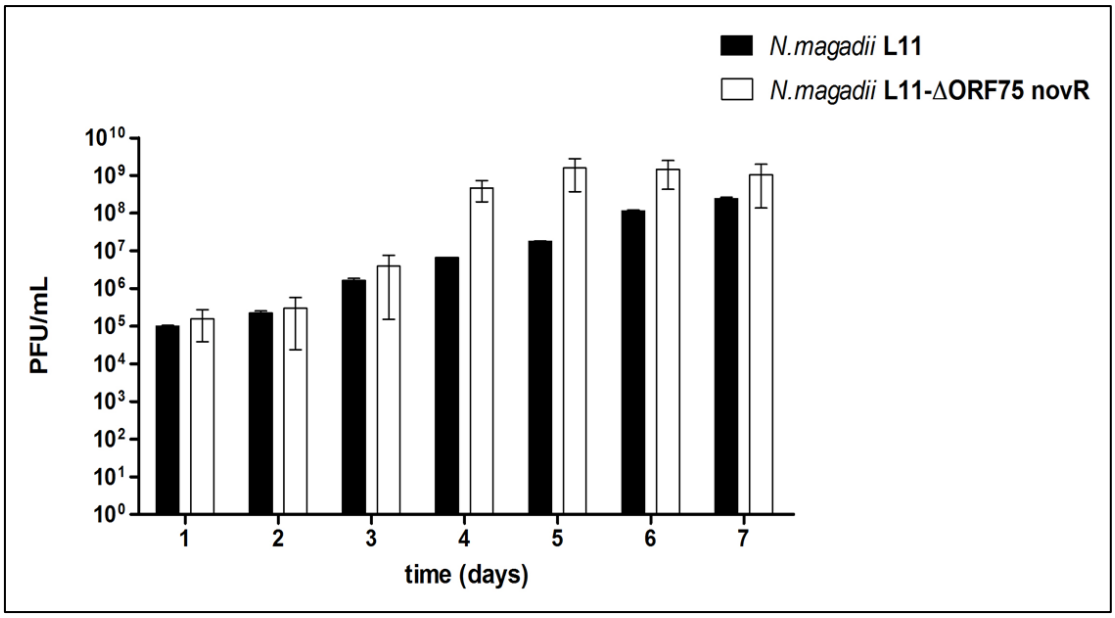

Figure 52. Plating efficiency and viral titer of *N. magadii* L11 and of *N. magadii* L11-ΔORF75 novR. *N. magadii* L11 was grown in NVM$^+$ CAA media for seven days and *N. magadii* L11-ΔORF75 novR was grown in NVM$^+$ CAA with novobiocin media for seven days. Every day the supernatant of *N. magadii* L11 (black bars) and *N. magadii* L11-ΔORF75 novR (white bars) was collected and used to infect the cured strain *N. magadii* L13, to estimate the viral titer**.** Error bars (±1SD) are indicated.

N. magadii L11 shows an increase in plaque forming units each day, with PFU/mL between 10^5 to 10^8. The lysis of the wildtype strain started on day four, after which an increase in viral load can be seen as expected (Figure 52). Similarly, for *N. magadii* L11-ΔORF75 novR an monotonous increase in viral titer each day could be observed, with PFU/mL between 10^5 to 10^9. On the third day started the lysis of the deletion strain, a slight increase in viral load can be seen from day two to day three. A big increase of plaque forming units occurred from day three to day four in the deletion strain (Figure 52).

Between the days four and seven the deletion strain shows higher PFUs/mL than the wildtype strain. This indicates that the deletion of the ORF75 has a positive impact in the quantity of the actively infectious viral particles after the fourth day. Since the lysis of the deletion strain started on the third day, but the significantly bigger increase of viral titer than the wildtype strain can only be observed form the fourth day on, it can be concluded that the deletion shows an earlier lysis but not an effect on earlier production of actively infectious virus particles and an effect on the higher production only after a day after the beginning of the lysis.

4.2.3.3 Western Blot analysis of *N. magadii* L11-ΔORF75 novR

Methyltransferase

The methyltransferase protein was detectable in *N. magadii* L11 from the third day on, which is the day before lysis started, since the viral proteins were synthesised shortly before the virus was released. *N. magadii* L11-ΔORF75 novR showed the onset of methyltransferase production on the third day, even though the lysis started the day before, but no significant increase in active virus particles can be seen in the viral titer analysis. The mutant strain shows a similar concentration pattern as the wild type strain, except with slightly but not significantly lesser methyltransferase on the days three and four (Figure 53 and Figure 54).

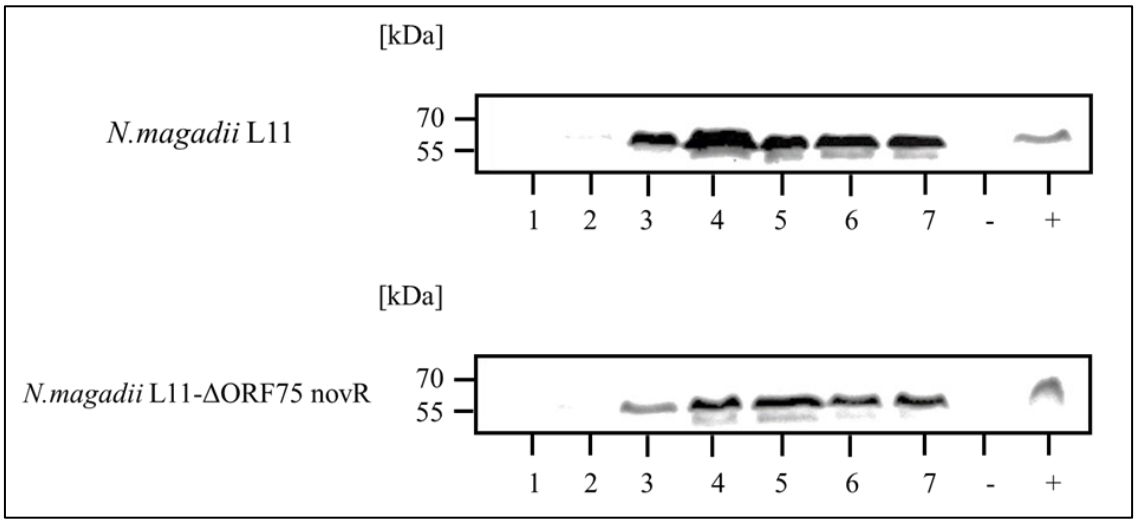

Figure 53. Western blot of *N. magadii* L11 and of *N. magadii* L11-ΔORF75 novR time series samples with antibodies against the methyltransferase. *N. magadii* L11 was grown in NVM$^+$ CAA media for seven days and *N. magadii* L11-ΔORF75 novR was grown in NVM$^+$ CAA with novobiocin media for seven days. Every day whole protein-extract samples of *N. magadii* L11 (top panel; Lanes 1-7) and *N. magadii* L11-ΔORF75 novR (bottom panel; Lanes 1-7) were collected and used for western blot analysis. As positive and negative control the whole protein-extract of *N. magadii* L11 (+) and *N. magadii* L13 (-), respectively, were used. For the detection of the methyltransferase the α - methyltransferase antibody was used, and the protein has a size of 46 kDa, calculated from the sequence. Due to the low pI, the protein migrates app at a size of 60kDa.

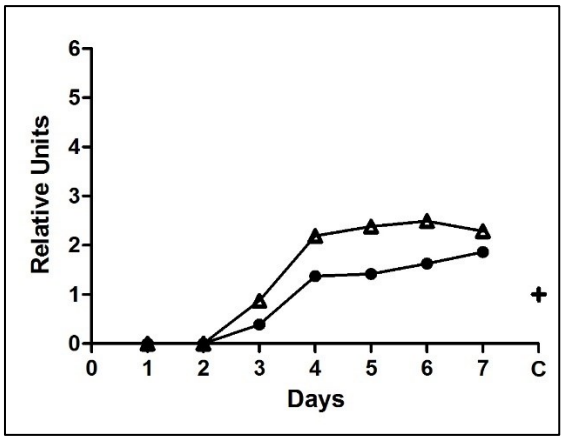

Figure 54. Relative protein levels of *N. magadii* L11 and of *N. magadii* L11-ΔORF75 novR with antibodies against the methyltransferase. Every day whole protein-extract samples of *N. magadii* L11 (●) and *N. magadii* L11-ΔORF75 novR (△) were collected and used for western blot analysis. As positive control the whole protein-extract of *N. magadii* L11 (+, C) was used. The relative values were calculated in respect to the positive control. For the western blot detection of the methyltransferase the α - methyltransferase antibody was used. The analysis was performed with Image Lab Software from Bio Rad.

protein E

The first signal of the major capsid protein E in *N. magadii* L11 and of *N. magadii* L11-ΔORF75 novR showed up at day three and the concentrations increased afterwards. The protein is thereby synthesised a day before lysis for *N. magadii* L11, but a day after lysis for *N. magadii* L11-ΔORF75 novR. When looking at the viral titer the amount of actively infectious viral particles stayed the same from day one to three. There was a slight decline in concentration on the last day of the time course in *N. magadii* L11. The concentrations of both strains show no significant difference of protein E (Figure 55 and Figure 56).

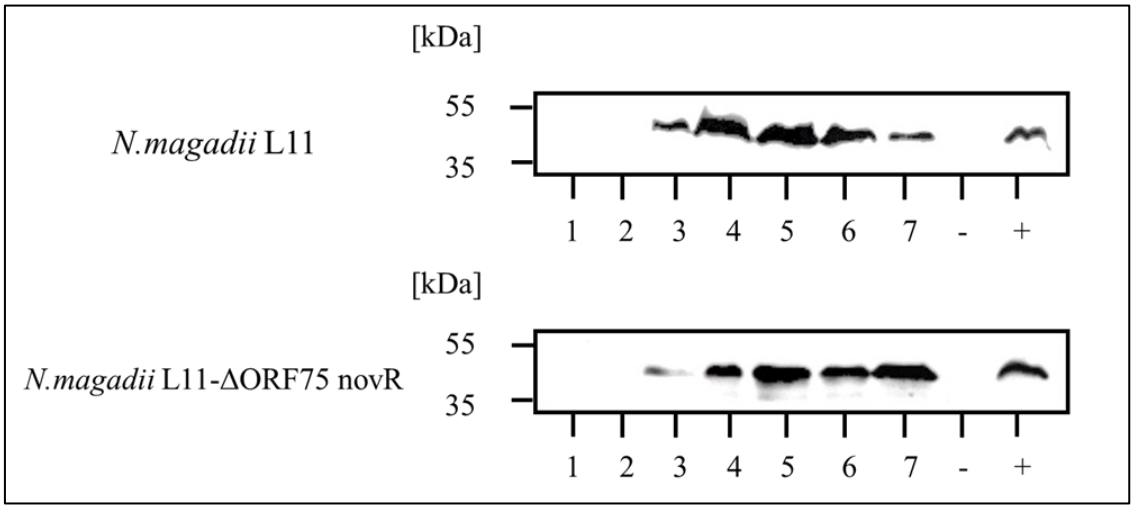

Figure 55. Western blot of *N. magadii* L11 and of *N. magadii* L11-ΔORF75 novR time series samples with antibodies against the major capsid protein E. *N. magadii* L11 was grown in NVM$^+$ CAA media for seven days and *N. magadii* L11-ΔORF75 novR was grown in NVM$^+$ CAA with novobiocin media for ten days. Every day whole protein-extract samples of *N. magadii* L11 (top panel; Lanes 1-7) and *N. magadii* L11-ΔORF75 novR (bottom panel; Lanes 1-7) were collected and used for western blot analysis. As positive and negative control the whole protein-extract of *N. magadii* L11 (+) and *N. magadii* L13 (-), respectively, were used. For the detection of the protein E the α- protein E antibody was used, and the protein has a size of 50 kDa.

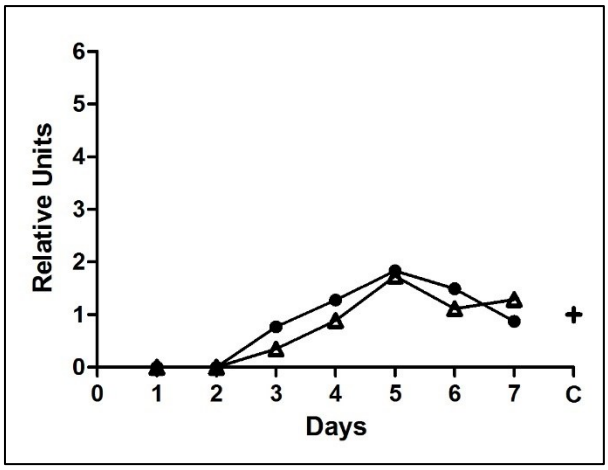

Figure 56. Relative protein levels of *N. magadii* L11 and of *N. magadii* L11-ΔORF75 novR with antibodies against the major capsid protein E. Every day whole protein-extract samples of *N. magadii* L11 (●) and *N. magadii* L11-ΔORF75 novR (△) were collected and used for western blot analysis. As positive control the whole protein-extract of *N. magadii* L11 (+, C) was used. The relative values were calculated in respect to the positive control. For the western blot detection of the protein E the α-protein E antibody was used. The analysis was performed with Image Lab Software from Bio Rad.

gp34

The viral tail fiber protein gp34 was measurable from day three onwards and increased until day seven for *N. magadii* L11. A similar concentration pattern was observed in *N. magadii* L11-ΔORF75 novR, with the only difference a slightly lower concentration on day three (Figure 57 and Figure 58). Here, as for the methyltransferase and protein E, the protein was detectable one day after the decline in the growth curve, and thereby after the beginning of lysis, but the viral titer showed no increase in active virus for *N. magadii* L11-ΔORF75 novR.

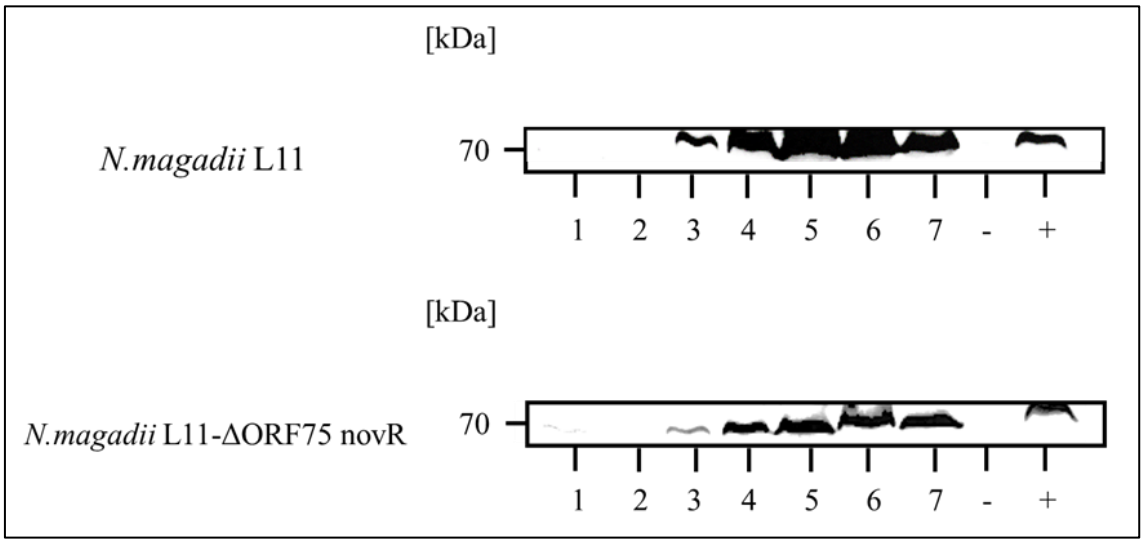

Figure 57. Western blot of *N. magadii* L11 and of *N. magadii* L11-ΔORF75 novR time series samples with antibodies against gp34. *N. magadii* L11 was grown in NVM$^+$ CAA media for seven days and *N. magadii* L11-ΔORF75 novR was grown in NVM$^+$ CAA with novobiocin media for ten days. Every day whole protein-extract samples of *N. magadii* L11 (top panel; Lanes 1-7) and *N. magadii* L11-ΔORF75 novR (bottom panel; Lanes 1-7) were collected and used for western blot analysis. As positive and negative control the whole protein-extract of *N. magadii* L11 (+) and *N. magadii* L13 (-), respectively, were used. For the detection of gp34 the α-gp34$_{52}$ (rabbit #20) antibody was used and the protein has a size of 66 kDa.

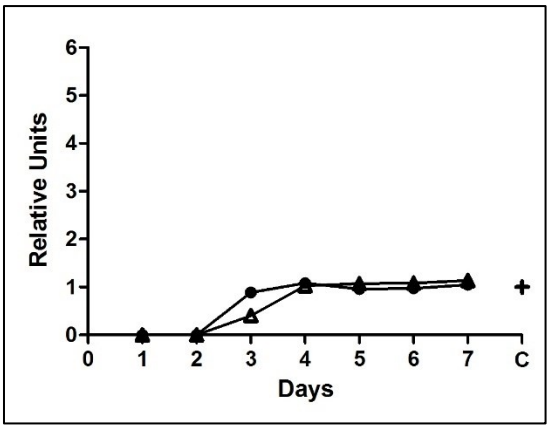

Figure 58. Relative protein levels of *N. magadii* L11 and of *N. magadii* L11-ΔORF75 novR with antibodies against gp34. Every day whole protein-extract samples of *N. magadii* L11 (●) and *N. magadii* L11-ΔORF75 novR (△) were collected and used for western blot analysis. As positive control the whole protein-extract of *N. magadii* L11 (+, C) was used. The relative values were calculated in respect to the positive control. For the western blot detection of gp34 the α-gp34$_{52}$ (rabbit #20) antibody was used. The analysis was performed with Image Lab Software from Bio Rad.

4.2.4 Discussion

Deleting the ORF75, from ΦCh1 in its natural host *N. magadii*, to investigate the effects and get further inside into its role in the lytic cycle, was shown to have worked. The ORF75 was deleted via homologous recombination of the novobiocin resistance cassette and then the growth behaviour, gene expression and viral titer was analysed to see if the lysis was affected. The deletion strain *N. magadii* L11-ΔORF75 novR showed to lyse a day earlier, on day two instead of three, and had a faster decline. This points towards a positive influence of the ORF75 on the growth and a negative effect on the lysis behaviour. The viral titer analysis showed that the deletion strain *N. magadii* L11-ΔORF75 novR produced more active virus particles than the wild type strain *N. magadii* L11, but only from day four on. Even though the earlier lysis was seen in the growth curve, the proteins methyltransferase, protein E and gp34, all important viral proteins, which normally are synthesized shortly before lysis, show up on the western blot analysis a day after lysis started. The protein concentrations are very similar in the deletion and the wild type strain, even though they showed to be slightly lighter at the beginning in the deletion strain. These findings show that the ORF75 plays a role in the growth and virus release, without significantly influencing the examined proteins. The underlying mechanism remains open and needs further investigation. How the ASCH domain plays a role in this regulation is still unclear, but these findings show that the lysis regulatory pathways are influenced by the gp75. Finding potential RNA targets of the ASCH domain- binding cleft could give further hints towards the underlying mechanism, this could be done with a CLIP/-seq analysis (Shema et al., 2020).

References

Ackermann, H. W. (1998). Tailed bacteriophages: the order caudovirales. *Advances in virus research*, *51*, 135–201. https://doi.org/10.1016/s0065-3527(08)60785-x

Ackermann, H. W., & Prangishvili, D. (2012). Prokaryote viruses studied by electron microscopy. *Archives of virology*, *157*(10), 1843–1849. https://doi.org/10.1007/s00705-012-1383-y

Albers, S. V., & Meyer, B. H. (2011). The Archaeal cell envelope. *Nature reviews. Microbiology*, *9*(6), 414–426. https://doi.org/10.1038/nrmicro2576

Allers, T., & Mevarech, M. (2005). Archaeal genetics - the third way. *Nature reviews. Genetics*, *6*(1), 58–73. https://doi.org/10.1038/nrg1504

Andrei, A. Ş., Banciu, H. L., & Oren, A. (2012). Living with salt: metabolic and phylogenetic diversity of Archaea inhabiting saline ecosystems. *FEMS microbiology letters*, *330*(1), 1–9. https://doi.org/10.1111/j.1574-6968.2012.02526.x

Baker, B. J., De Anda, V., Seitz, K. W., Dombrowski, N., Santoro, A. E., & Lloyd, K. G. (2020). Diversity, ecology and evolution of Archaea. *Nature microbiology*, *5*(7), 887–900. https://doi.org/10.1038/s41564-020-0715-z

Bamford, D. H. (2003). Do viruses form lineages across different domains of life?. *Research in microbiology*, *154*(4), 231–236. https://doi.org/10.1016/S0923-2508(03)00065-2

Baranyi, U., Klein, R., Lubitz, W., Krüger, D. H., & Witte, A. (2000). The Archaeal halophilic virus-encoded Dam-like methyltransferase M. phiCh1-I methylates adenine residues and complements dam mutants in the low salt environment of Escherichia coli. *Molecular microbiology*, *35*(5), 1168–1179. https://doi.org/10.1046/j.1365-2958.2000.01786.x

Bernander, R. (2000). Chromosome replication, nucleoid segregation and cell division in Archaea. *Trends in microbiology*, *8*(6), 278–283. https://doi.org/10.1016/s0966-842x(00)01760-1

Bertonati, C., Punta, M., Fischer, M., Yachdav, G., Forouhar, F., Zhou, W., Kuzin, A. P., Seetharaman, J., Abashidze, M., Ramelot, T. A., Kennedy, M. A., Cort, J. R., Belachew, A., Hunt, J. F., Tong, L., Montelione, G. T., & Rost, B. (2009). Structural genomics reveals EVE as a new ASCH/PUA-related domain. *Proteins*, *75*(3), 760–773. https://doi.org/10.1002/prot.22287

Bickle, T. A., & Krüger, D. H. (1993). Biology of DNA restriction. *Microbiological reviews*, *57*(2), 434–450. https://doi.org/10.1128/mr.57.2.434-450.1993

Breuert, S., Allers, T., Spohn, G., & Soppa, J. (2006). Regulated polyploidy in halophilic Archaea. *PloS one*, *1*(1), e92. https://doi.org/10.1371/journal.pone.0000092

Brown, J. R., & Doolittle, W. F. (1997). Archaea and the prokaryote-to-eukaryote transition. *Microbiology and molecular biology reviews : MMBR*, *61*(4), 456–502. https://doi.org/10.1128/mmbr.61.4.456-502.1997

Casadesús, J., & Low, D. (2006). Epigenetic gene regulation in the Bacterial world. *Microbiology and molecular biology reviews : MMBR*, *70*(3), 830–856. https://doi.org/10.1128/MMBR.00016-06

Cavicchioli, R. (Ed.). (2007). Archaea: Molecular and Cellular Biology. ASM Press. https://doi.org/10.1128/9781555815516.

Cavicchioli, R., Curmi, P. M., Saunders, N., & Thomas, T. (2003). Pathogenic Archaea: do they exist?. *BioEssays : news and reviews in molecular, cellular and developmental biology*, *25*(11), 1119–1128. https://doi.org/10.1002/bies.10354

Comai, L. (2005). The advantages and disadvantages of being polyploid. *Nature reviews. Genetics*, *6*(11), 836–846. https://doi.org/10.1038/nrg1711

Cook, G. M., Russell, J. B., Reichert, A., & Wiegel, J. (1996). The Intracellular pH of Clostridium paradoxum, an Anaerobic, Alkaliphilic, and Thermophilic Bacterium. *Applied and environmental microbiology*, *62*(12), 4576–4579. https://doi.org/10.1128/aem.62.12.4576-4579.1996

da Costa, M. S., Santos, H., & Galinski, E. A. (1998). An overview of the role and diversity of compatible solutes in Bacteria and Archaea. *Advances in biochemical engineering/biotechnology*, *61*, 117–153. https://doi.org/10.1007/BFb0102291

De Rosa, M., & Gambacorta, A. (1988). The lipids of archaebacteria. *Progress in lipid research*, *27*(3), 153–175. https://doi.org/10.1016/0163-7827(88)90011-2

DeLong, E. F. (1998). Everything in moderation: Archaea as 'non-extremophiles'. *Current opinion in genetics & development*, *8*(6), 649–654. https://doi.org/10.1016/s0959-437x(98)80032-4

Edgell, D. R., & Doolittle, W. F. (1997). Archaea and the origin(s) of DNA replication proteins. *Cell*, *89*(7), 995–998. https://doi.org/10.1016/s0092-8674(00)80285-8

Eme, L., Spang, A., Lombard, J., Stairs, C. W., & Ettema, T. J. G. (2017). Archaea and the origin of eukaryotes. *Nature reviews. Microbiology*, *15*(12), 711–723. https://doi.org/10.1038/nrmicro.2017.133

Forterre, P. (2013). The common ancestor of Archaea and Eukarya was not an archaeon. *Archaea (Vancouver, B.C.)*, *2013*, 372396. https://doi.org/10.1155/2013/372396

Fu, Y., Luo, G. Z., Chen, K., Deng, X., Yu, M., Han, D., Hao, Z., Liu, J., Lu, X., Dore, L. C., Weng, X., Ji, Q., Mets, L., & He, C. (2015). N6-methyldeoxyadenosine marks active transcription start sites in Chlamydomonas. *Cell*, *161*(4), 879–892. https://doi.org/10.1016/j.cell.2015.04.010

Gambacorta, A., Gliozzi, A., & De Rosa, M. (1995). Archaeal lipids and their biotechnological applications. *World journal of microbiology & biotechnology*, *11*(1), 115–131. https://doi.org/10.1007/BF00339140

Grant, W. D., Gemmell, R. T., & McGenity, T. J. (1998). Halobacteria: the evidence for longevity. *Extremophiles : life under extreme conditions*, *2*(3), 279–287. https://doi.org/10.1007/s007920050070

Guffanti, A. A., & Hicks, D. B. (1991). Molar growth yields and bioenergetic parameters of extremely alkaliphilic Bacillus species in batch cultures, and growth in a chemostat at pH 10.5. *Journal of general microbiology*, *137*(10), 2375–2379. https://doi.org/10.1099/00221287-137-10-2375

Guy, L., & Ettema, T. J. (2011). The Archaeal 'TACK' superphylum and the origin of eukaryotes. *Trends in microbiology*, *19*(12), 580–587. https://doi.org/10.1016/j.tim.2011.09.002

Haider, F. (2009). *Characterization of the DNA methyltransferase M .Nma Φ Ch1I and further characterization of a transformation system of haloalkaliphilic Archaea* (diploma's thesis, University of Vienna)

Haines, T. H., & Dencher, N. A. (2002). Cardiolipin: a proton trap for oxidative phosphorylation. *FEBS letters*, *528*(1-3), 35–39. https://doi.org/10.1016/s0014-5793(02)03292-1

Holmes, M. L., Nuttall, S. D., & Dyall-Smith, M. L. (1991). Construction and use of halobacterial shuttle vectors and further studies on Haloferax DNA gyrase. *Journal of bacteriology*, *173*(12), 3807–3813. https://doi.org/10.1128/jb.173.12.3807-3813.1991

Holmes, M. L., Scopes, R. K., Moritz, R. L., Simpson, R. J., Englert, C., Pfeifer, F., & Dyall-Smith, M. L. (1997). Purification and analysis of an extremely halophilic beta-galactosidase from Haloferax alicantei. *Biochimica et biophysica acta*, *1337*(2), 276–286. https://doi.org/10.1016/s0167-4838(96)00174-4

Horikoshi K. (1999). Alkaliphiles: some applications of their products for biotechnology. *Microbiology and molecular biology reviews : MMBR*, *63*(4), 735–750. https://doi.org/10.1128/MMBR.63.4.735-750.1999

Hug, L. A., Baker, B. J., Anantharaman, K., Brown, C. T., Probst, A. J., Castelle, C. J., Butterfield, C. N., Hernsdorf, A. W., Amano, Y., Ise, K., Suzuki, Y., Dudek, N., Relman, D. A., Finstad, K. M., Amundson, R., Thomas, B. C., & Banfield, J. F.

(2016). A new view of the tree of life. *Nature microbiology*, *1*, 16048. https://doi.org/10.1038/nmicrobiol.2016.48

Hunte, C., Screpanti, E., Venturi, M., Rimon, A., Padan, E., & Michel, H. (2005). Structure of a Na+/H+ antiporter and insights into mechanism of action and regulation by pH. *Nature*, *435*(7046), 1197–1202. https://doi.org/10.1038/nature03692

Iro, M. (2006). *Characterisation of the regulatory region of the virus ΦCh1 infecting Natrialba magadii*. (Dissertation, University of Vienna)

Iro, M., Klein, R., Gálos, B., Baranyi, U., Rössler, N., & Witte, A. (2007). The lysogenic region of virus phiCh1: identification of a repressor-operator system and determination of its activity in halophilic Archaea. *Extremophiles : life under extreme conditions*, *11*(2), 383–396. https://doi.org/10.1007/s00792-006-0040-3

Ito, M., Guffanti, A. A., Zemsky, J., Ivey, D. M., & Krulwich, T. A. (1997). Role of the nhaC-encoded Na+/H+ antiporter of alkaliphilic Bacillus firmus OF4. *Journal of bacteriology*, *179*(12), 3851–3857. https://doi.org/10.1128/jb.179.12.3851-3857.1997

Iyer, L. M., Burroughs, A. M., & Aravind, L. (2006). The ASCH superfamily: novel domains with a fold related to the PUA domain and a potential role in RNA metabolism. *Bioinformatics (Oxford, England)*, *22*(3), 257–263. https://doi.org/10.1093/bioinformatics/bti767

Jarrell, K. F., Jones, G. M., & Nair, D. B. (2010). Biosynthesis and role of N-linked glycosylation in cell surface structures of Archaea with a focus on flagella and s layers. *International journal of microbiology*, *2010*, 470138. https://doi.org/10.1155/2010/470138

Jarrell, K. F., Walters, A. D., Bochiwal, C., Borgia, J. M., Dickinson, T., & Chong, J. P. J. (2011). Major players on the microbial stage: why Archaea are important. *Microbiology (Reading, England)*, *157*(Pt 4), 919–936. https://doi.org/10.1099/mic.0.047837-0

Jones, P. A., & Takai, D. (2001). The role of DNA methylation in mammalian epigenetics. *Science (New York, N.Y.)*, *293*(5532), 1068–1070. https://doi.org/10.1126/science.1063852

Kamekura, M., Dyall-Smith, M. L., Upasani, V., Ventosa, A., & Kates, M. (1997). Diversity of alkaliphilic haloBacteria: proposals for transfer of Natronobacterium vacuolatum, Natronobacterium magadii, and Natronobacterium pharaonis to Halorubrum, Natrialba, and Natronomonas gen. nov., respectively, as Halorubrum vacuolatum comb. nov., Natrialba magadii comb. nov., and Natronomonas pharaonis comb. nov., respectively. *International journal of systematic bacteriology*, *47*(3), 853–857. https://doi.org/10.1099/00207713-47-3-853

Karner, M. B., DeLong, E. F., & Karl, D. M. (2001). Archaeal dominance in the mesopelagic zone of the Pacific Ocean. *Nature*, *409*(6819), 507–510. https://doi.org/10.1038/35054051

Kates, M., Kushner, D. & Matheson, A. T. (1993). The Biochemistry of Archaea (Archaebacteria). In New comprehensive biochemistry. https://doi.org/10.1016/s0167-7306(08)x6015-6

Keeling, P. J., Charlebois, R. L. & Doolittle, W. F. (1994). Archaebacterial genomes: eubacterial form and eukaryotic content. *Current Opinion in Genetics & Development*, *4*(6), 816–822. https://doi.org/10.1016/0959-437x(94)90065-5

Kim S. H. (1998). Shining a light on structural genomics. *Nature structural biology*, *5 Suppl*, 643–645. https://doi.org/10.1038/1334

Kim, B. N., Shin, M., Ha, S. C., Park, S. Y., Seo, P. W., Hofmann, A., & Kim, J. S. (2017). Crystal structure of an ASCH protein from Zymomonas mobilis and its ribonuclease activity specific for single-stranded RNA. *Scientific reports*, *7*(1), 12303. https://doi.org/10.1038/s41598-017-12186-w

Kim, H. J., Yi, J. Y., Sung, H. S., Moore, D. D., Jhun, B. H., Lee, Y. C., & Lee, J. W. (1999). Activating signal cointegrator 1, a novel transcription coactivator of nuclear receptors, and its cytosolic localization under conditions of serum deprivation. *Molecular and cellular biology*, *19*(9), 6323–6332. https://doi.org/10.1128/MCB.19.9.6323

Kitada, M., Hashimoto, M., Kudo, T. & Horikoshi, K. (1994). Properties of two different Na+/H+ antiport systems in alkaliphilic Bacillus sp. strain C-125. *Journal Of Bacteriology*, *176*(21), 6464–6469. https://doi.org/10.1128/jb.176.21.6464-6469.1994

Klein, R., Baranyi, U., Rössler, N., Greineder, B., Scholz, H., & Witte, A. (2002). Natrialba magadii virus phiCh1: first complete nucleotide sequence and functional organization of a virus infecting a haloalkaliphilic archaeon. *Molecular microbiology*, *45*(3), 851–863. https://doi.org/10.1046/j.1365-2958.2002.03064.x

Klein, R., Greineder, B., Baranyi, U., & Witte, A. (2000). The structural protein E of the Archaeal virus phiCh1: evidence for processing in Natrialba magadii during virus maturation. *Virology*, *276*(2), 376–387. https://doi.org/10.1006/viro.2000.0565

Klingl, A., Pickl, C., & Flechsler, J. (2019). Archaeal Cell Walls. *Sub-cellular biochemistry*, *92*, 471–493. https://doi.org/10.1007/978-3-030-18768-2_14

Krüger, D. H., & Bickle, T. A. (1983). Bacteriophage survival: multiple mechanisms for avoiding the deoxyribonucleic acid restriction systems of their

hosts. *Microbiological reviews*, *47*(3), 345–360. https://doi.org/10.1128/mr.47.3.345-360.1983

Kushner, D. J. (1978). Life in high salt and solute concentrations. In D. J. Kushner (Ed.), *Microbial life in extreme environments* (pp. 318-368). Academic Press.

Lanyi J. K. (1974). Salt-dependent properties of proteins from extremely halophilic Bacteria. *Bacteriological reviews*, *38*(3), 272–290. https://doi.org/10.1128/br.38.3.272-290.1974

Lanyi, J. K., Helgerson, S. L., & Silverman, M. P. (1979). Relationship between proton motive force and potassium ion transport in Halobacterium halobium envelope vesicles. *Archives of biochemistry and biophysics*, *193*(2), 329–339. https://doi.org/10.1016/0003-9861(79)90037-7

Lloyd, K. G., May, M. K., Kevorkian, R. T., & Steen, A. D. (2013). Meta-analysis of quantification methods shows that Archaea and Bacteria have similar abundances in the subseafloor. *Applied and environmental microbiology*, *79*(24), 7790–7799. https://doi.org/10.1128/AEM.02090-13

Luk, A. W., Williams, T. J., Erdmann, S., Papke, R. T., & Cavicchioli, R. (2014). Viruses of haloarchaea. *Life (Basel, Switzerland)*, *4*(4), 681–715. https://doi.org/10.3390/life4040681

Lurie-Weinberger, M. N., & Gophna, U. (2015). Archaea in and on the Human Body: Health Implications and Future Directions. *PLoS pathogens*, *11*(6), e1004833. https://doi.org/10.1371/journal.ppat.1004833

Ma, Y., Galinski, E. A., Grant, W. D., Oren, A., & Ventosa, A. (2010). Halophiles 2010: life in saline environments. *Applied and environmental microbiology*, *76*(21), 6971–6981. https://doi.org/10.1128/AEM.01868-10

Madern, D., Ebel, C., & Zaccai, G. (2000). Halophilic adaptation of enzymes. *Extremophiles : life under extreme conditions*, *4*(2), 91–98. https://doi.org/10.1007/s007920050142

Makarova, K. S., Krupovic, M., & Koonin, E. V. (2014). Evolution of replicative DNA polymerases in Archaea and their contributions to the eukaryotic replication machinery. *Frontiers in microbiology*, *5*, 354. https://doi.org/10.3389/fmicb.2014.00354

Malone, T., Blumenthal, R. M., & Cheng, X. (1995). Structure-guided analysis reveals nine sequence motifs conserved among DNA amino-methyltransferases, and suggests a catalytic mechanism for these enzymes. *Journal of molecular biology*, *253*(4), 618–632. https://doi.org/10.1006/jmbi.1995.0577

Margesin, R., & Schinner, F. (2001). Potential of halotolerant and halophilic microorganisms for biotechnology. *Extremophiles : life under extreme conditions*, *5*(2), 73–83. https://doi.org/10.1007/s007920100184

Marinus, M. G., & Morris, N. R. (1973). Isolation of deoxyribonucleic acid methylase mutants of Escherichia coli K-12. *Journal of bacteriology*, *114*(3), 1143–1150. https://doi.org/10.1128/jb.114.3.1143-1150.1973

May, M. S., & Hattman, S. (1975). Analysis of bacteriophage deoxyribonucleic acid sequences methylated by host- and R-factor-controlled enzymes. *Journal of bacteriology*, *123*(2), 768–770. https://doi.org/10.1128/jb.123.2.768-770.1975

Mayrhofer-Iro, M., Ladurner, A., Meissner, C., Derntl, C., Reiter, M., Haider, F., Dimmel, K., Rössler, N., Klein, R., Baranyi, U., Scholz, H., & Witte, A. (2013). Utilization of virus φCh1 elements to establish a shuttle vector system for Halo(alkali)philic Archaea via transformation of Natrialba magadii. *Applied and environmental microbiology*, *79*(8), 2741–2748. https://doi.org/10.1128/AEM.03287-12

Mesbah, N. M., Cook, G. M., & Wiegel, J. (2009). The halophilic alkalithermophile Natranaerobius thermophilus adapts to multiple environmental extremes using a large repertoire of Na(K)/H antiporters. *Molecular microbiology*, *74*(2), 270–281. https://doi.org/10.1111/j.1365-2958.2009.06845.x

Mevarech, M., Frolow, F., & Gloss, L. M. (2000). Halophilic enzymes: proteins with a grain of salt. *Biophysical chemistry*, *86*(2-3), 155–164. https://doi.org/10.1016/s0301-4622(00)00126-5

Modrich, P., & Lahue, R. (1996). Mismatch repair in replication fidelity, genetic recombination, and cancer biology. *Annual review of biochemistry*, *65*, 101–133. https://doi.org/10.1146/annurev.bi.65.070196.000533

Nelson, M., & McClelland, M. (1987). The effect of site-specific methylation on restriction-modification enzymes. *Nucleic acids research*, *15 Suppl*(Suppl), r219–r230. https://doi.org/10.1093/nar/15.suppl.r219

Norris, P. R., Burton, N. P., & Foulis, N. A. (2000). Acidophiles in bioreactor mineral processing. *Extremophiles : life under extreme conditions*, *4*(2), 71–76. https://doi.org/10.1007/s007920050139

Olsen, G. J., & Woese, C. R. (1997). Archaeal genomics: an overview. *Cell*, *89*(7), 991–994. https://doi.org/10.1016/s0092-8674(00)80284-6

Oren A. (1999). Bioenergetic aspects of halophilism. *Microbiology and molecular biology reviews : MMBR*, *63*(2), 334–348. https://doi.org/10.1128/MMBR.63.2.334-348.1999

Oren A. (2002). Diversity of halophilic microorganisms: environments, phylogeny, physiology, and applications. *Journal of industrial microbiology & biotechnology*, *28*(1), 56–63. https://doi.org/10.1038/sj/jim/7000176

Oren, A. (2006). The Order Halobacteriales. In: Dworkin, M., Falkow, S., Rosenberg, E., Schleifer, KH., Stackebrandt, E. (eds) *The Prokaryotes*. Springer, New York, NY. https://doi.org/10.1007/0-387-30743-5_8

Oren, A., Bratbak, G., & Heldal, M. (1997). Occurrence of virus-like particles in the Dead Sea. *Extremophiles : life under extreme conditions*, *1*(3), 143–149. https://doi.org/10.1007/s007920050027

Palmer, B. R., & Marinus, M. G. (1994). The dam and dcm strains of Escherichia coli--a review. *Gene*, *143*(1), 1–12. https://doi.org/10.1016/0378-1119(94)90597-5

Pikuta, E. V. (2011). Overview of Archaea. *Instruments, methods, and missions for astrobiology XIV*, 8152, 176-190.

Pikuta, E. V., Hoover, R. B., & Tang, J. (2007). Microbial extremophiles at the limits of life. *Critical reviews in microbiology*, *33*(3), 183–209. https://doi.org/10.1080/10408410701451948

Pohlschroder, M., Pfeiffer, F., Schulze, S., & Abdul Halim, M. F. (2018). Archaeal cell surface biogenesis. *FEMS microbiology reviews*, *42*(5), 694–717. https://doi.org/10.1093/femsre/fuy027

Prangishvili, D. (2013). The wonderful world of Archaeal viruses. *Annual review of microbiology*, *67*, 565–585. https://doi.org/10.1146/annurev-micro-092412-155633

Rodrigues-Oliveira, T., Belmok, A., Vasconcellos, D., Schuster, B., & Kyaw, C. M. (2017). Archaeal S-Layers: Overview and Current State of the Art. *Frontiers in microbiology*, *8*, 2597. https://doi.org/10.3389/fmicb.2017.02597

Rothschild, L. J., & Mancinelli, R. L. (2001). Life in extreme environments. *Nature*, *409*(6823), 1092–1101. https://doi.org/10.1038/35059215

Sakai, H. D., Nur, N., Kato, S., Yuki, M., Shimizu, M., Itoh, T., Ohkuma, M., Suwanto, A., & Kurosawa, N. (2022). Insight into the symbiotic lifestyle of DPANN Archaea revealed by cultivation and genome analyses. *Proceedings of the National Academy of Sciences of the United States of America*, *119*(3), e2115449119. https://doi.org/10.1073/pnas.2115449119

Sali A. (1998). 100,000 protein structures for the biologist. *Nature structural biology*, *5*(12), 1029–1032. https://doi.org/10.1038/4136

Sauer, T., & Galinski, E. A. (1998). Bacterial milking: A novel bioprocess for production of compatible solutes. *Biotechnology and bioengineering*, *57*(3), 306–313.

Schumacher, K., Heine, E., & Höcker, H. (2001). Extremozymes for improving wool properties. *Journal of biotechnology*, *89*(2-3), 281–288. https://doi.org/10.1016/s0168-1656(01)00314-5

Sehgal, S. N., & Gibbsons, N. E. (1960). Effect of some metal ions on the growth of Halobacterium cutirubrum. *Canadian journal of microbiology*, *6*, 165–169. https://doi.org/10.1139/m60-018

Shahmohammadi, H. R., Asgarani, E., Terato, H., Saito, T., Ohyama, Y., Gekko, K., Yamamoto, O., & Ide, H. (1998). Protective roles of bacterioruberin and intracellular KCl in the resistance of Halobacterium salinarium against DNA-damaging agents. *Journal of radiation research*, *39*(4), 251–262. https://doi.org/10.1269/jrr.39.251

Shema Mugisha, C., Tenneti, K., & Kutluay, S. B. (2020). Clip for studying protein-RNA interactions that regulate virus replication. *Methods (San Diego, Calif.)*, *183*, 84–92. https://doi.org/10.1016/j.ymeth.2019.11.011

Sleytr, U. B., & Beveridge, T. J. (1999). Bacterial S-layers. *Trends in microbiology*, *7*(6), 253–260. https://doi.org/10.1016/s0966-842x(99)01513-9

Sommerkamp, G. (2022). *Characterization of mutant ϕCh1-ΔORF94 and investigation of ORF75 of ϕCh1: does it encode an activator?* (master's thesis, University of Vienna)

Stolt, P., & Zillig, W. (1994). Transcription of the halophage phi H repressor gene is abolished by transcription from an inversely oriented lytic promoter. *FEBS letters*, *344*(2-3), 125–128. https://doi.org/10.1016/0014-5793(94)00347-5

Sturr, M. G., Guffanti, A. A., & Krulwich, T. A. (1994). Growth and bioenergetics of alkaliphilic Bacillus firmus OF4 in continuous culture at high pH. *Journal of bacteriology*, *176*(11), 3111–3116. https://doi.org/10.1128/jb.176.11.3111-3116.1994

Teichmann, S. A., Chothia, C., & Gerstein, M. (1999). Advances in structural genomics. *Current opinion in structural biology*, *9*(3), 390–399. https://doi.org/10.1016/S0959-440X(99)80053-0

Tenchov, B., Vescio, E. M., Sprott, G. D., Zeidel, M. L., & Mathai, J. C. (2006). Salt tolerance of Archaeal extremely halophilic lipid membranes. *The Journal of biological chemistry*, *281*(15), 10016–10023. https://doi.org/10.1074/jbc.M600369200

Tindall, B. J., Ross, H. N. M., & Grant, W. D. (1984). *Natronobacterium* gen. nov. and *Natronococcus* gen. nov., Two New Genera of Haloalkaliphilic Archaebacteria. *Systematic and Applied Microbiology, 5*(1), 41-57. https://doi.org/10.1016/S0723-2020(84)80050-8

Wais, A. C., Kon, M., MacDonald, R. E., & Stollar, B. D. (1975). Salt-dependent bacteriophage infecting Halobacterium cutirubrum and H. halobium. *Nature*, *256*(5515), 314–315. https://doi.org/10.1038/256314a0

Williams, T. A., Cox, C. J., Foster, P. G., Szöllősi, G. J., & Embley, T. M. (2020). Phylogenomics provides robust support for a two-domains tree of life. *Nature ecology & evolution*, *4*(1), 138–147. https://doi.org/10.1038/s41559-019-1040-x

Wilson G. G. (1991). Organization of restriction-modification systems. *Nucleic acids research*, *19*(10), 2539–2566. https://doi.org/10.1093/nar/19.10.2539

Witte, A., Baranyi, U., Klein, R., Sulzner, M., Luo, C., Wanner, G., Krüger, D. H., & Lubitz, W. (1997). Characterization of Natronobacterium magadii phage phi Ch1, a unique Archaeal phage containing DNA and RNA. *Molecular microbiology*, *23*(3), 603–616. https://doi.org/10.1046/j.1365-2958.1997.d01-1879.x

Woese C. R. (1994). There must be a prokaryote somewhere: microbiology's search for itself. *Microbiological reviews*, *58*(1), 1–9. https://doi.org/10.1128/mr.58.1.1-9.1994

Woese, C. R., & Fox, G. E. (1977). Phylogenetic structure of the prokaryotic domain: the primary kingdoms. *Proceedings of the National Academy of Sciences of the United States of America*, *74*(11), 5088–5090. https://doi.org/10.1073/pnas.74.11.5088

Woese, C. R., Kandler, O., & Wheelis, M. L. (1990). Towards a natural system of organisms: proposal for the domains Archaea, Bacteria, and Eucarya. *Proceedings of the National Academy of Sciences of the United States of America*, *87*(12), 4576–4579. https://doi.org/10.1073/pnas.87.12.4576

Yarza, P., Yilmaz, P., Pruesse, E., Glöckner, F. O., Ludwig, W., Schleifer, K. H., Whitman, W. B., Euzéby, J., Amann, R., & Rosselló-Móra, R. (2014). Uniting the classification of cultured and uncultured Bacteria and Archaea using 16S rRNA gene sequences. *Nature reviews. Microbiology*, *12*(9), 635–645. https://doi.org/10.1038/nrmicro3330

Zhou, M., Xiang, H., Sun, C., & Tan, H. (2004). Construction of a novel shuttle vector based on an RCR-plasmid from a haloalkaliphilic archaeon and transformation into other haloarchaea. *Biotechnology letters*, *26*(14), 1107–1113. https://doi.org/10.1023/B:BILE.0000035493.21986.20

Zillig W. (1991). Comparative biochemistry of Archaea and Bacteria. *Current opinion in genetics & development*, *1*(4), 544–551. https://doi.org/10.1016/s0959-437x(05)80206-0